

2

FTD-ID(RS)T-1340-80

AD A090523

FOREIGN TECHNOLOGY DIVISION



ANTENNAS

DTIC
ELECTE
OCT 14 1980
S B D



Approved for public release;
distribution unlimited.

DDC FILE COPY



80 10 8 069

UNEDITED MACHINE TRANSLATION

(10) FTD-ID(RS)T-1340-80 (11) 15 September 1980

MICROFICHE NR: FTD-80-C-001012

(6) ANTENNAS

(12) - 15

English pages: 307

Source: (21) *Un. 11771 in which...*
Antenny, Sbornik, Publishing House
~~... Moscow, No. 16, 1972,~~
~~pp. 1-7~~

Country of origin: (USSR) *716 p. 1-7 1972.*

This document is a machine translation

Requester: FTD/TQFE

Approved for Public release; distribution unlimited.

<p>THIS TRANSLATION IS A RENDITION OF THE ORIGINAL FOREIGN TEXT WITHOUT ANY ANALYTICAL OR EDITORIAL COMMENT. STATEMENTS OR THEORIES ADVOCATED OR IMPLIED ARE THOSE OF THE SOURCE AND DO NOT NECESSARILY REFLECT THE POSITION OR OPINION OF THE FOREIGN TECHNOLOGY DIVISION.</p>	<p>PREPARED BY: TRANSLATION DIVISION FOREIGN TECHNOLOGY DIVISION WP-AFB, OHIO.</p>
---	---

TABLE OF CONTENTS

U. S. Board on Geographic Names Transliteration System.....	11
Radio Interferometer of Byurakansk Observatory to the Wavelength 73.5 cm, by V. A. Sanamyan.....	2
Restoration of Antenna Radiation Patterns From the Field Known in the Limited Sector of Angles in the Fresnel Zone, by Yu. A. Kolosov, A. P. Kurochkin.....	54
Synthesis of the Linear of the Antenna in the Class Relay Functions of Current Distribution, by E. I. Krupitskiy, T. N. Sergeyenko.....	82
Synthesis of Arc and Spherical Antenna Arrays, by L. I. Ponomarev, I. S. Yuspraykh.....	111
Formation of the Antenna Radiation Patterns With the Help of the Passive Slotted Emitters, by I. V. Guzeyev, L. L. Zbarskaya.....	142
Research of the Consecutive Diaphragm-Forming Diagrams for Multiple-Wires Antenna, by M. A. Zhutikov, S. M. Mikhaev.	169
Algorithm of the Selection of the Optimum Location of the Emitters of Linear Antenna Array by the Method of Coordinate-by-Coordinate Sorting, by Yu. Kh. Vermishev, V. V. Gmurman, M. B. Zakson.....	194
Performance Calculation of Antenna Radiation with the Circular Aperture, by L. Z. Pazin, Yu. S. Petreykov.....	215
Characteristics of Two-Mirror Antenna, Which Forms Radiation Pattern of Sum-and-Difference Type, by L. N. Zakhar'yev, A. A. Lemanskiy, A. Ye. Tumanskaya.....	232
Approximate Computation of the Surface of a Small Mirror According to the Strains of Large Mirror in Cassegrain's Antenna, by A. L. Eizenberg, L. A. Dozorets.....	248
The Phase Center of Horn Radiators, by V. G. Yampol'skiy.....	265
Dispersive Characteristics of Multiturn Cylindrical Helical Antennas with Counter Winding, by O. A. Yurtsev.....	283

U. S. BOARD ON GEOGRAPHIC NAMES transliteration SYSTEM

Block	Italic	Transliteration	Block	Italic	Transliteration
А а	<i>А а</i>	A, a	Р р	<i>Р р</i>	R, r
Б б	<i>Б б</i>	B, b	С с	<i>С с</i>	S, s
В в	<i>В в</i>	V, v	Т т	<i>Т т</i>	T, t
Г г	<i>Г г</i>	G, g	У у	<i>У у</i>	U, u
Д д	<i>Д д</i>	D, d	Ф ф	<i>Ф ф</i>	F, f
Е е	<i>Е е</i>	Ye, ye; E, e*	Х х	<i>Х х</i>	Kh, kh
Ж ж	<i>Ж ж</i>	Zh, zh	Ц ц	<i>Ц ц</i>	Ts, ts
З з	<i>З з</i>	Z, z	Ч ч	<i>Ч ч</i>	Ch, ch
И и	<i>И и</i>	I, i	Ш ш	<i>Ш ш</i>	Sh, sh
Й й	<i>Й й</i>	Y, y	Щ щ	<i>Щ щ</i>	Shch, shch
К к	<i>К к</i>	K, k	Ъ ъ	<i>Ъ ъ</i>	" "
Л л	<i>Л л</i>	L, l	Ы ы	<i>Ы ы</i>	Y, y
М м	<i>М м</i>	M, m	Ь ь	<i>Ь ь</i>	'
Н н	<i>Н н</i>	N, n	Э э	<i>Э э</i>	E, e
О о	<i>О о</i>	O, o	Ю ю	<i>Ю ю</i>	Yu, yu
П п	<i>П п</i>	P, p	Я я	<i>Я я</i>	Ya, ya

*ye initially, after vowels, and after ъ, ь; e elsewhere.
When written as ě in Russian, transliterate as yě or ě.

RUSSIAN AND ENGLISH TRIGONOMETRIC FUNCTIONS

Russian	English	Russian	English	Russian	English
sin	sin	sh	sinh	arc sh	sinh
cos	cos	ch	cosh	arc ch	cosh
tg	tan	th	tanh	arc th	tanh
ctg	cot	cth	coth	arc cth	coth
sec	sec	sch	sech	arc sch	sech
cosec	csc	csch	csch	arc csch	csch

Russian	English
rot	curl
lg	log

ANTENNAS.

Accession For	
NTIS GRA&I	<input checked="" type="checkbox"/>
DTIC TAB	<input type="checkbox"/>
Unannounced	<input type="checkbox"/>
Justification	
By	
Distribution/	
Availability Codes	
Dist	Avail and/or Special
A	

Page 2.

No typing.

Page 3.

Radio interferometer of Byurakansk observatory to the wavelength 73.5 cm.

V. A. Sanamyan.

In the article is given detailed description of the radio interferometer of Byurakansk astrophysical observatory to the wave 73.5 cm, recently of introduced into action.

Introduction.

The described radio interferometer was created on the basis of earlier than worked on the wave 3.7 m radiotelescope [1] by its reconstruction for the shorter wave - 73.5 cm (408 MHz). In the volume of works on reconstruction they entered:

1. Increase in the length of western and average/mean east of

the antennas of radio interferometer respectively 2 and 1.6 times.

2. Alteration of reflecting surface of antenna dishes.

3. Development and production of swivel gears for rotating antennas with the help of central electric drive.

4. Development and production of a new system of vibraters.

5. Development and production of radiometer on 408 MHz (system of preamplifiers and main receiving-recording device/equipment).

As a result of reconstruction the total geometric antenna area of radio interferometer achieved 7700 m^2 , the extent of line the east - west - 540 m (736λ) with the gap in the middle on 180 m (245λ), i.e., considerably smaller than the length of its antennas. This system, as let us see below, has interference radiation pattern with the sharply pronounced central lobe/lug whose width at the level of half power is 6 min and actually is determined the resolution of radio interferometer on the right ascension.

The effective area of two fundamental antennas of radio interferometer (including losses in the feeders prior to the input of preamplifiers) comprises not less than 2000 m^2 , which makes it possible to reliably record radio sources with the density of the flow of 1-2 unity with the effective noise temperature of

preamplifier of 600°K, the band of receiver 1 MHz and time constant of end device 4 s.

After the replacement of electron-tube preamplifiers by the low-noise transistor amplifiers which at present are developed/processed, the sensitivity of radiotelescope considerably will be increased.

CONSTRUCTION/DESIGN OF RADIO INTERFEROMETER.

Antenna dishes. Radio interferometer consists of four antennas, general layout and sizes/dimensions of which are given in Fig. 1.

Page 4.

The reflecting surface of antenna dish has a form of the parabolic cylinder which is formed with the help of the flat/plane parabolic farms/trusses. The latter are mounted on the metallic struts, arranged at a distance of 9 m from each other (Fig. 2).

Mirror itself is formed by 1.5-mm compound wires, in parallel stretched to these farms/trusses at a distance of 5 cm from each other with the help of the compensative springs (at the ends of each wire) by the force of 10-12 kyf.

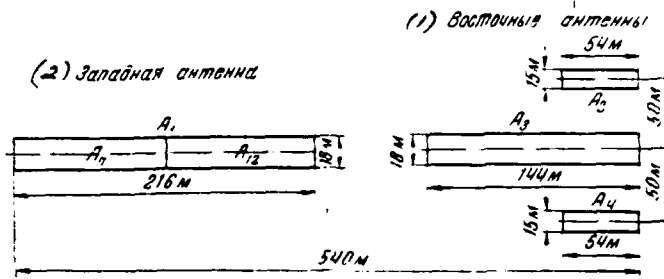


Fig. 1.

Key: (1). Eastern antennas. (2). Western antenna.

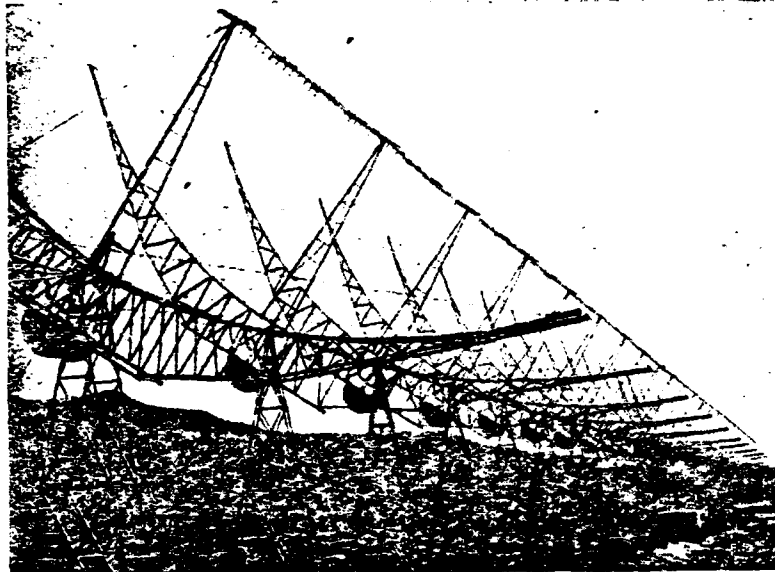


Fig. 2.

Page 5.

The system of irradiation and the cables of feed are placed

along the focal line of mirror, which passes at a distance of 5.5 m from its apex/vertex. Entire system of irradiation, cables of feed and coordinating elements/cells of the sections of antenna are suspended/hung from three in parallel stretched cables which, in turn, are held on the metallic focal struts.

System of the rotation of antenna. The antennas of radio interferometer rotate only in the meridian plane. In the initial version when radio interferometer worked on the ultrashort waves and, therefore, it had wide radiation pattern on the declination, the rotation of antenna was realized by hand, discretely through 2.5° . After transition/junction to the shorter waves the antenna radiation pattern on the declination sharply was throttled/tapered and this rotation of antenna proved to be insufficient. Furthermore, as showed practice, the operation of this system too labor-consuming and requires long time for the adjustment/exchange of the antennas of radio interferometer of one position into the other. It was suitable for the survey/coverage of the sky when infrequently it was necessary to vary antenna position. However, after the reconstruction of radiotelescope as a result of which were increased its resolution and sensitivity and, therefore, it became possible to use a radiotelescope for the solution of other radio-astronomical problems, arose the requirement to revolve the antenna of radiotelescope rapidly, to smoothly and establish/install it with the large

accuracy. For this was worked out the new rotary device/equipment whose overall kinematic diagram was given in Fig. 3.

The rotation of the eastern and western antennas of radio interferometer is realized independently with the help of electric drive. For obtaining the necessary delay/retarding/deceleration are used three standard reducers of brand RTSD-250 with the coefficient of the reduction of each 1-24. In the reducer is used the electric motor of the type ACO-12/4 with the number of revolutions $N=1360$ r/min and the power $W=2.3$ kW. In parallel to the horizontal rotational axis of antennas is carried out the common shaft which in the middle is connected directly with bilateral output shaft of reducer. At each parabolic farm/truss of antenna dish, in the center of its rotation, is mounted the block with a diameter of 1 m, and under it, on the axis of drive, is put on another block with a diameter of 0.5 m. Both these of block are mutually connected by 8-mm steel cable whose ends/leads are fixed/recorded on the housings of blocks. This diagram is very simple and at the same time it ensures the linear connection/communication between the rotation of drive shaft and the antenna dish. One turn of drive shaft corresponds to the rotation of antenna in the limits of the operating range of angles of depression. For the target the decreases of frictional force on drive shaft of the axis of blocks are based on the ball bearings.

The permissible maximum shaft stress of reducer is equal to 0.5 t, which by an order exceeds the general/common/total force of the imbalance of antenna. This makes it possible to work in the presence of small wind pressure.

Page 6.

With the high winds and when radiotelescope is not found in running order, antenna dishes are fixed. Is developed/processed the braking system of antenna dish, which will make it possible to work, also, with moderate winds.

The degree scales are attached directly on the shaft of electric drive in its middle and at the ends/leads, and also on the rotational axis of the outer and average/mean supporting farms/trusses of antenna dish.

The antenna dishes of radio interferometer are turned around the horizontal axis in limits of 0-160°, beginning from the southern horizon/level. The speed of rotation of mirror is equal to 8°/min, the accuracy of focusing/induction in the declination - 15-20 min.

At present the rotation of separate antennas is realized independently. Are developed/processed the systems of automation for the synchronization of rotation and control of all antennas of radio interferometer from the central control desk.

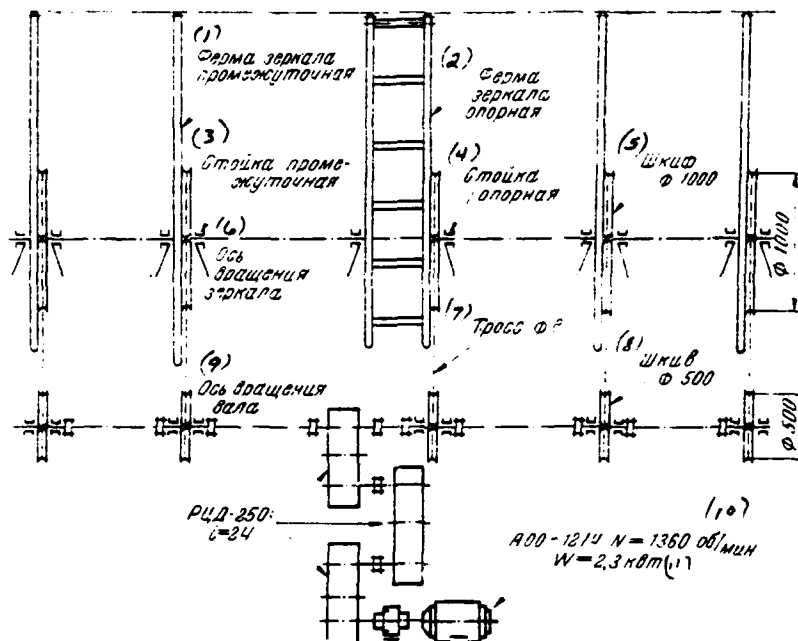


Fig. 3.

Key: (1). Fermat mirror is intermediate. (2). Fermat mirror supporting/reference. (3). Strut intermediate. (4). Strut supporting/reference. (5). Cabinet. (6). Rotational axis of mirror. (7). Cable. (8). Block. (9). Rotational axis of shaft. (10). r/min. (11). kW.

Page 7.

SYSTEM OF VIBRATORS.

Half-wave dipole with the coaxial slotted feed. As primary sensor (irradiator) was selected a 75- ohm symmetrical half-wave vibrator which is supplied from the coaxial line with the longitudinal quarter-wave slot (Fig. 4a). The selection of this system is caused by three fundamental requirements:

- obtainings possibly of more uniform current distribution along the focal line of antenna, which will lead to an increase in the effective antenna area;

- guarantee of reliable protection of primary feeders and vibrator itself from the moisture;

- guarantee of compactness and lightest possible weight of radiation system.

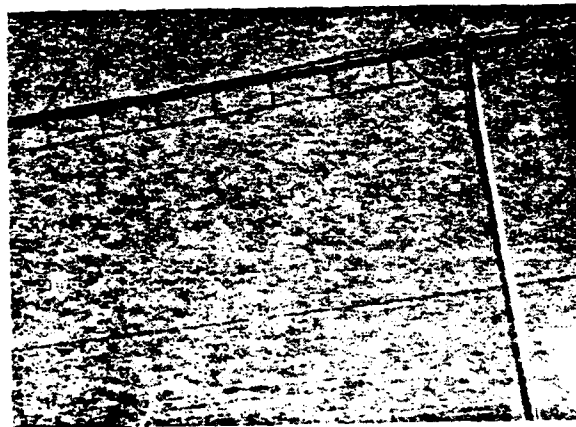
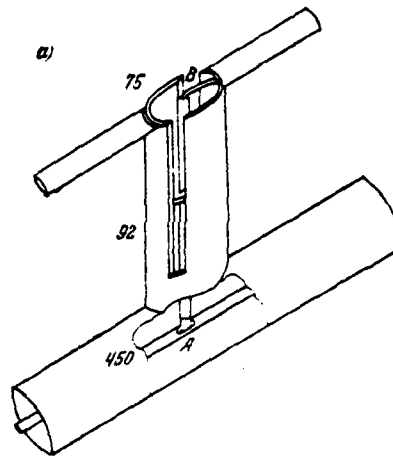


Fig. 4.

Page 8.

Four-wave slot simultaneously transforms the resistor/resistance of vibrator to the input of general/common/total feeder with relationship/ratio [2]

$$R_A = 4R_0^2/R_s; \quad R_T = 2R_0. \quad (1)$$

where R_0 - wave impedance of coaxial feeder; R_T - wave impedance of the section of slot (Fig. 4a, between points A and B); R_s - output resistance of vibrator; R_A - transformed to the common line resistor/resistance (Fig. 4a, point A).

As shows formula (1) when $R_s < R_T$, slot is step-up impedance transformer. This property simplifies the power-supply system of a large number of parallel-connected low-resistance emitters, which occurs in the case of the described radiotelescope.

Location of vibrators on the antenna. For the elongation/extent nine meters of the focal line of antenna are placed 24 half-wave vibrators. This group of vibrators subsequently we will count for one section of antenna. Each section, in turn, is divided/marked off into two parts on 12 vibrators in each. They cophasally are connected up the general/common/total coaxial feeder through a 92- ohm coaxial line with the slot.

The feed of group of 12 vibrators is produced in its center. It cophasal, which is achieved by the selection of the junction of the internal vein/strand of line to the left or right edge of the slot of vibrator. The distance between two adjacent vibrators is equal $\lambda/2$.

This means that two groups, on 6 vibrators in each (resistor/resistance of which it transforms itself to the common coaxial feeder as 450 ohms), in parallel they are connected between themselves, and then through a 150-ohm quarter-wave transformer to the general/common/total input of sections.

Diagram of one of the vibrators with the indication of the value of resistance at different points is given in Fig. 4a, and 4b is shown the photo of one group of vibrators. By trial and error of the parameters slots, diameter of internal wiring and thickness of the fastening insulators of the line of the value of resistors/resistances were selected by such that general/common/total output resistance of group of 12 vibrators would be equal to the wave impedance of the feeding cable (75 ohms). In the groups of vibrators were not used the tuning elements/cells. Before carrying out serial production of the groups of vibrators, in the experimental samples/specimens with the large thoroughness were selected the sizes/dimensions of all elements/cells of vibrator, line and coordinating elements/cells, and then during the production, with aid of special attachment, they observed a strict identity of all groups. As a result of this was achieved/reached almost ideal value coefficient this was achieved/reached the almost ideal value of standing-wave ratio (k_{sv}) for all groups: 1.05±0.05 in the band of frequencies of 10 MHz about the operating frequency and 1.15-1.20 in

the band of frequencies (395-420) MHz.

Page 9.

Section of 24 vibrators is the independent system, which is tuned on the earth/ground, and then is suspended on the antenna along its focal line with the help of the cables and special holders. The sizes/dimensions of the latter were selected so as to compensate the sagging of cables and sections themselves. The divergence of the line of vibrators from the focal line of mirror does not exceed 0.05λ in the worst (from the point of view of sagging) antenna position. Since the antenna radiation pattern in the plane of declination is not very narrow, this shift cannot introduce essential error into the results of measurements.

Counter-reflector. The system of cables, the feeders of feed, holders and matching elements/cells are placed on the plane of the counter-reflector of antenna.

Counter-reflector also and antenna dish, is formed with the help of the in parallel stretched wires. It has flat/plane form for the western antenna (by width $\sim\lambda$) and angle mold for the eastern antennas (aperture of angle of $\sim 140^\circ$). The sizes/dimensions of counter-reflector, the distance of vibrator from the focal line and

from the plane of counter-reflector were selected experimentally so that edge antenna dishes would be irradiated by the power, which does not exceed 100% of the power by the center, but the line of phase centers would pass along the focal line.

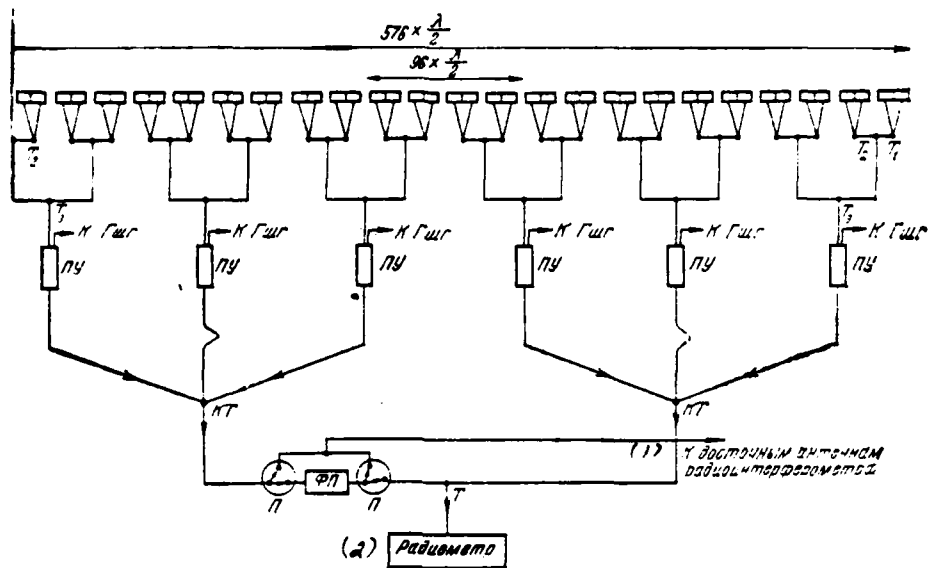


Fig. 5.

Key: (1). To the eastern antennas of radio interferometer. (2). Radiometer.

Page 10.

Feeders of feed. The overall diagram of the feed of the vibrators of entire antenna is given in Fig. 5, where T, T₁, T₂, T₃ - matched tee-transformers; TK - crosspiece-transformer; GShG - cap of noise generator; P - switch of feeders and FP - phase switch. Two halves section of 24 vibrators are connected between themselves by the cable of a small attenuation (HK-78) and by quarter-wave tee-

transformer. The sections between themselves are combined in pairs. The lengths of all cables from the center of the primary group of vibrators to the input of main receiver are identical. This, as we will see below, it ensures sufficiently broadband for entire radio interferometer. Groups also and sections, are connected between themselves with the help of the specially prepared quarter-wave branch-transformers which are well matched with cable (ksv-1.1) and are hermetically sealed. Before placing feeders on the antenna, their electrical lengths with the help of the grad line they were selected with the large accuracy. The phase error in the arms of antenna does not exceed one-two degrees.

At the output of every four sections (96 half-wave vibrators) occurs the preliminary amplification of signal. The subsequent intermediate amplification of signal occurs at the input of each antenna of radio interferometer.

Power loss in the cables from the preamplifier (PU) to the general/common/total input of antenna (Fig. 5) is equal 3 dB -- 2 of times), and from the input of antenna to the main receiver 8 dB (6 chasubles). Losses in the section from the vibrator to PU experimentally were not determined. Then carried to the losses of antenna. Calculated values of these losses is 1.1 dB.

USE OF ANTENNAS IN A COMPOSITION OF RADIO INTERFEROMETER.

The selected system of feeders and preamplifiers makes it possible to use each antenna as the separate independent and as composite/compound component part of entire radio interferometer. Moreover both western and average/mean eastern of antenna separately can be used as the system, in which occurs periodic switching of the phase of signal in the cable of the feed of one half antenna fabric.

In the composition of fundamental radio interferometer they are used average/mean eastern and western antennas. The effective area of two outer eastern antennas in comparison with the total effective area is small, they cannot make a significant contribution to the formation of radiation pattern and improvement in the sensitivity of entire radio interferometer; therefore they in essence will be used together with average eastern antenna or with its part when will arise the need for making more precise the declination of radio source or its structure in the vertical plane. For this case is provided the possibility to differently combine three eastern antennas: all three together, extreme between themselves and average/mean with the extreme ones.

In the feeders, which go to the outer eastern antennas, are phase inverters for the shift of interference pattern in the vertical plane, which are the graduated segments of the coaxial line of the variable/alternating length, in each arm which smoothly vary the phase of signal in limits of 0 to 180°. These lines are uniform and well matched between themselves; therefore a change in their length with the phasing of interferometer does not introduce further errors.

Outer eastern antennas can be combined with two halves the western antenna and to have two independent interferometers whose bases are deflected to the different sides relative to line the east - west. This gives the possibility to raise the accuracy of the determination of the right ascension of radio source by its simultaneous observation by these interferometers.

Is provided also the possibility with the help of the automatically operational system of phase inverters to scan interference radiation pattern in the vertical plane so that to immediately solve the radio sources which simultaneously are within the limits the antenna radiation pattern. This problem can be solved also by the use/application of the well untied between themselves multichannel feeder and receivers.

CHARACTERISTICS OF ANTENNA FEEDER UNIT.

The antenna radiation pattern of radio interferometer in the vertical plane is the radiation pattern of parabolic reflector with the aperture 18 and 15 m for the western and eastern antennas respectively. Since the edge of mirrors they are irradiated weakly, radiation pattern in the vertical plane is obtained somewhat wider than the calculated. Due to this is reduced the dissipation of energy on the side lobes of antenna. According to calculation data the width of radiation pattern in this plane composes $2^{\circ} 5'$ for the western antenna and 3° for the eastern antennas.

The antenna radiation pattern in the horizontal plane is determined by the formula of coplanar grating which in the units of power and in the standardized/normalized form is expressed by formula (2) [3]

$$F_{PN}(\theta) = \left[\frac{\sin\left(\frac{N\varphi}{2}\right)}{N \sin\left(\frac{\varphi}{2}\right)} \right]^2; \quad \varphi = dk \sin \theta. \quad (2)$$

Here θ - angular distance of source from the normal to the plane of antenna aperture, the secant of interferometer spacing; $d = \lambda/2$ - distance between the adjacent elements/cells of grating; λ - wavelength; N - number of elements/cells in the grating, equal to 576.384 and 144 for western (A_1), average/mean the eastern (A_3) and outer eastern (A_2 and A_4) antennas of radio interferometer

respectively (Fig. 1); $\kappa = 2\pi/\lambda$ - wave number.

Page 12.

When two halves antenna are connected between themselves through the device/equipment, which periodically changes over the phase of signal on 180° , radiation pattern [5]

$$F_N(\theta) = 4F_{N/2}(\theta)F_H(\theta); \quad F_H(\theta) = \cos\left(\frac{N}{2}\varphi + \psi\right);$$

$$F_{N/2}(\theta) = \left[\frac{\sin\left(\frac{N\varphi}{4}\right)}{\frac{N}{2}\sin\left(\frac{\varphi}{4}\right)} \right]^2,$$

where ψ - permanent phase difference; $F_H(\theta)$ - interference factor. Fig. 6a gives calculated radiation patterns for the western and eastern antennas of radio interferometer (curves F_1 and F_2 respectively), obtained in the machine "Nairi-2". Is to the right given the recording of radio source Deva-A (3C274), obtained on antenna A_1 . Scale corresponds to one angle degree. On the dotted graphs is shown the curve F , which corresponds to this recording. The conformity of experimental design data, as we see, satisfactory.

In Fig. 6b are introduced radiation pattern of side lobes on the increased scale along the axis of ordinates.

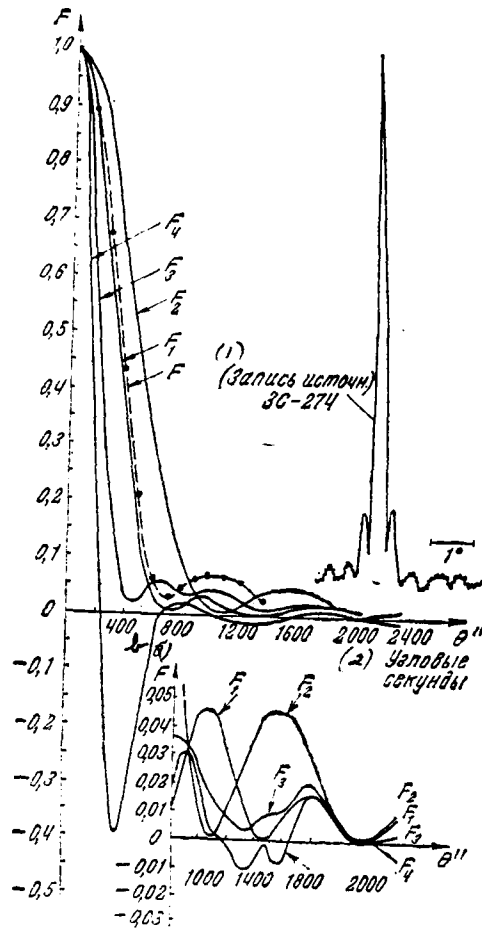


Fig. 6.

Key (1). (Recording by source). (2). Seconds of arc.

Interference diagram. For the fundamental antennas of radio interferometer (A_1 and A_3) in the plane of right ascension interference diagram in the composite form

$$F_{nA_1A_3}(\theta) = F_{A_1}(\theta) + F_{A_3}(\theta) e^{i(\beta + \psi_0)};$$

$$\beta = \frac{\kappa D}{\cos \alpha} \sin(\theta - \alpha); \quad \psi_0 = \kappa D \operatorname{tg} \alpha \sin(\gamma - \alpha),$$

where $F_{A_1}(\theta)$ and $F_{A_3}(\theta)$ - antenna radiation pattern A_1 and A_3 on the strength of field; D - interferometer spacing the east - west in the plane of the horizon/level; $\alpha = 0.5^\circ$ - angle of the slope of true interferometer spacing from horizontal line of $\gamma = 40.5^\circ$ - latitude of Byurakan.

After simple conversion for the interference function, expressed in the units of power, we will obtain

$$F_{n p}(\theta) \equiv |F_{nA_1A_3}(\theta)|^2 = F_{A_1}^2 + F_{A_3}^2 + 2F_{A_1}F_{A_3} \cos(\beta + \psi_0).$$

If in the interferometer is applied the device/equipment, which periodically changes over the phase of signal in one arm on 180° , then [4]

$$F(\theta) = F_{n p}(\beta + \psi_0 + \pi) - F_{n p}(\beta + \psi_0) = 4F_{A_1}F_{A_3} \cos(\beta + \psi_0). \quad (3)$$

In the arms of interferometer are introduced the further segments of the line of variable/alternating length for the compensation for a phase difference ψ_0 by the caused difference in the levels of antennas A_1 and A_3 . In this case in expression (3) it is possible to take $\psi_0 = 0$.

Effective antenna area was evaluated according to the flow of the series/row of the supporting/reference sources of cosmic radio-frequency radiation. All losses of antenna and antenna feeder units prior to the input PU (Fig. 5) referred to the losses of antenna. Separately were determined the effective areas of one section of antenna, four sections and entire antenna. For the coefficients of the use of an area respectively were obtained the values: 0.5; 0.4 and 0.34. The method of measuring these coefficients is in detail presented below. From given data it follows that the noticeable part of the energy of useful signal is lost in the cables between the output of sections and the input PU, that, in turn, he indicates the need for the selection of an optimum number PU and their approximation/approach to an output of sections.

Level of lateral lobes. The radiation pattern of multiunit antenna unavoidably has side lobes. For a decrease in the level of these lobes/lugs into the antenna to technology are applied different methods, in particular, is selected the corresponding law of current distribution according to the antenna dish or according to its elements/cells. As a rule, the current strengths on the edges of mirror or on the extreme elements/cells reduce on the specific law.

In the described radiotelescope a decrease in the side-lobe level in the vertical plane, as it was noted, is achieved by the weak

irradiation of the edges of cylindrical mirror (about 5-10% relative to the power, which falls to the middle part of the mirror).

Distribution of the current strength according to the vibrators of the sections of the antennas of radio interferometer uniform along the focal line.

Page 14.

Consequently, in the plane of right ascension the side-lobe level is obtained not less than it is determined by the given higher formula. True, the length of mirror on $(2-3)\lambda$ more in comparison with the length of the line of vibrators, and the current strengths in the extreme groups of vibrators are somewhat reduced in comparison with the average groups; however, this does not significantly vary common diffraction pattern. In this plane the side-lobe level in essence is characterized by the heterogeneity of antenna feeder unit (on the phase and by the amplitude of current in them). Therefore were applied all possible measures, in order these heterogeneities to reduce to a minimum.

The decrease of the side-lobe level of common interference pattern favorably is manifested the following fact. In the line the east - west the sizes/dimensions of the mirrors of the eastern and

western antennas of radio interferometer are different, they relate as by 2:3. Because of this the maximums and zero radiation patterns of one antenna are displaced relative to maximums and zero another. And when interferometer works by the method of phase switching, with which the radiation patterns of two antennas are multiplied, a number of side lobes increases in the limits of the solid angle of interference diagram, and their level, beginning from the second, noticeably it is reduced (Fig. 6, the curve F_4). The appearance of a large negative lobe/lug does not accordingly make the resolution worse of radio interferometer, since it is within the limits of main thing and the first of side lobes and, furthermore, with this form of curve one can see well the presence of adjacent source. The advantages of this method are in more detail presented in work [5]. This system has another advantage. If this source is observed twice: one time by simple interference method, and another time by single switching, then from the analysis of the recordings of observations error-free it is possible to determine, it is this recording the signal of real source of this is trace from the intense source, accepted by the side lobe of antenna. If recording is the signal of real source, then transit time must not depend on the method of observations.

RECEIVER.

Preamplifier. At the height of each group of four sections of antenna is connected one cascade/stage PU (Fig. 7), carried out on the diagram "grounded grid". It is assembled on the high-frequency ceramic triodes of the type 6C17K ¹).

FOOTNOTE ¹. At present these amplifiers are replaced transistor with the factor of the noise -3 dB. ENDFOOTNOTE.

Resonators coaxial are connected in the circuit of anode and cathode of tube. Their tuning for the resonance frequency and to the optimum coupling is realized with the help of variable/alternating air capacitors, entering the construction/design of resonators themselves.

Page 15.

Output signal is removed/taken from the grounded end/lead of coaxial cavity near the current antinode. This low-resistance inclusion/connection simplifies the agreement of the output of amplifier with the cable. Noise factor is equal to 2.8 (-4.5 dB), power gain 36 (-16 dB). The resonance frequency of 408 MHz, passband (8-10) MHz. With the work of antenna in the system of the interferometer between its input and main cable is switched on by intermediate the preamplifier of signal (PPU).

Fundamental receiver - superheterodyne type. Its input amplifiers are also assembled on the triodes 6C17K and have the same construction/design as PU. Mixer - crystal, with the coaxial cavity. The frequency of heterodyne 383.86 MHz is stabilized by quartz (55th crystal harmonics). This noticeably improves the stability of entire receiver. In the intermediate frequency - 24 MHz main receiver branches to two channels with the bands of frequencies of 1 MHz for interference observations and 3 MHz for the observations with one antenna. The overall gain of main receiver can be regulated in the limits of 100-120 dB. The time constant of end device varies through discrete/digital values of 0.05; 0.1; 0.5 and 4 s. The remaining units of receiver are usual.

Phase antenna switch (FP) is carried out on the semiconductor changing over diodes of the type D501Zh (approach also diodes D501A and D501Ye). Its schematic diagram is given in Fig. 8.

For the exception/elimination of sharp transitions/junctions the switch is designed in the form of coaxial ring. At the ends/leads of the quarter-wave sections are variable/alternating disc capacitors - C_{var} for tuning of switch for the operating frequency. Changing over reference sine voltage 0.6-0.8 ^{with} V frequency of 37 Hz is supplied

from the standard audio signal generator (ZG-10) of stable feed. Switching the phase of signal on 180° is realized with the error not more than one degree. Power losses in the switch compose 70/o (0.3 dB). Analogous diagram has amplitude switch. In it at point A (see Fig. 8) ring is cut into two branches to which are connected the antenna and the equivalent noise source.

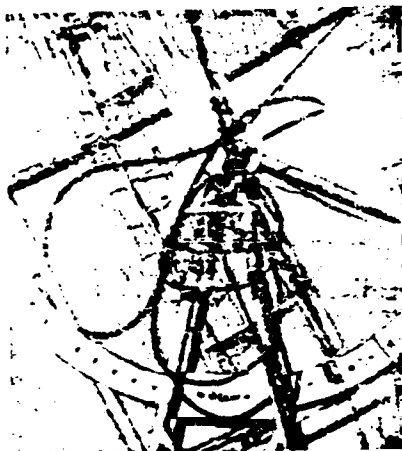


Fig. 7.

Page 16.

CALIBRATION OF RADIO INTERFEROMETER.

The calibration of multiunit radiotelescopes with the help of the local standard noise sources in the majority of the cases is connected with the great technical difficulties or is almost impossible. In such cases, as a rule, calibrates itself main receiver, and system PU and feeder circuit remain without the control/checking. As the most perfect, naturally, is considered the calibration of multiunit antenna systems with the help of the supporting/reference space sources; however, this not completely sufficient, since always after the arrival of the signal of the observed source it is impossible to directly record the signal of supporting/reference source. Virtually frequently it is necessary signal from the latter to write/record through several hours during which can be changed the parameters of antenna feeder circuit and radiometer. Does not remain constant and the effective antenna ambient temperature in the directions of the measured and supporting/reference sources. By another difficult, by most essential, problem is the realization of control/checking of the

quality of the work of the individual sections of multiunit antennas. This problem even more is complicated, when system extended also in each element/cell or group of elements/cells occurs the preliminary amplification of signal with the sufficiently high coefficient of power gain. In that case the calibration of radiometer from the input of main receiver is insufficient for calibrating the radiation source, since noises and instability of equipment in essence will depend work of PU.

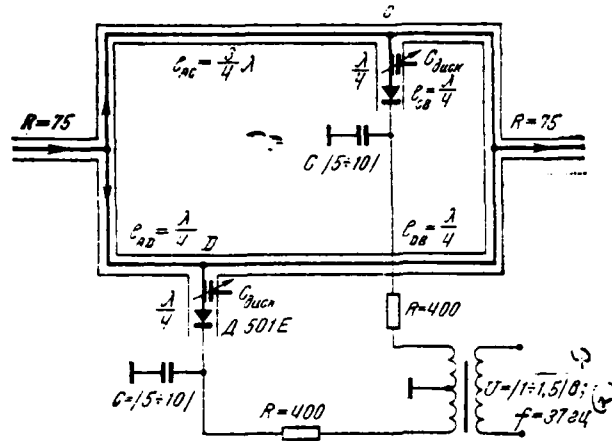


Fig. 8. Key: (1). V. (2). Hz.

Page 17.

Furthermore, in the multiunit extended systems when the length of feeder lines from PU to the main receiver composes hundred or thousands of wavelengths and they are badly/poorly shielded from the effect of ambient conditions (change in the temperature, humidity, different electrical focusings/inductions and others), and a number of tuning and coordinating elements/cells reaches ten and hundred, the characteristics of antenna feeder circuit in the time can vary and it is essential to affect the results of measurements. Is important the fact that the parameters of PU themselves also can vary in the time by very differently.

On reasons indicated above appears the need for calibrating or, at least, to monitor mode/conditions of the work of radiotelescope at least in the section from the inputs of preamplifiers - all amplifiers together and each individually.

In the described radio interferometer for the partial solution of this problem it is provided in each PU to place the separate cap of noise generator GShG (see Fig. 7), which in parallel with the section of antenna constantly is connected to the input of PU through the directional coupler. The feed of noise caps and corresponding measuring meters general/common/total for all amplifiers is arranged/located on the main receiver. Feed to the separate noise caps can be supplied separately to each or simultaneously to all. This gives possibility periodically, also, without the large expenditure of time to calibrate both entire system as a whole and its separate sections, beginning from the input of PU. But the latter are sufficiently closely conducted/supplied to the primary vibrators (length of the line between them only of 50 wavelengths), and, furthermore, these lines are done from the cable of a small attenuation, it is well shielded from the penetration of moisture and are located under identical temperature conditions. As showed experiment, the parameters of these sections substantially do not

vary in the small time interval, determined by the transit time of the radio source through the antenna radiation pattern and time of recording reference signal. It is completely sufficient, if these sections of line, just as entire radiotelescope, two or three times will calibrate itself according to the well selected intense space radio sources.

Of course for the full/total/complete calibration it would be desirable standard noise signal to supply not by an the input of amplifier, but directly to the primary irradiator. This problem is technically difficult, since the remote zone in which it is necessary to place the standard noise source, composes hundreds of kilometers and virtually it is not possible to ensure the reception of reference signal of necessary amplitude and stability. However, it is possible the standard generator to place also in the near zone such that by the branched from it power to irradiate primary vibrators or groups of vibrators. The creation of this system, in the principle, possibly, and a question of its practical implementation is studied.

A question of the use/application of PU in the multiunit antenna systems is examined in works [6, 7]. Here it will be examined in connection with the described interferometer, mainly, from the point of view of the absolute calibration of the multiunit antenna systems, which contain numerous PU.

Page 18.

During the computations we will disregard the noises of the galactic background. This will not introduce significant error, since radio interferometer in the majority of the cases will work by the method of phase switching and the antenna radiation pattern is sufficiently narrow in order to exclude the reception/procedure of the radio emission of galactic background. As far as regions are concerned separate of the intense radio emission of the background of galaxy, then we will carry them to the group of the extended galactic radio sources, about which it will be said below.

For the absolute calibration of the radio emission adopted our antenna we will consider as the system, which consists of n of the linear, in parallel connected four-poles. Number n we will take as the equal to a number of PU. If we to the input of the i -th of these four-poles supply noise power p_i , then the total power of signal at the input of the main cable

$$P_c = \sum_{i=1}^n \eta_i g_i p_i \quad p_i = A_{3i} \Delta f_i S, \quad (4)$$

where: η_i - transmission factor of the power of the i branch of line;

g_i - coefficient of the power gain of the i amplifier; A_{3i} the

effective area of the i group of the sections of antenna taking into account the loss in the cables in the section up to PU; Δf_i the band of frequencies of the i amplifier; S - density of the flow of the radiation/emission adopted, which we will consider constant in all sections of antenna aperture. In particular, when amplifiers and corresponding branches are identical, i.e., when

$$\eta_i = \eta, \quad g_i = g, \quad A_{oi} = A_o, \quad n, \quad p_i = p \quad \text{and} \quad \Delta f_i = \Delta f \quad \text{for all values of index } i$$

then

$$P_c = n \eta g p = \eta g \Delta f S A_o; \quad p = \frac{S A_o \Delta f}{n}. \quad (5)$$

This power is further amplified by main receiver, and it is possible to rate/estimate simply: $p_o = p c g_f \eta_o$, where η_o the transmission factor of the power of main cable, and the led to the band coefficient of the power gain of the main receiver

$$g_f = g_o \frac{\Delta f_o}{\Delta f}, \quad (6)$$

g_o and Δf_o - factor of amplification and band of the frequencies of the main receiver adopted respectively. We accept $\Delta f_o < \Delta f$. Comparing the measured by method indicated above power of radio source with the equivalent horsepower of noise generator, from equality $P = P_n$ let us determine the value of the antenna temperature of radio source T_a [8].

It is here necessary to focus attention on two facts. Completely

it is clear that the signals, which go from the different standard generators, are incoherent white noises, and in order to compare them with the signal of observed point source, coherent at the output all PU, it is necessary to use a compensative or amplitude-modulation radiometer; this comparison will be full/total/complete.

Page 19.

When is used the phase-switching device/equipment at the input of fundamental receiver, then signals from the noise caps are not modulated, in contrast to the useful signal whose phase varies with the passage of the radio source through the antennas of interferometer and, therefore, is modulated during the switching. But since the sections of antenna are not ideally matched with the cable and switching system itself is not also ideal, then at the output of radiometer will be always different from zero signals from the noise caps, which we will call the error signal. If it are calibrated by the signal of known radio source, it is possible to measure the signals also of other sources, since, beginning from the input of PU, any change in the parameters of radiometer will equal affect the value of the measured signal and error signal.

SENSITIVITY OF RADIOTELESCOPE.

By sensitivity of radiotelescope is understood the minimum flux of radio emission, which can be distinguished at the level of the normal noises, which appear in all its nodes, from the antenna to output amplifier. For ultimate sensitivity they usually accept the half the power of noise path/track.

If all noises (galactic background, antenna itself, feeder circuit, preamplifiers and fundamental receiver) are related to the input of antenna and equivalent noise temperature are designated through T_0 , then the sensitivity of radiotelescope, which corresponds to the half power of noise path/track, will be expressed by the known formula:

$$S_{min} = \frac{2kT_0(N_s - 1)}{A_s \Delta f \tau} = \frac{2kT_0}{A_s \Delta f \tau} \quad (7)$$

where $T_0 \approx 300^\circ\text{K}$ - ambient temperature; $N_s = (T_s + T_0)/T_0$ the equivalent factor of the noise of entire radiotelescope; A_s effective antenna area; Δf - bandwidth of the reception/procedure; τ - time constant of output device; k - Boltzmann constant.

As can be seen from formula (7), for determining the sensitivity or, which is the same, for the precise measurement of weak flows is necessary and is sufficient accurately to measure T_0 and A_s for this radiotelescope, which, by the way, presents great practical difficulty, especially in the case of multiunit radio

interferometers. Determination Δf and r difficulty does not present.

For definition T_s each branch of the antenna (section from the section to its input) of radio interferometer, in turn, we will consider as the system of series-connected active and passive networks with all inherent noise and transmission factors of power (Fig. 9).

Page 20.

If these branches are identical and everywhere occurs the full/total/complete agreement of four-poles with the feed lines, then for the equivalent noise temperature it is possible to write following expression [9, 10]:

$$T_s = T_{am} + \frac{T_{Y1}}{\eta_{K1}} + \frac{T_{K2}}{\eta_{K1} g_{Y1}} + \frac{T_{Y2}}{\eta_{K1} \eta_{K2} g_{Y1}} + \frac{T_{K3}}{\eta_{K1} \eta_{K2} g_{Y1} g_{Y2}} + \frac{T_{PP}}{\eta_{K1} \eta_{K2} \eta_{K3} g_{Y1} g_{Y2}}$$

Here T_{am} the total noise temperature of the background of galaxy, antenna and cable up to PU; $T_K = T_0(1 - \eta_K)$ - the noise temperature of the corresponding cut cables; $\eta_{K1}, \eta_{K2}, \eta_{K3}$ and T_{K1}, T_{K2}, T_{K3} - the transmission factors of the power of the corresponding sections of line; g_{Y1}, g_{Y2} and T_{Y1}, T_{Y2} factors of amplification and noise temperatures of PU and PPU respectively; T_{PP} the noise temperature of fundamental receiver. Table 1 gives the values of the coefficients, entering into formula (8) for the western antenna A₁ (analogous characteristics has

the eastern antenna of radio interferometer), while in Table 2 - value T_e , N_s and S_{min} for different cases of connecting of preliminary and through repeaters, and also values of their characteristics. During the computation of equivalent antenna temperature were accepted the following values of the parameters: $\Delta f = 1$ MHz, $\tau = 4$ s and $A_s = 2000$ m². Data of table show that with assigned magnitude A_s and the characteristics of cable the value of minimum flow which can be recorded by the given radiotelescope, strongly it depends on a number, characteristics and connection point of PU and PPU.

During the determination of the sensitivity of radiotelescope the noises of the radiic emission of galactic background included/connected in the composition of antenna noises whose value in the direction Earth's north pole was determined by the following method.

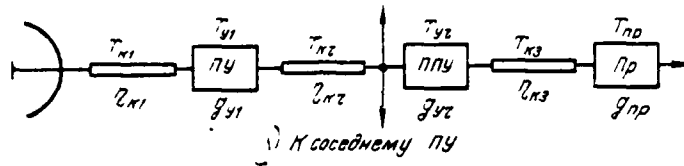


Fig. 9. Key: (1). To adjacent PU.

Table 1.

(1) Коэффициент передачи кабелей			(2) Шумы кабелей, °К			(3) Коэффициент усиления предусилителей, дБ	
η_{k1}	η_{k2}	η_{k3}	T_{k1}	T_{k2}	T_{k3}	ϵ_{y1}	ϵ_{y2}
0.75	0.50	0.10	75	150	270	16	16

Key: (1). Transmission factor of cables. (2). Noises of cables. (3). Factor of amplification of preamplifiers, dB.

Page 21.

Antenna they directed toward the pole and was fixed/recorded the conditional level of the output noises of simple compensative radiometer. Then to input of one of the amplifiers instead of the cable, which goes from four sections of antenna, they included/connected the matched load and at an ambient temperature again was fixed/recorded the level of output noises. Finally, matched impedance they transferred to the input of one section and was fixed/recorded a change in the level of output noises. The further

corresponding jumps of the level of output noises calibrated by the located in preamplifier standard noise generator. After simple computations for T_{aw} were obtained values of $\sim 250^{\circ}\text{K}$.

The problem of computing the value A_e for the multiunit antenna systems more complicated, and, as a rule, calculation and real data do not coincide, since not always it is possible to accurately determine field distribution in antenna aperture or to measure its precise radiation pattern. For this reason A_e also were determined experimentally - measurement of the antenna temperature of the series/row of the intense space radio sources, spectral flow distribution of which is well known. The recording of the signals of several sources, obtained with the help of the western antenna of radio interferometer ($A_{\text{geom}} \approx 3900 \text{ m}^2$) together with reference signal of the noise generator $T=30^{\circ}\text{K}$, is given in Fig. 10.

Table 2.

Схема включения и характеристики ПУ (1)	T_e , °K	N_s	S_{min}^{20} поток
Без применения ПУ (3)	12 000	43	10
Один каскад ПУ на входе каждой группы из четырех секций на лампах 6С17К с коэффициентом усиления мощности 16 дБ и собственными шумами 600°K (4)	1 200	5	1.0
То же, плюс общий усилитель на входе главного кабеля (действующий вариант) (5)	900	4	0.7
По два каскада ПУ на каждую группу из четырех секций с теми же характеристиками (6)	750	3.5	0.6
Один каскад параметрического усилителя на каждую группу из 12 секций антенны с коэффициентом усиления 20 дБ и собственными шумами 100°K (7)	570	2.9	0.5
Транзисторный усилитель на каждые 2 секции антенны с усилением 25 дБ и шумами 350°K (8)	750	3.5	0.6
Один каскад ПУ на входе каждой группы из четырех секций на лампах 6С17К с коэффициентом усиления мощности 16 дБ и собственными шумами 600°K, но приемник на входе антенн А ₁ и А ₂ (9)	900	5	≈1.0

Note. Given in the table data correspond to the average/mean characteristics of the working or developed/processed in the USSR amplifiers.

Key: (1). Circuit diagram and characteristic of PU. (2). un. of flow. (3). Without use/application of PU. (4). One cascade/stage of PU at input of each group of four sections on tubes 6S17K with coefficient of power gain of 16 dB and inherent noise of 600°K. (5). The same, plus general/common/total amplifier at input of main cable (operating version). (6). On two cascades/stages of PU to each group of four

sections with the same characteristics. (7). One cascade/stage of parametric amplifier to each group of 12 sections of antenna with factor of amplification 20 dB and inherent noise of 100°K. (8). Transistor amplifier to every 2 sections of antenna with amplification 25 dB and noises of 350°K. (9). One cascade/stage of PU at input of each group of four sections on tubes 6S17K with coefficient of power gain of 16 dB and inherent noise of 600°K, but receiver at input of antennas A_1 and A_3 .

Page 22.

The values of the effective area of this antenna (A_{13}), calculated according to the value of antenna temperature (T_{ant}) and flux of radio emission (S_n) of these sources [11] according to the formula

$$A_{13} = 2kT_e/S_n, \quad (9)$$

and also the corresponding values of the coefficient of the use of an antenna area are given in Table 3.

Data of table show that the average/mean value of the coefficient of the use of an antenna area composes 340/o, what is sufficiently good result for diffraction type antennas. Some disagreements of the value of this coefficient, obtained on the basis of different sources, are caused by the fact that in the period of

these control measurements the antenna was turned through the discrete/digital values of declinations and radio source is not always passed strictly on the maximum of diagram. For the introduction of the corresponding correction the antenna temperatures of sources 3S75 and 3S70 respectively increased 1.4 and 1.1 times (according to the data of radiation pattern on the declination).

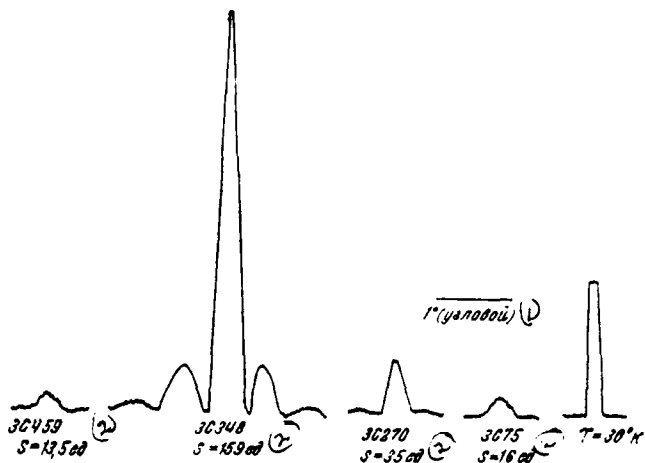


Fig. 10. Key: (1). angular. (2). unit.

Table 3.

Радиостанция (1)	Антенная температура $T_{ан}$, °K (2)	Плотность потока $S_{ан}$, ед. потока (3)	Эффективная площадь $A_{1э}$ (4)	Коэффициент использования площади (кпп) антенны A_1 (5)
ЗС75	5.1	16	1250	0.32
ЗС270	13.2	35	1200	0.31
ЗС384	90.0	159	1500	0.38
ЗС459	3.8	13.5	1400	0.36
Среднее значение кпп антенны A_1 по четырем измерениям			~1340	~0.34

Key: (1). Radio source. (2). Antenna temperature. (3). Density of flow $S_{ан}$ un. of flow. (4). Effective area. (5). Coefficient of use of area (stalks) of antenna A_1 . (6). Average/mean value of stalks of antenna A_1 on four measurements.

A comparatively large disagreement of values of effective area is caused by the fact that the flows of radio sources in the catalogs are given with the accuracy $\pm (5-10)\%$.

On the basis of given in Table 2 data it is not difficult to conclude that during the use/application of more sensitive parametric or transistor amplifiers or by multistaging in the operating amplifiers and approaching the place of their inclusion to primary radiations it is possible 1.5-2 times to increase the sensitivity of radiotelescope. Without the special work two times it is possible to raise sensitivity by an increase Δf and ν . Then ultimate sensitivity of radiotelescope achieves 0.25 unity of flow. If we consider that technical sensitivity two times lower than ultimate sensitivity, then it is obtained, that the radio sources with the flow of 0.5 unity can be observed with the help of the described radiotelescope during the use of all its real possibilities. Of this it is possible to be convinced also from the following simple analysis of the recordings of radio sources, given in Fig. 10. In them the temperature of noise path/track composes $\sim 0.5^\circ\text{K}$, which for $A_{10} = 1350 \text{ m}^2$ and $T_{10} = 1000^\circ\text{K}$ corresponds to the critical angle of $S=1$ unity. For entire radio interferometer when simultaneously are used all antennas in effective area not less than 2000 m^2 , this number decreases approximately

doubly.

SCIENTIFIC PROGRAM.

In conclusion it is possible to say several words about the program of research which it is proposed to carry out with the help of described interferometer. It switches on the study of galactic and extragalactic radio sources (discrete/digital and extended), the study of pulsars, the measurement of the angular dimensions of radio sources, etc. Interferometer makes it possible with the large accuracy to conduct the measurement of the flows of extragalactic sources, which is necessary for studying the low-frequency spectra of radio galaxies and quasars, conducted together with other observatories. Such measurements will make it possible to explain a question about a slow change of the intensity of the radiation/emission of quasars in the range of decimeter waves. Effective can prove to be the use/application of an interferometer for studying of the extended galactic sources, including the center of our galaxy, that also is planned/glided to do.

Are of definite interest the well coordinated observations of pulsars, conducted on radioastronomy station of the physical institute of the Academy of Sciences on the ultrashort waves and in Byurakan on the wave 73.5 cm.

Page 24.

In the domain of definition of the angular dimensions of the sources of work it is planned to carry out in two directions. Will be continued the determination of the angular dimensions of radio sources by the experiment of the measure for the glimmer of their brightness in the heterogeneities of circumsolar plasma. Furthermore, radiotelescope together with other distant and conveniently arranged/located radiotelescopes of other observatories can be used for the interferometry of radio sources by the method of the self-contained reception/procedure of radio signals.

The possibilities of radiointerferometer are not contained by the enumerated above problems. It is possible to enumerate number of other scientific and applied problems at solution of which it is possible successfully to work with the help of the described radiotelescope.

The author thanks the colleagues of the department of the radio astronomy of Byurakan observatory, who took part in the creation of radiotelescope. He expresses gratitude also to academician V. A. Ambartsumyan and corresponding member of the AS USSR, professor A. A.

Pistol'kors, who attentively looked over article and who did a series/row of useful observations.

REFERENCES.

1. V. A. Sanamyan, G. S. Minasyan. Communications/reports of Byurakan observatory. Iss. XXII, 1959, 35.
2. A. Runman. "Telefunkeuztg", 24, 237, 1947, No 93.
3. A. A. Pistol'kors. Antennas. M., "Soviet radio", 158, 1947.
4. M. Ryle. "Proc. Royal Soc.", 211A, 351, 1952.
5. V. A. Sanamyan. Communications/reports of Byurakan observatory. Iss. XXXX, 69, 1969.
6. B. M. Chikhachev. Transactions of the Lebedev physics inst., 17, 135, 1962.
7. R. D. Dagkesamanskiy, S. N. Ivanov, Yu. P. Ilyasov. Transactions of the Lebedev physics inst., 38, 29, 1967.
8. J. L. Pozi, R. N. Breysuel. Radio astronomy. M., "Foreign

literature", 57, 1958.

9. M. S. Zhuk, Yu. B. Molochkov. Design of antenna feeder units. L., "Energy", 99, 1966.

10. N. S. Kreyngeľ. Noise parameters of radio receiving equipment. L., "Energy", 85, 1969.

11. P. W. Hopton, R. G. Conway and E. P. Daintry. Mon. Not. R. astr. Soc. vol. 143, 1969, p. 245.

Received 6/IV 1971; after revision - 1/X 1971.

Page 25.

RESTORATION OF ANTENNA RADIATION PATTERNS FROM THE FIELD KNOWN IN THE LIMITED SECTOR OF ANGLES IN THE FRESNEL ZONE.

Yu. A. Kolosov, A. P. Kurocnkin.

The accuracy of the determination of the antenna radiation patterns according to the results of measuring the field at the relatively small distance from the aperture depends substantially on the value of sector, in which is fixed/recorded the field. In the article are given the results of theoretical and experimental study by choice of sector in which should be carried out field measurements of antennas in the Fresnel zone for purposes of further restoration/reduction of radiation patterns. Experimental research was conducted by means of the optical simulation of problem.

Introduction.

The possibility of the definition of radiation patterns (DN) according to the results of measuring the field at the relatively small distance from antenna aperture has important practically value conformably both to the large-size antennas when the direct

measurement of DN is very difficult, as a result of the large distance of the boundary of remote zone, and to the antennas of the moderate sizes/dimensions in the case when characteristic measurements are conducted in the small locations. There are several methods of determining DN from field measurements of antenna of nearer than the boundary of remote zone.

In work [1] for determining DN of optical-type antennas it is proposed to take out irradiator from the focus of mirror. In this case the defocusing, which appears as a result of the carrying out of irradiator, compensates the defocusing of antenna, caused by final distance of the zone of measurement. For the antennas with the linear and flat/plane apertures the refocusing for the purpose of "approaching remote zone", in the principle, can be achieved/reached via corresponding to strain radiating surface [2].

Another group of methods is based on the initial measurement of field during a comparatively small distance from the antenna and the subsequent restoration/reduction of field distribution in the remote zone. The operation of restoration/reduction can be implemented either with the help of TsVM [digital computer] as this proposed in works [3], [4], or with the use of a method of optical simulation [5] which is realized most simply if the field of antenna measured in the Fresnel zone or directly in the aperture. The enumerated methods do

not require the interference in to the divergence of the measured characteristics from the true parameters of antenna in the remote zone.

Page 26.

In two latter/last methods of determining DN the accuracy of the final result depends on the value of sector, in which is fixed/recorded the field near the antenna. It is obvious, in the case when radiation field is known on certain locked surface, which encompasses antenna, the most precise possible restoration/reduction of DN. Virtually, however, field measurement is conducted only on the part of the surface where it has even more noticeable value. However, the values of field on the remaining part of the surface remain unknowns and are usually assumed/set by equal to zero, in consequence of which DN is located approximately. In the present work are given the considerations about the selection of sector in which should be carried out field measurements of antenna in the Fresnel zone for purposes of further restoration/reduction of DN in the assigned sector.

For simplicity is examined the line-source antenna with uniform cophasal field distribution in the aperture. The obtained results remain valid and in the case of antennas with the flat/plane

aperture.

STRUCTURE OF THE FIELD OF LINE-SOURCE ANTENNA IN A FRESNEL ZONE.

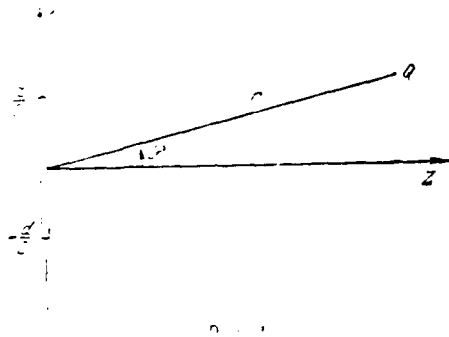
Field $E(r, \varphi)$ of line source in the Fresnel zone with an accuracy to permanent factor is connected with the field in aperture $E(x)$ with the following relationship/ratio (Fig. 1):

$$E(r, \varphi) = \int_{-\frac{d}{2}}^{\frac{d}{2}} E(x) e^{ik \left(x \sin \varphi - \frac{x^2}{2r} \cos^2 \varphi \right)} dx. \quad (1)$$

In the case of the uniform cophasal distribution ($E(x)=1$) expression (1) after integration takes the form

$$E(r, \varphi) = \frac{i}{\cos \varphi} \sqrt{\frac{\lambda r}{2}} e^{i \frac{kr}{2} \cos^2 \varphi} \{ [C(t_2) - C(t_1)] - i [S(t_2) - S(t_1)] \}, \quad (2)$$

where $C(t)$ and $S(t)$ - Fresnel's integrals;



$$\begin{aligned}
 t_1 &= -\frac{d}{\sqrt{2\lambda r}} \cos \varphi + \\
 &+ \sqrt{\frac{2r}{\lambda}} \operatorname{tg} \varphi; \\
 t_2 &= \frac{d}{\sqrt{2\lambda r}} \cos \varphi - \\
 &- \sqrt{\frac{2r}{\lambda}} \operatorname{tg} \varphi.
 \end{aligned} \quad (3)$$

Fig. 1.

Page 27.

The means of distribution (2) depends both on the electrical length of antenna and on distance of r . In the measurements are of interest the smallest allowed values r , for which also correctly Fresnel approximation/approach. It is possible to show that this distance by approximately the order of less than the distance of the boundary of the remote zone for the antennas by length into several ten wavelengths and almost to two orders for the antennas by length into several hundred waves. Characteristic amplitude distributions of the field of large and small antennas are depicted in Fig. 2a ($r=10d$, $d=500\lambda$) and 2b ($r=3d$, $d=6.4\lambda$).

In the problem in question it is necessary to know, to what interval of the values φ it is possible to be bounded when DN will be

determined correctly in the required sector, which encompasses principal maximum and part of the near to it side lobes.

The interval of the values of angle θ is conveniently decomposed into three parts, which correspond to the illuminated region (zone of direct radiation), the region of penumbra and shadow. The most clearly indicated regions can be isolated in the field of antenna with the large electrical length.

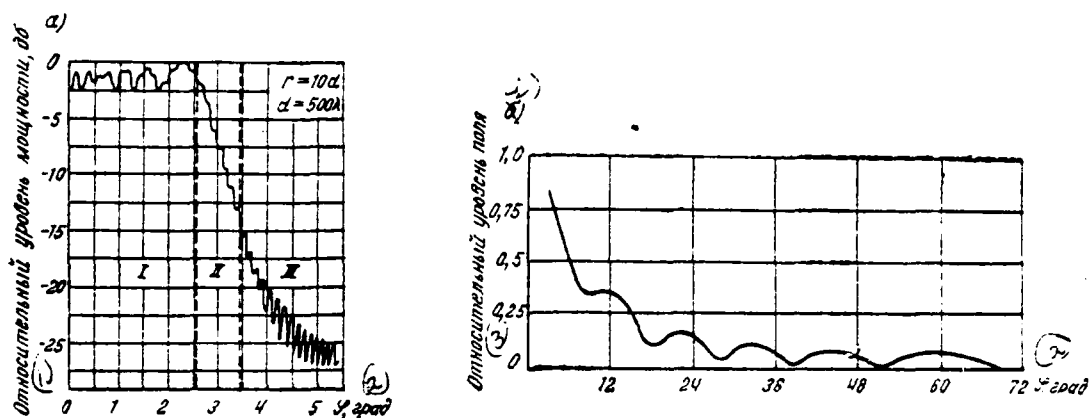


Fig. 2. Key: (1). Relative power level, dB. (2). deg. (3). Relative level of field.

Page 28.

In Fig. 2a these three regions of distribution are noted by numerals I, II, III.

We trace the structure of field in the shadow zone, for which let us determine the angular position of maximums and minimums of the lobes/lugs of field distribution (2). Let us equate with to zero derivatives on ϕ of the function, which describes the amplitude of this distribution with fixed/recorded r . The analysis of the obtained equation shows that the extreme points of field (2) are distributed on ϕ unevenly. However, using a first approximation of the asymptotic representation of Fresnel's integrals [6]

$$C(t) = \frac{1}{2} + \frac{1}{\pi} \frac{\sin \frac{\pi t^2}{2}}{t}, \quad S(t) = \frac{1}{2} - \frac{1}{\pi} \frac{\cos \frac{\pi t^2}{2}}{t}. \quad (4)$$

which correctly at sufficiently high values of t , it is possible to find that the extreme points are determined by equation

$\cos \varphi \sin \frac{2\pi}{\lambda} d \sin \varphi = 0$, whence

$$\sin \varphi = \frac{n}{2} \frac{\lambda}{d}, \quad (5)$$

where n - whole numbers.

From equality (5) it follows that the position of maximums and minimums of the lobes/lugs of field distribution in the shadow zone of Fresnel zone (it is more precise, in that part of space r, ϕ , where is correct approximation/approach (4)) the same as in the remote zone. Consequently, the trajectories of the maximums and minimums from the Fresnel zone into the remote zone are straight lines, and it means, between the adjacent side lobes the redistribution of energy is absent.

Let us rate/estimate the region of the applicability of approximation/approach (4). We will consider that remaining components/terms/addends in the asymptotic representation of Fresnel's integrals can be disregarded/neglected, if the maximum value of the first rejected term by an order is lower than the

minimum value of the sum of the remaining terms. Then minimum permissible value φ_{min} is equal to 1.5, whence we find the relationship/ratio

$$\operatorname{tg} \varphi_{min} = \frac{d}{2r} \cos \varphi_{min} = \frac{3}{2} \left] \frac{\lambda}{2r} \right. \quad (6)$$

being determining with this r the interval of values $\varphi > \varphi_{min}$, for which the correctly considered/examined approximation/approach. For the antennas with a large electrical length of $\varphi_{min} \ll 1$ and, consequently, $\varphi_{min} = \frac{d}{2r} - \frac{3}{2} \left] \frac{\lambda}{2r} \right.$ Let us note that the boundary of the region of shadow is determined by condition $\varphi_r = 1$, whence $\operatorname{tg} \varphi_r = \frac{d}{2r} \cos \varphi_r = \left] \frac{\lambda}{2r} \right.$ Comparing latter/last expression with (6), we find that approximation/approach (4) it is possible to use virtually in the entire shadow zone.

Page 29.

Using approximation/approach (4) for Fresnel's integrals, it is possible to also simplify field expression (2):

$$E(r, \varphi) = \frac{1}{\pi \cos \varphi} \left] \frac{\lambda r}{2} e^{i \frac{kr}{2} \operatorname{tg}^2 \varphi} \left[\frac{\sin \frac{\pi t_2^2}{2}}{t_2} - \frac{\sin \frac{\pi t_1^2}{2}}{t_1} \right] - i \left[\frac{\cos \frac{\pi t_2^2}{2}}{t_2} - \frac{\cos \frac{\pi t_1^2}{2}}{t_1} \right] \right. \quad (7)$$

From formula (7) at the high values \bullet it follows that

$$E(r, \varphi) = d \frac{\sin \frac{\pi d}{\lambda} \sin \varphi}{\frac{\pi d}{\lambda} \sin \varphi} \quad (8)$$

i.e. that amplitude field distribution (2) in the values θ indicated corresponds to field distribution of emitter in the remote zone.

Fig. 3 gives the graph by the envelope of distribution (2) and the envelope of lobes/lugs, calculated on the basis of approximate formula (7). It is evident that in the shadow zone both curves virtually coincide. This fact confirms the validity of the accepted during evaluation estimate θ_{min} criterion.

Thus, under condition (6) field in the Fresnel zone in the shadow zone is described by the function of form (7) and is characterized by the fact that in it there is no redistribution of the energy between the adjacent side lobes. But then this part of the field must not participate in shaping of DN in the sector of angles

$$|\theta| \leq \theta_{min}$$

Thus, value θ_{min} determined by expression (6), can be taken as the boundary of sector, measurement in which ensures correct restoration/reduction of DN in the same sector.

The given considerations by choice of the boundary of the region in which it is necessary to measure the field of antenna for the

subsequent restoration/reduction of DN, were checked by the numerical calculations of DN according to strict formulas and the method of the optical simulation of problem.

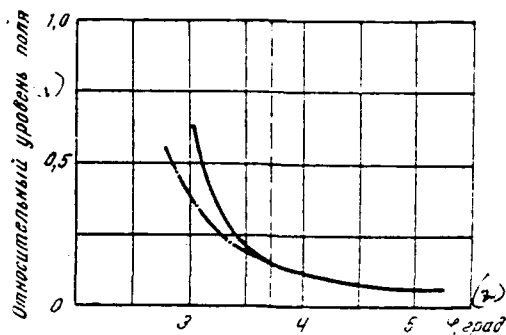


Fig. 3. Key: (1). Relative level of field. (2). deg.

Page 30.

CALCULATION METHOD AND NUMERICAL RESULTS.

By the model of antenna serves band with a width of d , gashed in the infinite flat/plane ideally conducting shield. It is known [for 7] that, solving the system of equations of Maxwell in the cylindrical coordinate system and taking into account boundary conditions on surface of shield, field at any point of space $r > d/2$ it is possible to present in the form of the series/row

$$E(r, \varphi) = \sum_{n=1}^{\infty} A_n H_n^{(2)}(kr) \cos n \varphi, \quad (9)$$

where A_n the coefficients, which depend on the function of field distribution in the aperture; $H_n^{(2)}(kr)$ the Hankel function of the second order of order n ; $k=2\pi/\lambda$ - parameter.

Applying the asymptotic representation of the Hankel function at the high values of r (at the large removal/distance from the antenna), from expression (9) we will obtain DN:

$$E(\varphi) = \int \frac{2}{\pi kr} e^{-i(kr - \frac{\pi}{4})} \sum_{n=1}^{\infty} i^n A_n \cos n \varphi. \quad (10)$$

In this problem it is examined restoration/reduction of DN for the case when on circumference $r=r_0$ in the interval of angles $[\varphi_1, \varphi_2]$ field distribution coincides with the true value, and out of this interval it is equal to zero. Line $r=r_0$, $\varphi_1 \ll \varphi \ll \varphi_2$ can be conditionally taken for the new radiating aperture and its field to record in the form

$$E_1(r, \varphi) = \sum_{n=1}^{\infty} B_n H_n^{(2)}(kr) \cos n \varphi, \quad (11)$$

where r varies from r_0 to ∞ , moreover coefficients B_n are such, that

$$E_1(r_0, \varphi) = \begin{cases} E(r_0, \varphi), & \text{если } \varphi_1 \leq \varphi \leq \varphi_2, \\ 0, & \text{если } \varphi < \varphi_1, \varphi > \varphi_2. \end{cases} \quad (12)$$

Key: (1). If.

On the basis of expressions (11) and (12) coefficients B_n it is easy to express through coefficients A_n :

$$B_n = \frac{2}{\pi H_n^{(2)}(kr_0)} \sum_{m=1}^{\infty} A_m H_m^{(2)}(kr_0) J_{nm}, \quad (13)$$

where

$$J_{nm} = \frac{1}{2} \left[\frac{\sin(n-m)\varphi}{n-m} + \frac{\sin(n+m)\varphi}{n+m} \right]_{\varphi_1}^{\varphi_2}. \quad (14)$$

Page 31.

Thus, for that obtaining as a result of reduction of DN we have the following expression:

$$E_1(\varphi) = j \frac{2}{\pi kr} e^{-j(kr - \frac{\pi}{4})} \sum_{n=1}^{\infty} i^n B_n \cos n\varphi. \quad (15)$$

where coefficients B_n are determined by formulas (13) and (14).

For calculating the field $E_1(\varphi)$ it is necessary to know coefficients A_n which on the basis of expression (11), can be calculated as the coefficients of Fourier series a precise DN. It is possible to also find them, if we consider as the given one field distribution in antenna aperture.

By the obtained formulas were calculated reduced DN, and also field distributions at different distances from the aperture. Calculation was performed with different value of the sector of angles $\phi_2 = -\phi_1 = \alpha$.

As an example in Fig. 4 are represented DN of antenna with a

length of $d=6.4\lambda$ for case of $r_0=3d$, that comprises $0.2 \frac{d^2}{\lambda}$ at values of $\alpha=20^\circ, 35^\circ, 50^\circ, 65^\circ$ and 90° , and in Fig. 2b - the amplitude characteristic of field on circumference $r_0=3d$ with the center in the middle of aperture.

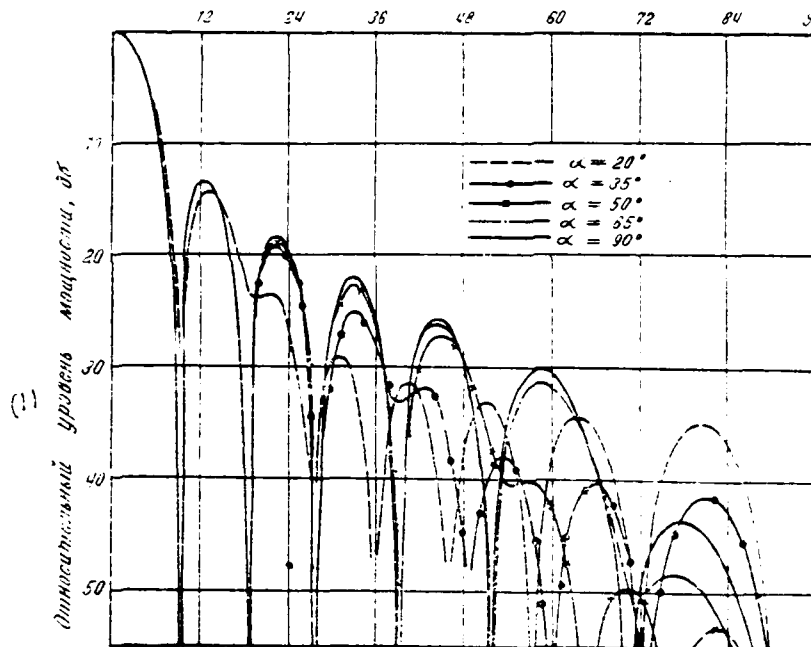


Fig. 4.

Key: (1). Relative level of power, dB.

Page 32.

The special feature/peculiarity of the field of antenna with the small electrical sizes/dimensions is the fact that already at comparatively small distances from the aperture field distribution as a whole reminds DN. In this field already it is possible to isolate a major lobe and corresponding to the size/dimension of antenna

quantity of side lobes. A fundamental difference in this field distribution (see Fig. 2b) from DN is in the significant magnitude of field in the minimums, and also in a difference in the side-lobe levels from their values in the remote zone.

For the case in question value φ_{min} , determined by expression (6), composes 22° . Calculations show that at values of $\alpha > 22^\circ$ in the reduced DN correctly are reproduced the levels and the position of the lobes/lugs, which fall into the interval $[-\alpha, \alpha]$, in which the field is assumed/set by the equal to the true field of antenna. This result confirms done above the conclusion that in the shadow zone the transformation of field from the near zone into the remote occurs in such a way that the angular redistribution of energy occurs in essence between the directions of the minimums and the adjacent side lobe.

Out of the interval $[-\alpha, \alpha]$ DN noticeably is distorted: vary levels and are displaced the directions of side lobes, appears the noticeable level of field in the minimums, appear further side lobes. The reason for such distortions consists in the fact that during the restoration/reduction is excluded from the examination that part of the field of antenna, which forms DN out of the interval $[-\alpha, \alpha]$.

The practical conclusion/output which follows from the

aforesaid, consists in the fact that for a precise restoration/reduction of DN of antenna with the small electrical sizes/dimensions in the assigned sector it is necessary to measure the field in the Fresnel zone in the same (or somewhat larger in order to completely take the latter from the measured side lobes) sector of angles.

OPTICAL SIMULATION OF PROBLEM.

For calculating restored/reduced DN and field in the Fresnel zone in the case of antenna with the large electrical length it would be possible to use formulas of the previous section. However, the number of terms of series/row, which must be in this case taken, is extremely large. In this case it proved to be convenient to use for the solution of problem the method of optical simulation.

Was assembled the diagram, depicted in Fig. 5. On the path of the luminous flux with the flat/plane wave front was placed slot 1, which played the role of the radiating aperture. At certain distance from it was placed slot 2, which cuts off the part of the light field, diffracted on the first slot.

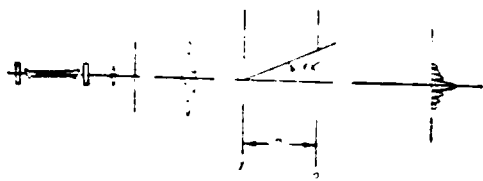


Fig. 5.

Page 33.

As a result of the transformation of field at certain distance from the second slot is formed/shaped DN. Form of this DN depends on the value of the angle 2α , at which is visible the second diaphragm from the center of the first. The measurement of field distribution was conducted with the help of the photoelectric diagram.

In the first part of the experiments was traced the structure of the field of uniform cophasal aperture in the Fresnel zone with different distances from the aperture. The second slot in this case was absent. The process of formation DN can be clearly traced in Fig. 6a, b in which are represented the photographs of field distribution in the space, beginning from the near zone. As the emitter is selected the aperture with the electrical size/dimension of $d=500\lambda$ ($\lambda=6328\text{\AA}$). In the photograph with the smaller delay (Fig. 6) is well visible the process of the formation of major lobe of DN, while in the photograph with the larger delay - process of the formation of

side lobes. On the character of a change in field distribution in proportion to removal/distance from the aperture it is possible to judge also by of the curves of Fig. 7a, b, c, d, where are represented experimentally taken/removed field distributions of aperture $d=500\lambda$ at distances of r , equal to $5d$, $20d$, $60d$, $200d$ respectively.

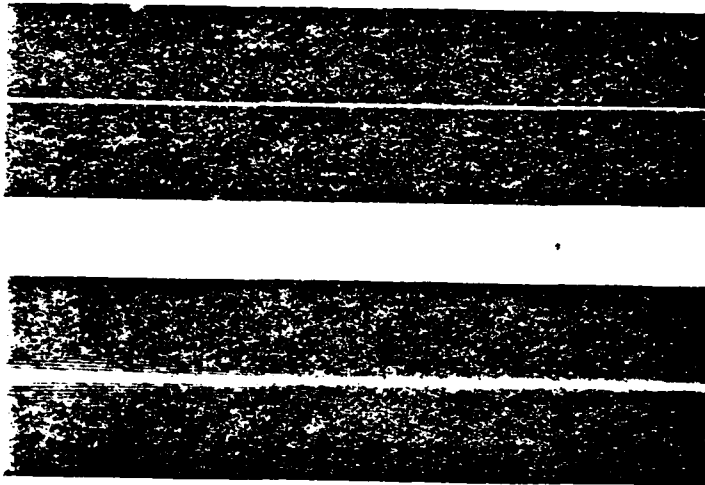


Fig. 6.

Page 34.

Analyzing the form of these curves, it is possible to note that:

- the envelope of the lobes/lugs of distribution in the shadow zone with an accuracy to permanent factor close to function $\frac{1}{\sqrt{\lambda z}}$
- in proportion to removal/distance from the aperture appear the new, adjacent to the principal maximum side lobes;
- angular dimensions of lobes/lugs in the shadow zone are approximately equal and compose value on the order of 0.114° , while

in the region of penumbra somewhat more. This tells about the fact that the trajectories of lobes/lugs in the region of penumbra yet are not straight lines;

- form of field curve at a distance of $r=200d$ reminds DN, i.e., at a distance on the order of this value field distribution completely is divided into the principal maximum and the side lobes.

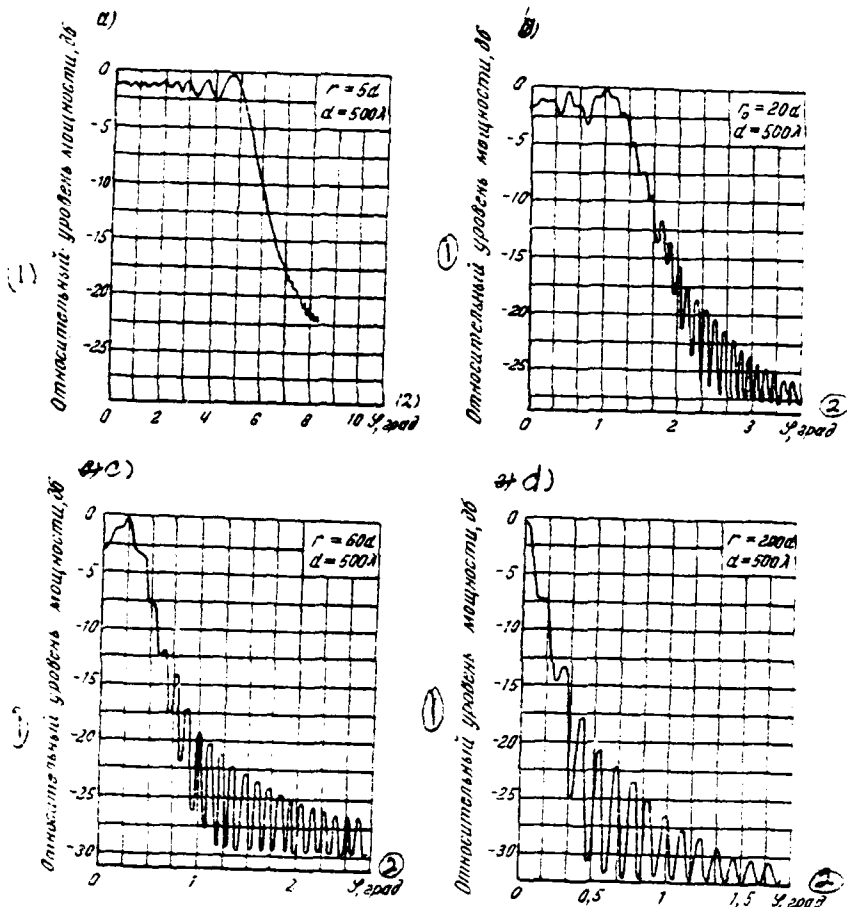


Fig. 7.

Key: (1). Relative power level, dB. (2). deg.

Page 35.

Thus, in the field of aperture first are formed/shaped distant

lobes/lugs with the large reference numbers. Then, in proportion to removal/distance from the aperture, an increasing quantity of near to the principal maximum side lobes is disengaged "pelestal", also, upon reaching of distance of $r=d^2/4\lambda$, for which on the aperture is placed one Fresnel zone, actually is drawn entire/all DN. These results coincide with the results of the numerical calculations, given in work [2].

Let us note that analogous situation for the antennas with small apertures it begins considerably earlier (see Fig. 2b), i.e., field distribution reminds DN already in the near part of the Fresnel zone, what is the corollary of different dependence from the electrical sizes/dimensions of the aperture of distances to lower boundary of Fresnel zone, and to the region where the distribution is similar on DN.

The second part of the experiments consisted in the measurement of DN in the presence of the second slot, which cuts off the part of the field in the Fresnel zone. Fig. 8a, b, c, d depicts those measured DN depending on the value of angle α for aperture $d=500\lambda$ with $r=10d$. For the comparison Fig. 8f gives a precise DN, i.e., field distribution in the output plane in the absence of the second slot. However, the distribution of the field of the initial radiating aperture in the plane of the location of the second slot is

represented in Fig. 2a. The analysis of distributions shows that, if the sector, in which is fixed/recorded the field in the Fresnel zone, exceeds value φ_{min} determined by expression (6), then DN is restored correctly in the same sector. To this case corresponds the curve, depicted on Reed. 8e, since, on the basis of expression (6), for antenna aperture with opening $d=500\lambda$ at a distance of $r=10d$ $\varphi_{min}=3^{\circ}43'$. But if in the measurements is not considered the part of the field, which is included in the region of direct radiation or penumbra, then during the restoration/reduction of DN are observed considerable changes in its form, up to the first side lobes. Of this it is possible to be convinced, analyzing the form of the curves, depicted in Fig. 8a, b, c, d. This confirms the correctness of the obtained above evaluation/estimate of the boundary of the region of measurements and it makes it possible to claim that condition (6) is not only sufficient, but also necessary.

Thus, the results of the optical simulation of problem show that for the correct determination of DN of large antennas according to the results of field measurement in the Fresnel zone it is necessary that subsequently its restoration/reduction compulsorily would participate the field, included in the sector of angles $|\varphi| < \varphi_{min}$ where φ_{min} is determined by expression (6). If it is necessary to determine DN by the sector, which exceeds φ_{min} then in the Fresnel zone it is necessary to measure the field by the sector, equal or

somewhat exceeding the given one.

Page 36.

CONCLUSION.

Thus, the analysis of the structure of field in the Fresnel zone, and also calculation and optical simulation DN make it possible to do the conclusion that for the correct restoration/reduction of field distribution to remote zone in the limits of the sector, which encompasses a principal maximum and the defined number of side lobes, is sufficient at the final distance from the aperture to measure the field in the sector whose value is not less as the interval of angles in which it is necessary to determine DN (first condition), so also the interval, determined by expression (6) (second condition).

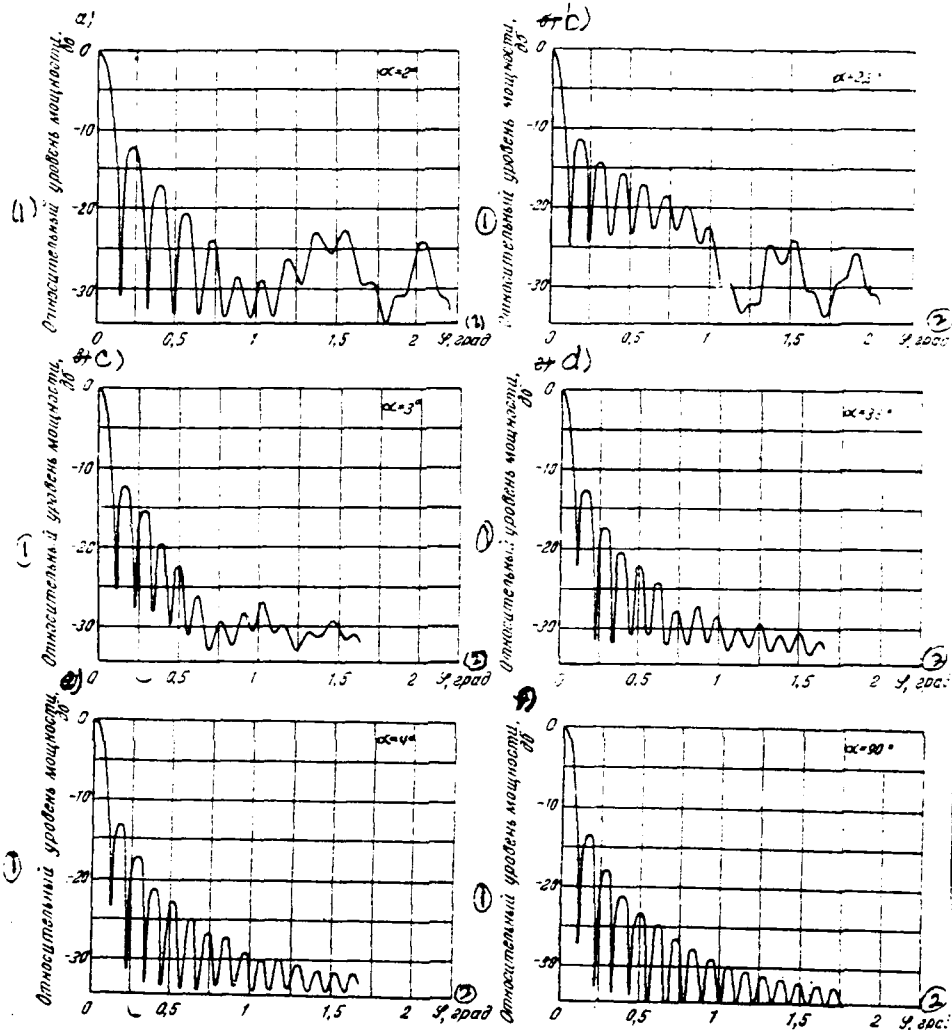


Fig. 8.

Key: (1). Relative power level, dB. (2). deg.

Page 37.

For the antennas with by the small the electrical sizes/dimensions (to 20λ) basic is the first condition, i.e., the sector of measurement must be approximately equal to the sector in which it is

necessary to determine DN. It occurs antennas with the large electrical sizes/dimensions it predominates the second condition also for determining DN necessary to measure the field in the region of direct radiation, penumbra and part of the shadow zone, determined by expression (6).

In conclusion we use the possibility to express a deep gratitude to A. A. Lemanskiy and N. I. Dmitriyeva for the consultations and the aid in conducting of calculations.

REFERENCES

1. N. A. Yesapkina. Reports of the AS USSR, 1957, 113, I, 94.
2. Blakey J. R. Near field Measurements and determination of Aerial Patterns. — «The Radio and Electronic Engineer», 28, 1964, № 5, p. 296.
3. Brown J., Jull E. V. The Prediction of Aerial Radiation Patterns from near Field measurements. — «Proc. IEE» (London), 108 B, november 1961, № 42, p. 635.
4. Martin W. W. Computation of antenna Radiation-Pattern from Near-Field measurements. — «IEEE Trans. Antennas Propagation», 15, march 1967, № 2, p. 316.
5. L. D. Bakhrakh, A. P. Kurocukin. Reports of the AS USSR, Vol. 171, 1966, No 6, page 1309.
6. A. Ango. Mathematics for the the electro- and the wireless engineers. M., "Science", 1964.
7. P. M. Morse, G. Feshbakh. The methods of theoretical physics. M., "Foreign literature", 1958.

Submitted 1/X 1970.

Page 38.

Synthesis of the linear of the antenna in the class relay functions of current distribution.

E. I. Krupitskiy, T. N. Sergeyenko.

In the work is examined the solution of the problem of the synthesis of line-source antenna in the class of the relay functions of current distribution according to the assigned real or amplitude to radiation patterns (DN).

Is used the numerical minimization of the functional of error.

Are given the results of calculations with the use of ETSVM [911BM - digital computer].

The known methods of approximate solution of the problem of the synthesis of line-source antenna lead to the continuous at the length of antenna distribution functions. In the present work is proposed the solution of the problem of the synthesis of line-source antenna in the class of disruptive-permanent distribution functions.

The synthesis of line-source antenna in this class is of interest for two reasons: first, it logically applies to the case of the antenna, which consists of the separate elements/cells with the continuous current distribution; in the second place, in a number of cases it leads to the more simply realizable current distribution.

From entire variety of the problems of the synthesis of line-source antenna, noted in work [1], in this article is examined the problem of the synthesis of line-source antenna in the class of the relay functions of current distribution according to the assigned real or assigned amplitude of DN ¹.

FOOTNOTE ¹. By relay functions it is accepted to call disruptive-permanent functions of form $I(x) = I_0 \operatorname{sign}(\psi(x)) = \pm I_0$, where $\psi(x)$ - arbitrary continuous function, and I_0 - certain constant, in particular, $I_0=1$. The class of relay functions we will further designate through Ω . ENDFOOTNOTE.

This problem has much in common with problem synthesis of the phase-keyed signals, and for its solution can be used the known asymptotic methods and the minimization of the functional of error, realized with the help of TsVM [2]. Let us note that the method, proposed in [2], is generalized to the case of the synthesis of the important class of antennas - discrete-commutation.

SYNTHESIS OF LINE-SOURCE ANTENNA IN A CLASS OF RELAY FUNCTIONS OF THE ASSIGNED REAL DAY.

The examined in this section case is of special interest for the synthesis of the line-source antenna, arranged/located perpendicular to the well conducting flat surface, in particular if necessary for swinging beam of DN.

The amplitude of current distribution along the antenna is assigned constant, and phase varies by jump on 180° , i.e., $I(x) \in \Omega$.

Page 39.

With the synthesis of this antenna unknown are only the points of the commutation of the phase of current on 180° (point of switching the relay function $I(x)$). Let us designate them through x_k . Thus, it is necessary to determine the function of current distribution $I(x) \in \Omega$ of the condition for the best approximation to given one $F_{\text{зад}}(\theta)$, where θ - angle, calculated off the normal to the axis of antenna.

Let us introduce into the examination the standard-exponential

weighed error in the approximation/approach of DN of antenna $F(\theta)$ to $F_{\text{зад}}(\theta)$:

$$\varepsilon = \left\{ \frac{2}{\pi} \int_0^{\pi/2} |F_{\text{зад}}(\theta) - F(\theta)|^p \rho(\theta) d(\theta) \right\}^{\frac{1}{p}} = \left\{ \frac{2}{\pi} J[I] \right\}^{\frac{1}{p}}, \quad (1)$$

where $p \geq 1$; $\rho(\theta)$ - positive weight function.

Weight function $\rho(\theta)$ makes it possible to redistribute the accuracy of approximation/approach to the assigned DN in different sections of gap/interval $(0, \pi/2)$ in accordance with the practical considerations.

Error ε is determined by the value of the functional

$$J[I] = \int_0^{\pi/2} |F_{\text{зад}}(\theta) - F(\theta)|^p \rho(\theta) d(\theta). \quad (2)$$

The best approximation $F(\theta)$ to $F_{\text{зад}}(\theta)$ in the space metrics $L_p[0, \frac{\pi}{2}]$ ($p \geq 1$) will be equivalent to the determination of this function $I(x) \in \Omega$, which minimizes functional (2). Let us note that in the limit in $p \rightarrow \infty$ of minimization $J[I]$ it corresponds to the best approximation in the space metrics $C[0, \pi/2]$, i.e., to the best uniform approximation.

The relay function $I(x)$, which has N of the points of switching at the length of antenna, with an accuracy to sign is determined by N by parameters x_k .

Functional (2) always can be represented in the form

$$J[I(x)] = \Phi(x_1, x_2, \dots, x_N) = \Phi(\bar{x}_N). \quad (3)$$

where $\Phi(\bar{x}_N)$ - certain continuous function N of variable/alternating x_k , \bar{x}_N - n -dimensional vector with components x_k .

Thus, for each N problem is reduced to the determination of the minimum of the function of many variable/alternating. This problem can be solved by ETSVM with the help of the detailed at present multistage methods of the search of the extrema of the functions of many variable/alternating [2, 3]. In this case it is necessary to consider that these methods make it possible to find the local minimum of functional (3), in connection with which finding the zero approximation, close to the global minimum of error, it is independent and important problem.

Page 40.

It must be noted that in this case it is feasible and another method of the minimization of functional (2), based on the solution of special nonlinear integral equation [2]. In the specific example of synthesis, given below, is used only first method.

DN of the antenna, arranged/located vertically above the ideally conducting plane, is described by the function

$$F(\theta, \theta_0) = \int_{h_1}^{h_2} \left\{ \begin{array}{l} \cos \left[\frac{2\pi}{\lambda} x \sin \theta \right] \\ \sin \left[\frac{2\pi}{\lambda} x \sin \theta \right] \end{array} \right\} I(x, \theta_0) dx = A[I(x)], \quad (4)$$

where h_1 and h_2 - distances of the lower and upper ends/leads of the antenna from the conducting surface;

θ_0 - angle at which is oriented principal maximum DN of antenna in the case of oscillation.

The selection of cosine or sine in the curly braces is determined by the polarization of currents (by longitudinal or transverse respectively).

As is shown the given below example of synthesis, the use of relay functions of current distribution makes it possible to effectively control the sharp/acute DN of similar antennas by changing the coordinates of the points of switching these functions.

As an example was examined the case of the synthesis of antenna with DN of the following form:

$$F_{\text{max}}(\theta, \theta_0) = \frac{\sin \left[\frac{2\pi}{\lambda} h (\sin \theta - \sin \theta_0) \right]}{\frac{2\pi}{\lambda} h (\sin \theta - \sin \theta_0)}, \quad (5)$$

where θ_0 - required angle of deflection of principal maximum DN;

h - height of antenna ($h_1=0$; $h_2=h$).

Was examined line-source antenna with the longitudinal and cross polarization by length 5λ . The angle of deflection of fundamental ray/beam of DN θ_0 was changed from 10° to 70° .

Problem was solved for the case of the root-mean-square criterion of approximation/approach ($p=2$) DN of line-source antenna (4) to the assigned DN of form (5) on the assumption that weight function $\rho(\theta)=1$.

For the determination of the zero approximation of the coordinates of the points of the commutation of the distribution function it is expedient to use the continuous current distribution, which corresponds to the accurately realizable DN of the form

$$F(\theta, \theta_0) = \frac{\sin \left[\frac{2\pi}{\lambda} h (\sin \theta - \sin \theta_0) \right]}{\frac{2\pi}{\lambda} h (\sin \theta - \sin \theta_0)} = \frac{\sin \left[\frac{2\pi}{\lambda} (\sin \theta - \sin \theta_0) \right]}{\frac{2\pi}{\lambda} h (\sin \theta - \sin \theta_0)}, \quad (6)$$

where plus sign corresponds to longitudinal, and minus - cross polarization.

Page 41.

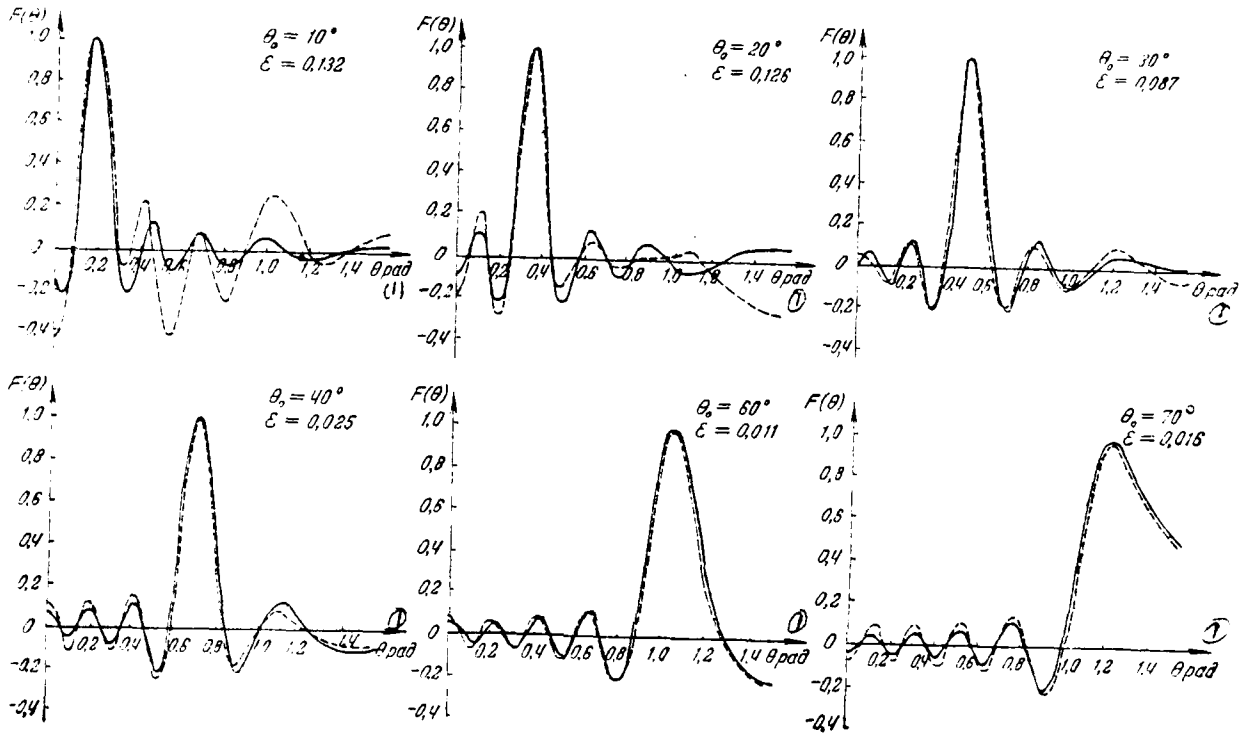


Fig. 1.

Key: (1). rad.

Page 42.

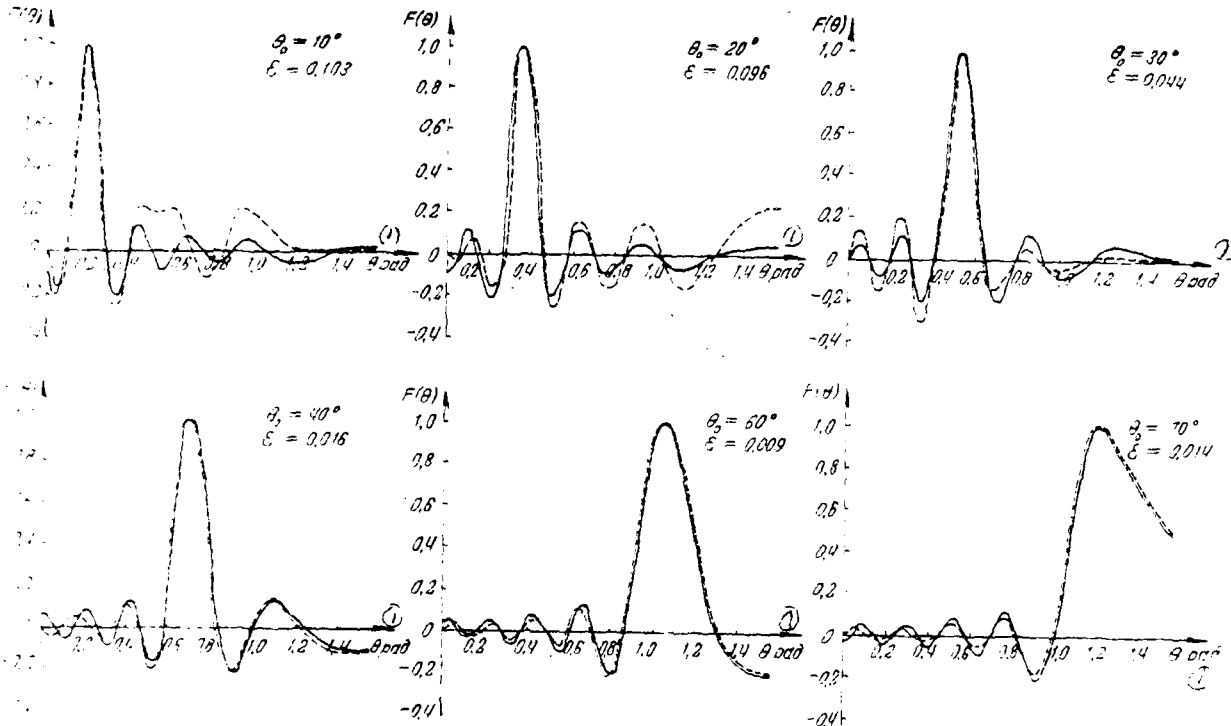


Fig. 2.

Key: (1). rad.

Page 43.

DN of form (6) under condition $\frac{2\pi}{\lambda} h \sin \theta_0 \gg 1$ very close to the assigned DN (5). It is not difficult to see that DN (6) will correspond the current distribution according to the law

$$I(x, \theta_0) = \begin{pmatrix} \cos \left[\frac{2\pi}{\lambda} x \sin \theta_0 \right] \\ \sin \left[\frac{2\pi}{\lambda} x \sin \theta_0 \right] \end{pmatrix} \quad (7)$$

where the upper expression corresponds to longitudinal, and lower - cross polarization.

As the zero approximation for the points of the commutation of the relay function of current distribution were undertaken zero functions (7).

Those obtained as a result of calculation on ISVM DN are depicted on Fig. 1 (dotted line) for the longitudinal polarization and ^{on Fig.} 2 for the cross polarization.

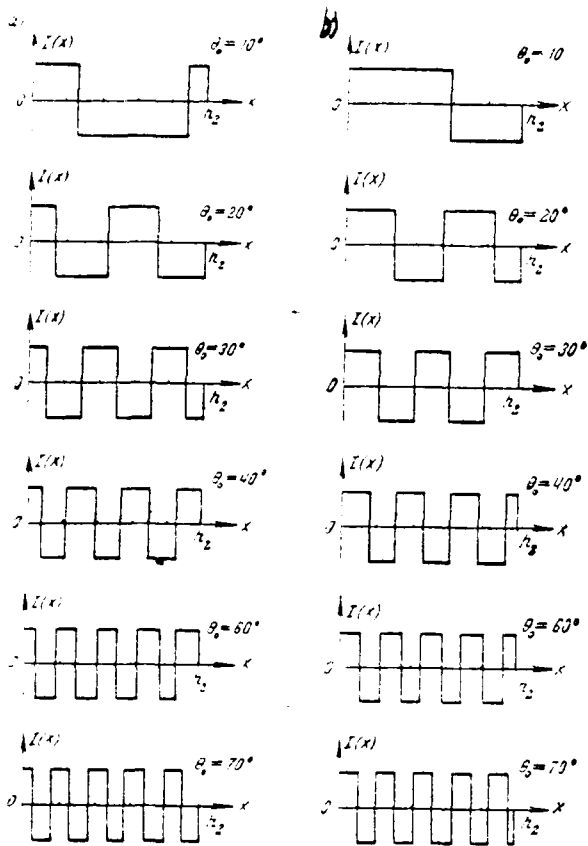


Fig. 3.

AD-A090 523

FOREIGN TECHNOLOGY DIV WRIGHT-PATTERSON AFB OH
ANTENNAS (U)

F/G 9/5

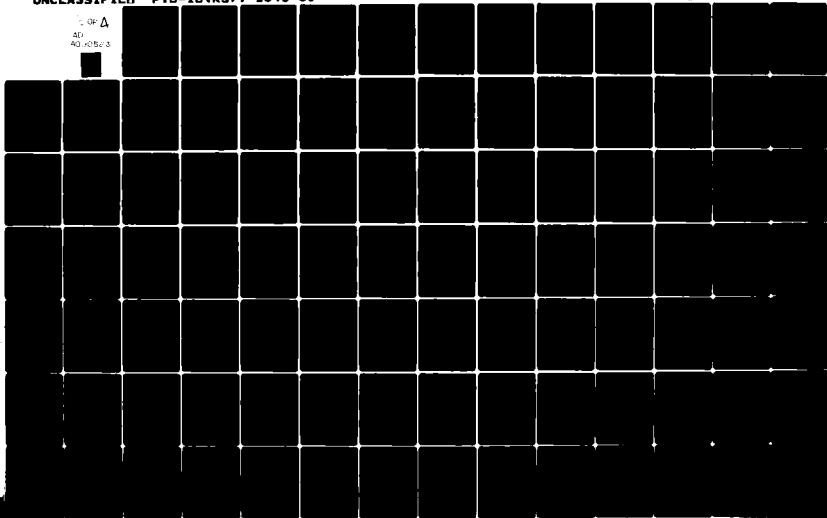
SEP 80

UNCLASSIFIED

FTD-ID(RS)T-1340-80

NL

1 OF 1
AD
AD A090 523



Page 44.

The given DN are depicted as solid line. It should be noted that root-mean-square error of approximation/approach ϵ to by the assigned DN does not exceed 0.132. For the large angles of deflection (more than 40°) coincidence with the assigned DN sufficiently good.

Fig. 3 gives the character of a change in the current distribution along the antenna at different angles of oscillation DN (a - longitudinal polarization, b - transverse). With an increase in the angle θ_0 , grows a number of commutations of the phase of current at the permanent length of antenna.

SYNTHESIS OF ANTENNA IN A CLASS OF RELAY FUNCTIONS OF THE ASSIGNED MODULUS/MODULE COMPOSITE DN.

Let us assume that it is assigned on the modulus/module the composite DN $F(u)$, and current distribution is sought in the class Ω . In this case appears the need of solving the nonlinear integral equation of the following form:

$$|F(u)|^2 = \int_{-L}^L \int_{-L}^L I(x) I^*(x') e^{i m u (x-x')} dx dx'; \quad u = \sin \theta; \quad m = \frac{2\pi}{\lambda}. \quad (8)$$

where $I^*(x')$ - the complex conjugate current distribution.

For further synthesis more expediently to pass in to another equation which is obtained by the Fourier transform of left and of right sides (8):

$$\begin{aligned} \int_{-\infty}^{\infty} |F(u)|^2 e^{-imuy} du &= \int_{-L}^L \int_{-L}^L \int_{-\infty}^{\infty} I(x) I^*(x') e^{im(u-x-x')} du dx' dx = \\ &= \frac{1}{m} \int_{-L}^L I(x) I^*(x-y) dx. \end{aligned} \quad (9)$$

Introducing the designation

$$R(y) = \int_{-\infty}^{\infty} |F(u)|^2 e^{-imuy} du, \quad (10)$$

we come to the equation

$$R(y) = \frac{1}{m} \int_{-L}^L I(x) I^*(x-y) dx; \quad y \in (-\infty, \infty), \quad (11)$$

where $I(x) \equiv 0$ with $|x| > L$.

It is important to note that function $R(y)$ is completely determined by the assigned modulus/module composite DN. Function $R(y)$ it is possible to call the autocorrelation function of current distribution.

If $I(x) \in \Omega$, then function $R(y)$ will be real, and then we come to the equation

$$R(y) = \frac{1}{m} \int_{-L}^L I(x) I(x-y) dx; \quad y \in (-\infty, \infty), \quad (12)$$

where all entering functions real and $I(x) = 0$ when $|x| > L$. In this case, the connection/communication of autocorrelation function with DN will be determined by the relationship/ratio

$$R(y) = 2 \int_0^{\infty} F(u)^2 \cos(mu y) du, \quad (13)$$

which is obtained taking into account the parity of modulus/module DN $F(u)$. The parity of function $|F(u)|$ follows from that fact that with $\text{Im} [I(x)] = 0$ $F(-u) = F^*(u)$.

Equation (12) is analogous with the equation of the synthesis of the phase-keyed (PM) signal for the assigned autocorrelation function. In connection with this for its solution also can be used the apparatus, proposed in [2].

For the purpose of simplification in the use of an apparatus of synthesis of PM signals according to the assigned autocorrelation function let us change the beginning of reading of coordinate x along the antenna so that the expression DN would take the form

$$F(u) = \int_0^{2L} e^{imx} I(x') dx'. \quad (14)$$

Let be assigned DN $|F_{3a2}(u)|$ in segment $[-1,1]$, which corresponds to the region of real angles $\theta \left(-\frac{\pi}{2} \leq \theta \leq \frac{\pi}{2}\right)$. Let us continue it into the region of the imaginary angles, as usually this is done with the synthesis of relatively long antennas (with $2L/\lambda \approx 5-10$) [4], assuming that $|F_{3a2}(u)| = 0$ when $|u| > 1$.

Then for determining the assigned autocorrelation function we will have a relationship/ratio

$$R_{3a2}(y) = 2 \int_0^1 |F_{3a2}(u)|^2 \cos(muy) du. \quad (15)$$

The problem of synthesis is reduced to the determination of function $I(x') \in \Omega$, which ensures approximation/approach $R_{3a2}(y)$ with real nonlinear operator (12).

Page 46.

For the realization of approximation/approach $R(y)$ to $R_{3a2}(y)$ it is expedient to normalize these functions to unity. Since maximum value of functions always corresponds $y=0$, and to $I(x') = \pm 1$, then one should take

$$R(y) = \frac{1}{2L} \int_0^{2L} I(x') I(x'-y) dx' \quad (16)$$

and

$$R_{3a2}(y) = \frac{1}{A} \int_0^1 |F_{3a2}(u)|^2 \cos(muy) du. \quad (17)$$

where

$$A = \int_0^1 |F_{\text{max}}(u)|^2 du. \quad (18)$$

Functional of the error, the subject of minimization, by the force of parity $R(y)$ takes the form

$$J[I] = \int_0^{2L} |R_{\text{max}}(y) - R(y)|^p \rho(y) dy, \quad (19)$$

where $\rho(y)$ - non-negative weight function.

Since as the final result us interests the approximation/approach to function $|F_{\text{max}}(u)|$, then arises the question: does ensure the minimization of functional (19) best approximation of DN $|F(u)|$ to assigned DN $|F_{\text{max}}(u)|$ in the appropriate space.

Most simply response/answer to this question succeeds in obtaining in the case of $p=2$ and $\rho(y)=1$.

Actually/really, let the assigned DN be calibrated so that

$$2 \int_0^{\infty} |F_{\text{max}}(u)|^2 du = 1,$$

then

$$R_{\text{max}}(y) - R(y) = 2 \int_0^{\infty} \{ |F_{\text{max}}(u)|^2 - |F(u)|^2 \} \cos(muy) du. \quad (20)$$

Using Parseval equality for the functions, converted according to Fourier theorem, we will obtain

$$\int_0^{\infty} |R_{\text{max}}(y) - R(y)|^2 dy = \frac{1}{m} \int_0^{\infty} \{ |F_{\text{max}}(u)|^2 - |F(u)|^2 \}^2 du. \quad (21)$$

Taking into account that $R(y) \equiv 0$ with $y > 2L$ and (21), we have

$$\begin{aligned}
 J[I] &= \int_0^{2L} [R_{322}(y) - R(y)]^2 dy = \frac{1}{m} \int_0^{\infty} \{ |F_{322}(u)|^2 - |F(u)|^2 \}^2 du - \\
 &- \int_{2L}^{\infty} R_{322}^2(y) dy = \frac{1}{m} \int_0^1 \{ |F_{322}(u)|^2 - |F(u)|^2 \}^2 du + \\
 &+ \frac{1}{m} \int_1^{\infty} |F(u)|^4 du - \int_{2L}^{\infty} R_{322}^2(y) dy. \quad (22)
 \end{aligned}$$

Second term in expression (22) determines the reactance of antenna, since it corresponds to the integration for the region of imaginary angles θ .

Page 47.

Latter/last composed with the assigned DN always can be computed its value it limits the rms error for the approximation/approach of DN of antenna to the given one, which with a small reactance of antenna cannot be less than this value.

Expression (22) shows that the minimization of functional $J[I]$ does not guarantee the simultaneous minimization of an error in the approximation/approach of this function of DN of antenna $|F(u)|$: it is minimized the sum of "error" and of "reactance". In spite of the deficiency/lack in this method of the synthesis of line-source

antenna indicated, it is remarkable fact that it does not require the assignment to phase DN and makes it possible to use only with the real functions.

According to the obtained current distribution amplitude of DN it can be calculated according to the formula

$$|F(u)| = \left\{ \left[\int_0^{2L} I(x') \cos(\mu x') dx' \right]^2 + \left[\int_0^{2L} I(x') \sin(\mu x') dx' \right]^2 \right\}^{1/2}. \quad (23)$$

which can be given also to another equivalent form.

Let us designate the points of the commutation through x'_k ($k=1, 2, \dots, N-1$), and the coordinates of the ends/leads of the antenna through $x'_0=0$ and $x'_N=2L$. Then, calculating integral composite DN (14) according to the sections, we obtain

$$F(u) = \pm \sum_{k=0}^{N-1} (-1)^k \int_{x'_k}^{x'_{k+1}} e^{i\mu x'} dx' = \pm \frac{1}{i\mu} \sum_{k=0}^N C_k e^{i\mu x'_k}, \quad (24)$$

where

$$C_k = 2(-1)^{k+1}, \quad C_0 = 1, \quad C_N = (-1)^{N+1} \\ (k=1, 2, \dots, N-1).$$

The sign before the sum must coincide with the sign of function $I(x')$ in the first section $[x'_0, x'_1]$. From (24) it follows that the amplitude of DN

$$|F(u)| = \frac{1}{|\mu|} \left[a_0 + 2 \sum_{k=1}^N a_k \cos(\mu x'_k) \right]^{1/2}, \quad (25)$$

where

$$a_k = \sum_{n=0}^{N-k} C_n C_{n-k}; \quad k=0, 1, 2, \dots, N.$$

Expression for $|F(0)|$ to more simply obtain directly from formula (24), assuming in it $u=0$. Then

$$|F(0)| = \left| \sum_{k=0}^{N-1} (-1)^k (x'_{k-1} - x'_k) \right| \quad (26)$$

Formulas (25) and (26) are completely equivalent (23).

Page 48.

It should be noted that this method of synthesis can be easily propagated to that case when amplitude current distribution according to the antenna is fixed/recorded, but it differs from uniform. In this case, naturally, function $I(x)$ will not belong to the class of relay ones. However, it is possible to represent in the form

$$I(x') = q(x') I_p(x'), \quad x' \in [0, 2L], \quad (27)$$

where $q(x')$ - assigned amplitude distribution of current;

$I_p(x')$ - unknown relay function, determined by the points of the commutation of the phase of current on 180° .

The methodology of the solution of the problem of synthesis remains previous with the only difference that the instead of formula (16) function $R(y)$ must be assigned by the expression

$$R(y) = \frac{\int_0^{2L} q(x') q(x' - y) I_p(x') I_p(x' - y) dx'}{\int_0^{2L} q^2(x') dx'} \quad (28)$$

The use of relay or quasi-relay ($I = qI_p$) functions of current

distribution is of fundamental interest from the point of view of the expansion of DN of long antennas. In this case this method is simple during the practical realization and allows/assumes the use of programmed control. Using this method in the antennas with electrical beam swinging, it is possible operationally to pass from the mode/conditions of the "consecutive" survey/coverage of space by the narrow scanning beam to the mode/conditions of "parallel" survey/coverage by wide motionless ray/beam; in this case for the creation of relay current distribution it is possible to use the same control units of the phase of the oscillations/vibrations which serve for the oscillation of narrow beam.

In conclusion let us present some examples of the synthesis of line-source antennas by method examined above on the assumption that weight function $\rho(y)=1$ and $p=2$.

Example 1. As the assigned DN let us take sector, i.e.,

$$F_{321}(u) = \begin{cases} 1; & u < u_0, \\ 0; & u > u_0. \end{cases} \quad (29)$$

Then

$$R_{321}(y) = \frac{\sin\left(\frac{2\pi}{\lambda} u_0 y\right)}{\frac{2\pi}{\lambda} u_0 y}; \quad 0 < y < 2L. \quad (30)$$

The zero approximation for distributing the points of commutation x_k of function $I(x)$, which corresponds to expression (30), let us determine with the help of the formula

$$\frac{x_k}{2L} = \sqrt{\frac{2k - \frac{1}{2}}{\gamma}}; \quad k = 1, 2, \dots, \quad (31)$$

where γ - certain coefficient, analogous to contraction coefficient of FM signal.

In work [5] the fixed points of the commutation of phase and the autocorrelation function of signal of the formulas, similar (31) and (30).

Coefficient γ in the example in question is determined through the length of antenna $2L$ and the width of DN u_0 as follows:

$$\gamma = \frac{2u_0 2L}{\lambda}. \quad (32)$$

The longer the antenna, the greater the coefficient γ and the better will be the approximation/approach $R(\gamma)$ to function $R_{\text{opt}}(\gamma)$.

For an example were examined the antennas by length 10λ and 50λ with the width of sector $u_0=0.5$. For these parameters the coefficient γ is equal to 10 and 50, and the function of current has 5 and 25 points of commutation at the length of antenna respectively (Fig. 4). In Fig. 4 dotted line showed current distribution in the zero approximation.

According to the obtained current distribution it was calculated the DN of antenna, represented in Fig. 5 by solid line for $2L=50\lambda$ and the dot-dash for $2L=10\lambda$. The assigned DN is depicted as dotted line.

The calculations conducted show that the obtained current distribution differs significantly from the zero approximation, which corresponds to asymptotic formula (31) only for the antenna of small length. It is obvious that in this case the described above method is effective.

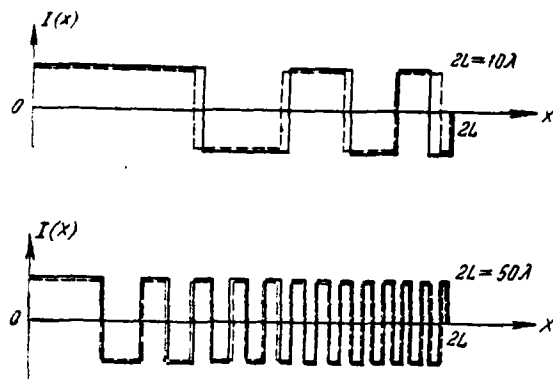


Fig. 4.

Page 50.

For the large ones γ , which corresponds to the antennas of large length, the minimization of the functional of the error for noticeable improvements does not give, proves to be sufficient the use of the asymptotic solutions.

Example 2.

DN is assigned in the form of the function

$$|F_{\text{зад}}(u)| = \left| \frac{\sin\left(\frac{2\pi}{\lambda} 2L_1 u\right)}{\frac{2\pi}{\lambda} 2L_1 u} \right|, \quad (33)$$

where $2L_1$ - length of the equivalent cophasal line-source antenna, which has the wide DN (this value can be much less than the length of

the synthesized antenna).

Problem lies in the fact that the same DN to obtain with the help of the long line-source antenna due to an alternation in the significance in the current distribution $I(x)$.

Corresponding autocorrelation function of the current

$$R_{\text{aut}}(y) = \begin{cases} \frac{-y}{4L_1} + 1; & 0 < y < 2L_1, \\ 0; & 2L_1 < y < 2L. \end{cases} \quad (34)$$

Zero approximation for distributing the points of commutation $I(x)$ is located through formula (31), where the coefficient

$$\gamma = \frac{L}{2L_1}. \quad (35)$$

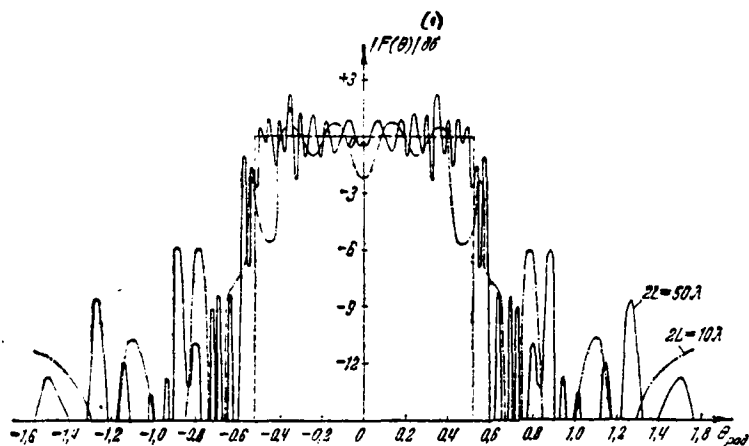


Fig. 5.

Key: (1). dv.

Page 51.

As an example were taken antennas of length 10λ and 50λ . It was necessary with the help of these antennas to obtain DN, which corresponds to half-wave dipole, i.e., $2L_1 = \lambda/2$.

Fig. 6 depicts the assigned DN for the half-wave dipole (dotted line), and those also obtained as a result of calculations DN of line-source antennas as length 10λ (dot-dash line) and 50λ (solid line) during the corresponding current distribution $I(x)$, shown in Fig. 7 (zero approximation is shown by dotted line).

From Fig. 6 it is evident that the character of a change of DN in the line-source antennas with variable distribution corresponds to DN of half-wave dipole. Due to variable current distribution $I(x)$ occurs considerable expansion of DN. For the antenna by length 10λ the expansion of DN occurs 20 times, and at the length $50\lambda - 100$ times.

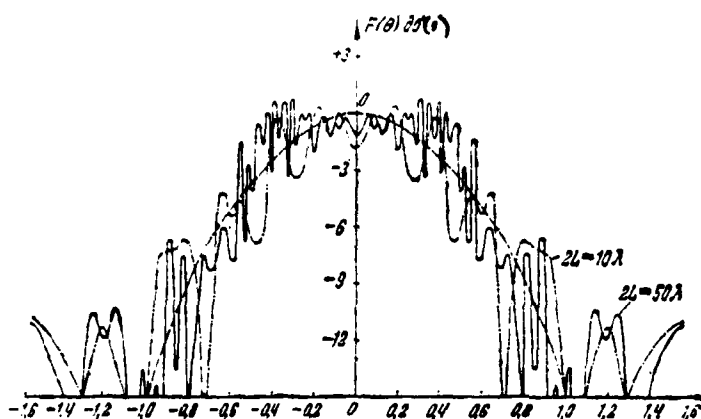


Fig. 6.

Key: (1) . dB.

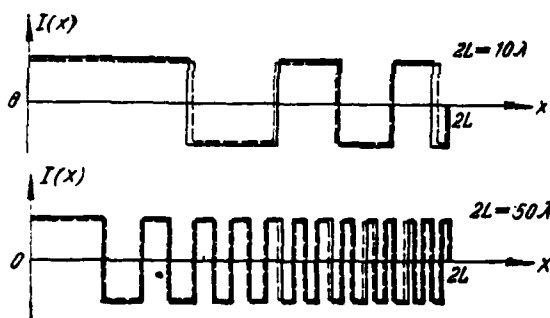


Fig. 7.

Page 52.

CONCLUSION.

Work examines the problem of the synthesis of line-source

antennas in the class of the relay functions of current distribution according to the assigned real or amplitude of DN. The given in the work examples of calculations confirm the possibility of obtaining the given DN during the phase control of current distribution along the antenna. In this case, in the case of antennas with the large extent, sufficiently effective prove to be the asymptotic methods of obtaining the corresponding current distribution. The minimization of the functional of error proposed it is desirable to use for the short antennas where it makes it possible to make more precise the found with asymptotic method current distribution.

The results of work can be useful from the point of view of the construction of the antennas, arranged/located above the well conducting flat surface, and also the expansion of the possibilities of long antennas with the phase control of DN.

REFERENCES

1. L. D. Bakhrakh, V. I. Troitsky. Mixed problems of the synthesis of antennas. - "radio engineering and electronics", Vol. 12, 1967, No 3, 473.
2. E. I. Krupitskiy, T. N. Sergeyenko. Problem of the minimization of the functional of the error in the class of relay functions and its

application/appendix to the synthesis of FM signals and line-source antennas. - "radio engineering and electronics", Vol. 15, 1970, No 2.-/

3. B. T. Polyak. Minimizatioms of the function of many variable/alternating. - "economy and mathematical methods", 1967, No 6.

4. Ye. G. Zelkin. Construction of radiating system according to the assigned radiation pattern. M., Gosenergoizdat, 1963.

5. D. Ye. Vakman. Regular method of synthesis of FM signals. M., "Soviet radio", 1967.

Submitted 6/VII 1970; after treatment/processing - 16/VIII 1971.

Page 53.

Synthesis of arc and spherical antenna arrays.

L. I. Ponomarev, I. S. Yuspraykh.

Are given the algorithms of the solution of the problem of the synthesis of convex antenna arrays by the assigned vector radiation

pattern in space L^2 with the use of an apparatus of vector eigenfunctions to the concrete/specific/actual relationships/ratios of synthesis for the arc and spherical gratings.

Are analyzed the results of the numerical calculations of the synthesis of arc antenna array from the longitudinal slots, arranged/located on the surface of the ideally conducting cylinder, for the wide interval of the values of an electrical radius of cylinder, step/pitch between the emitters and the angular dimension of grating.

In the work is examined one of the possible methods of the solution of the problem of the synthesis of antenna arrays by the assigned vector radiation pattern $\bar{F}_{\text{зад}}(\theta, \varphi)$ with the use of an apparatus of its own vector functions. Moreover best approximation to $\bar{F}_{\text{зад}}(\theta, \varphi)$ is sought in space L^2 .

The method in question can be used for the synthesis of the antenna arrays of arbitrary form the radiation field of which can be presented in the form of the set of its own waves. There is special interest in the use/application of this method for the synthesis of convex antenna arrays (arc, circular, spherical), because the known methods of the synthesis of linear antenna arrays with the synthesis of convex gratings do not always prove to be effective.

FORMULATION OF THE PROBLEM.

Let us designate through $\bar{F}(\theta, \phi)$ the radiation pattern of the synthesized antenna array in the remote zone. Then the condition for the best root-mean-square approximation $\bar{F}(\theta, \phi)$ to the assigned radiation pattern $\bar{F}_{\text{зад}}(\theta, \phi)$ will be the achievement of the minimum of the expression

$$\int_{S_1} |\bar{F}(\theta, \phi) - \bar{F}_{\text{зад}}(\theta, \phi)|^2 ds. \quad (1)$$

where S_1 - spherical surface of a single radius.

Let us present $\bar{F}(\theta, \phi)$ and $\bar{F}_{\text{зад}}(\theta, \phi)$ in the form of series/row along the system of its own orthonormalized on S_1 vector functions $\bar{f}_m(\theta, \phi)$:

$$\bar{F}(\theta, \phi) = \sum_m C_m \bar{f}_m(\theta, \phi); \quad \bar{F}_{\text{зад}}(\theta, \phi) = \sum_m A_m \bar{f}_m(\theta, \phi). \quad (2)$$

where composite coefficients $A_m = A'_m + iA''_m$ are calculated from the formula

$$A_m = \int_{S_1} (\bar{F}_{\text{зад}}, \bar{f}_m) ds. \quad (3)$$

but coefficients C_m are determined through the composite amplitudes of currents in radiators of array and can be recorded in the form

$$C_m = \sum_{j=1}^N dm_j J_j - d_{m0}. \quad (4)$$

where $I_j = I_j + iI_j'$ - composite amplitude of current in the j emitter; N - is determined by a number of radiators in the array; $d_{mj} = d'_{mj} + i d''_{mj}$ - some coefficients, which depend on the type of grating and on the conditions for the standardization of radiation pattern.

$$\int_{S_1} \vec{T}_m \cdot \vec{T}_n^* ds = \delta_{mn}$$

FOOTNOTE 1. The condition of orthonormalization takes form \wedge where δ_{mn} - Kronecker's -symbol, and expression $(\vec{T}_m \cdot \vec{T}_n^*)$ designates scalar product \vec{T}_m and \vec{T}_n^* . asterisk indicates the sign of composite coupling. ENDFOOTNOTE.

FOOTNOTE 2. If on $\vec{F}(\theta, \varphi)$ it is superimposed no limitations, then in expression (4) coefficients $d_{m0} = 0$ and N are equal to a number of emitters K . During the imposition on $\vec{F}(\theta, \varphi)$ of the condition for the standardization of form $\vec{F}(\theta, \varphi_0) = \vec{i}_0$, where \vec{i}_0 - certain single transverse unit vector, coefficients $d_{m0} \neq 0$, and N in general early $(K-2)$. ENDFOOTNOTE.

Substituting expansion (2) into formula (1), we will obtain

$$\int_{S_1} |\vec{F}(\theta, \varphi) - \vec{F}_{\text{std}}(\theta, \varphi)|^2 ds = \int_{S_1} \left| \sum_m (C_m - A_m) \vec{F}_m(\theta, \varphi) \right|^2 ds. \quad (5)$$

In expression (5) coefficients A_m are not depended between

themselves, whereas coefficients C_m are connected with each other by means of relationship/ratio (4) and cannot be selected arbitrarily. Therefore the solution of the problem of the synthesis of the antenna arrays mathematically is reduced to the determination of the minimum of expression (5) under condition (4).

Before passing to the solution of this problem, let us note that, after excluding the possibility of obtaining superdirectional solutions, expansion (2) for $\bar{F}(\theta, \varphi)$ into S_1 to any degree of accuracy it is possible to approximate by the final sum of the form

$$\bar{F}(\theta, \varphi) = \sum_{m=0}^M C_m \bar{f}_m(\theta, \varphi). \quad (6)$$

where a number of members of sum M depends on the electrical size/dimension of antenna. So it is known [1], for the cylindrical antenna arrays of radius a with $M=2\kappa a$ ($\kappa = \frac{2\pi}{\lambda}$ — wave number) the accuracy of this approximation at each point proves to be not worse than 20/o.

Page 55.

Let us compare value N , connected with a number of emitters in the grating, with value M . If $M \ll N$, then relationship/ratio (4) is not limiting when selecting of coefficients C_m i.e. in this case they can be selected independently of each other and the minimum of

expression (5) is reached at the condition

$$C_m = A_m; \quad m \leq M. \quad (7)$$

Condition $M \leq N$ corresponds to the case of a large quantity of emitters in the grating when the distance between two adjacent emitters proves to be less $\lambda/2$ and according to its results this case is close to the case of continuous current distribution in the antenna.

In practice in the antenna arrays usually the distance between two adjacent emitters is more or equal to $\lambda/2$, which corresponds to condition $M > N$. In this case coefficients C_m no longer can be selected independently and it is necessary to solve problem of the best root-mean-square approximation $\bar{F}(\theta, \phi)$ to $\bar{F}_{3a2}(\theta, \phi)$ under condition (4).

About the best root-mean-square approximation $\bar{F}(\theta, \phi)$ to $\bar{F}_{3a2}(\theta, \phi)$

Let us consider a question the best root-mean-square approximation $\bar{F}(\theta, \phi)$ to $\bar{F}_{3a2}(\theta, \phi)$ under condition (4). For this purpose, after substituting (6) in (1), let us make simple conversions. As a result we will obtain

$$\int_{S_1} |\bar{F}(\theta, \phi) - \bar{F}_{3a2}(\theta, \phi)|^2 ds = \int_{S_1} |\bar{F}_{3a2}(\theta, \phi)|^2 ds + \sum_{m=0}^M |A_m - C_m|^2 - \sum_{m=0}^M |A_m|^2 \quad (8)$$

As it follows from expression (8), for the minimization of integral (1) it suffices to minimize the sum

$$\Delta^2 = \sum_{m=0}^M |A_m - C_m|^2. \quad (9)$$

Substituting in (9) the values of coefficients C_m from condition (4), we will obtain

$$\Delta^2 = \sum_{m=0}^M \left| A_m - \sum_{j=1}^N d_{mj} J_j - d_{m0} \right|^2. \quad (10)$$

In relationship/ratio (10) the composite amplitudes of currents J_j of already independent variables, and therefore the necessary condition of achieving the minimum of value Δ^2 is the equality to zero of partial derivatives of Δ^2 on real and imaginary part J_j ($j=1, 2, \dots, N$). As a result we will obtain the system $2N$ of linear equations from which it is possible to determine values J_j' and J_j'' , and then from (4) and values of coefficients C_m ensuring the minimum of integral (1).

Page 56.

Let us note that the equality of zero first-order particular derivatives determines only the necessary condition of extremum Δ^2 , however, since the second particular derivatives of Δ^2 , in this case are positive, then this extremum is the minimum.

Lowering intermediate linings/calculations, let us give the final type of system for determination J_j and J_{j+1} ensuring the best root-mean-square approximation $\bar{F}(\theta, \phi)$ to $\bar{F}_{\text{зад}}(\theta, \varphi)$ under condition

(4):

$$\begin{bmatrix} \beta_{ij}^{\prime} & -\beta_{ij}^{\prime\prime} \\ \beta_{ij}^{\prime\prime} & \beta_{ij}^{\prime} \end{bmatrix} \begin{bmatrix} J_j^{\prime} \\ J_j^{\prime\prime} \end{bmatrix} - \begin{bmatrix} Y_i^{\prime} \\ Y_i^{\prime\prime} \end{bmatrix} = 0. \quad (11)$$

where

$$\left. \begin{aligned} \beta_{ij}^{\prime} &= \sum_{m=0}^M (d'_{mi} d'_{mj} - d''_{mi} d''_{mj}), \\ \beta_{ij}^{\prime\prime} &= \sum_{m=0}^M (d''_{mi} d'_{mj} - d'_{mi} d''_{mj}), \\ Y_i^{\prime} &= \sum_{m=0}^M (-A'_m d'_{mi} + d'_{m0} d'_{mj} - A''_m d''_{mi} + d''_{m0} d''_{mj}), \\ Y_i^{\prime\prime} &= \sum_{m=0}^M (A'_m d''_{mi} - d'_{m0} d''_{mj} - A''_m d'_{mi} + d''_{m0} d'_{mj}). \end{aligned} \right\} (12)$$

The solution of system (11) is the solution of stated problem of the synthesis of antenna arrays by the assigned radiation pattern.

It should be noted that the method of the construction of the solution presented is the variety of the known receptions/procedures of the theory of the synthesis of antennas with the use of a system of orthogonal partial radiation patterns [7.8].

THE SYNTHESIS OF ARRAYS WITH THE MAXIMUM DIRECTIVE GAIN.

The problem of the synthesis of antenna arrays with the maximum

directive gain (knd) in the direction θ_0, ϕ_0 during the assigned polarization of emitted in this direction field can be considered as a special case of the problem of the best root-mean-square approximation of the standardized/normalized radiation pattern $\bar{F}(\theta, \phi)$ ($\bar{F}(\theta_0, \phi_0) = \bar{i}_0$) to a vector delta-function $\delta(\theta - \theta_0, \phi - \phi_0) \bar{i}_0$ [2, 7]. Having this in mind, let us present the radiation pattern of antenna array from K emitters in the form of sum (6), where the coefficients

$$C_m = \sum_{j=1}^K b_{mj} J_j, \quad (13)$$

and $b_{mj} = a_{mj} - ib_{mj}^*$ — some complex numbers, which depend only on the type of antenna array.

Page 57.

Introducing the condition for the standardization of radiation pattern

$$\bar{F}(\theta_0, \phi_0) = \sum_{m=0}^M C_m \bar{f}_m(\theta_0, \phi_0) = \bar{i}_0, \quad (14)$$

from relationships/ratios (13) and (14) not difficult to obtain expression for coefficients C_m or form (4), where N is in general equal K-2.

Therefore further solution of the problem of the synthesis of antenna with maximum knd can be reduced to the solution of system

(11.12), where as coefficients A_m should be taken the coefficients of the expansion of delta-function $\delta(\theta-\theta_0, \phi-\phi_0)\bar{i}_0$ in the series/row in terms of the system of the eigenfunctions:

$$A_m = (\bar{i}_0, \bar{j}_m(\theta_0, \phi_0)).$$

The value of the maximum and in this case can be counted on the following relationship/ratio:

$$D_{max} = \frac{4\pi}{\Delta_{min}^2 - 2 - \sum_{m=0}^M |A_m|^2} \quad (15)$$

where Δ_{min}^2 — minimum value (10), obtained with the substitution in (10) of the solution of system (11).

INITIAL RELATIONSHIPS/RATIOS OF SYNTHESIS FOR THE ARC AND SPHERICAL ARRAYS.

Let us consider the obtained above general solution of the problem of synthesis in appendix to the concrete/specific/actual arc and spherical gratings.

Arc grating with the longitudinal emitters. Grating is the system of the longitudinal half-wave slots, gashed on the ideally conducting surface of the infinitely long round cylinder of an electrical radius kA in the plane, normal to its axis (Fig. 1a).

Eigenfunctions $\bar{j}_m(\theta, \varphi)$ for this antenna are written/recorded in

the form [3]

$$\bar{f}_m(\theta, \varphi) = \frac{H_m^{(1)'}(\kappa a)}{\sqrt{N_m \epsilon_m \pi} H_m^{(1)'}(\kappa a \sin \theta)} \frac{\cos\left(\frac{\pi}{2} \cos \theta\right)}{\sin^2 \theta} \left\{ \frac{\cos m \varphi}{\sin m \varphi} \right\} \bar{f}_m. \quad (16)$$

where

$$\epsilon_m = \begin{cases} 2^{\alpha} \pi \kappa & m = 0, \\ 1 & m \neq 0; \end{cases}$$

$$N_m = \int_0^{\pi} \left(\frac{\cos\left(\frac{\pi}{2} \cos \theta\right)}{\sin^2 \theta} \right)^2 \left| \frac{H_m^{(1)'}(\kappa a)}{H_m^{(1)'}(\kappa a \sin \theta)} \right|^2 \sin \theta d\theta.$$

Key: (1). when. $H_m^{(1)}$ — Hankel function of the 1st order, and prime designates its derivative on the argument.

Page 58.

Coefficients

$$b_{mj} = \sqrt{\frac{N_m}{\epsilon_m \pi}} \frac{e^{-i m \frac{\pi}{2}}}{H_m^{(1)'}(\kappa a)} \left\{ \frac{\cos m \varphi_j}{\sin m \varphi_j} \right\}. \quad (17)$$

With the synthesis of this grating with the the maximum knd in the directions $\theta_0 = \pi/2$, $\varphi_0 = 0$ coefficients d_{mj} are respectively equal to:

$$d_{mj} = b_{mj} \frac{\sum_{m=0}^M b_{mj} \frac{1}{\sqrt{N_m \epsilon_m \pi}}}{\sum_{m=0}^M b_{mK} \frac{1}{\sqrt{N_m \epsilon_m \pi}}} b_{mK}. \quad (18)$$

$$d_{m0} = \frac{b_{mK}}{\sum_{m=0}^M b_{mK} \frac{1}{\sqrt{N_m \epsilon_m \pi}}}.$$

but value N is equal to $K-1$.

Arc grating with the transverse emitters. Grating is the system of the azimuth half-wave slots, gashed on the surface of the ideally conducting infinite cylinder (Fig. 1b).

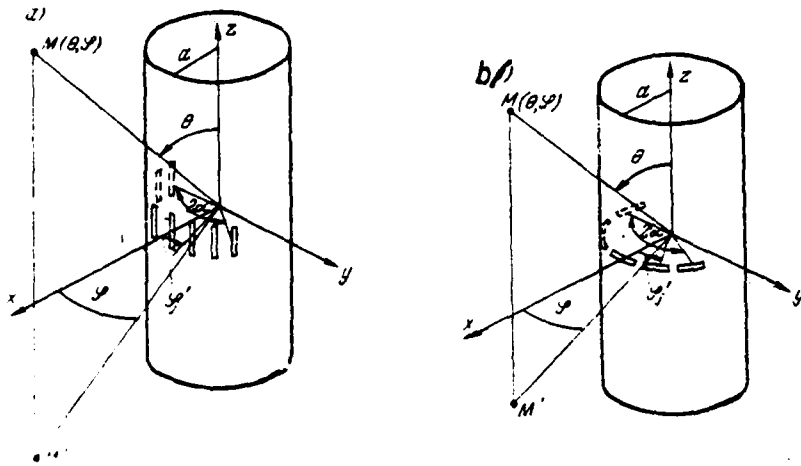


Fig. 1.

Page 59.

The eigenfunctions of this antenna [3, 4]

$$\begin{aligned} \vec{f}_m(\theta, \varphi) = \frac{e^{-im\frac{\pi}{2}}}{N_m} & \left[\frac{1}{\sin\theta H_m^{(1)}(\kappa a \sin\theta)} \begin{pmatrix} \cos m\varphi \\ \sin m\varphi \end{pmatrix} \vec{i}_\theta - \right. \\ & \left. + \frac{m \operatorname{ctg}\theta}{\kappa a \sin\theta H_m^{(1)'}(\kappa a \sin\theta)} \begin{pmatrix} \sin m\varphi \\ -\cos m\varphi \end{pmatrix} \vec{i}_\varphi \right]. \end{aligned} \quad (19)$$

where

$$N_m = e_m \pi \int_0^\pi \left[\frac{1}{\sin^2\theta |H_m^{(1)}(\kappa a \sin\theta)|^2} + \frac{m^2 \operatorname{ctg}^2\theta}{(\kappa a)^2 \sin^2\theta |H_m^{(1)'}(\kappa a \sin\theta)|^2} \right] \sin\theta d\theta.$$

and coefficients

$$b_{mj} = \frac{1}{e_m \pi} \frac{\kappa a}{(\kappa a)^2 - m^2} \cos m \frac{\pi}{2} \begin{pmatrix} \cos m\varphi_j \\ \sin m\varphi_j \end{pmatrix}. \quad (20)$$

Spherical array. The problem of the synthesis of the spherical gratings of emitters is more complicated in comparison with the problem of the synthesis of cylindrical gratings, since unknowns are not only amplitude and phase of the excitation of emitters, but also their polarization. Its solution with the help of method examined above is possible only in two cases: if is assigned the orientation of emitters on the spherical surface or if there are no limitations for the polarization of emitters. Let us give the initial relationships/ratios of synthesis with the given one of the orientations of elementary slotted emitters on the ideally conducting spherical surface of the electrical radius ka . The length of emitters let us designate through l_m .

In this case the system of its own waves $\overline{T}_p^{\mu}(\theta, \varphi)^1$ takes form

[1]

$$\begin{aligned} \overline{T}_p^i(\theta, \varphi) &= (-i)^{n+1} \sqrt{\frac{(2n+1)(n-m)!}{2\pi\epsilon_{mn}(n+1)(n+m)!}} \left[\frac{\partial P_n^m(\cos \theta)}{\partial \theta} \begin{vmatrix} \cos m\varphi \\ \sin m\varphi \end{vmatrix} \right. \\ &\quad \left. \times \overline{i}_\theta + \frac{m}{\sin \theta} P_n^m(\cos \theta) \begin{vmatrix} -\sin m\varphi \\ \cos m\varphi \end{vmatrix} \overline{i}_\varphi \right]; \quad (21) \\ \overline{T}_p^\mu(\theta, \varphi) &= (-i)^{n+1} \sqrt{\frac{(2n+1)(n-m)!}{2\pi\epsilon_{mn}(n+1)(n+m)!}} \\ &\quad \times \left[\frac{m}{\sin \theta} P_n^m(\cos \theta) \begin{vmatrix} -\sin m\varphi \\ \cos m\varphi \end{vmatrix} \overline{i}_\theta - \frac{\partial P_n^m(\cos \theta)}{\partial \theta} \begin{vmatrix} \cos m\varphi \\ \sin m\varphi \end{vmatrix} \overline{i}_\varphi \right]. \end{aligned}$$

where $P_n^m(\cos \theta)$ - the associated functions of Legendre.

FOOTNOTE 1. Index p here designates the double index mn , and superscripts 1 or μ relate to the electrical or magnetic waves.

ENDFOOTNOTE.

Page 60.

Since along the length of elementary slot the field of the m its own wave varies insignificantly, then coefficients b_{mj} can be found from the following expressions:

$$b_{mj}^i = \left[\frac{(2n-1)(n-m)!}{\epsilon_m n(n+1)(n-m)!} \frac{I_m}{\xi_n(\kappa a)} \right. \\ \left. \times \left[-m \sin \alpha_j P_n^m(\cos \theta_j) \begin{Bmatrix} -\sin m \varphi_j \\ \cos m \varphi_j \end{Bmatrix} - \frac{\partial P_n^m(\cos \theta)}{\partial \theta} \Big|_{\theta=\theta_j} \sin \theta_j \cos \alpha_j \begin{Bmatrix} \cos m \varphi_j \\ \sin m \varphi_j \end{Bmatrix} \right] \right] \\ b_{mj}^u = \left[\frac{(2n-1)(n-m)!}{\epsilon_m n(n+1)(n+m)!} \frac{I_m}{i \xi_n(\kappa a)} \times \right. \\ \left. \times \left[\sin \alpha_j \frac{\partial P_n^m(\cos \theta)}{\partial \theta} \Big|_{\theta=\theta_j} \sin \theta_j \begin{Bmatrix} \cos m \varphi_j \\ \sin m \varphi_j \end{Bmatrix} + m \cos \alpha_j P_n^m(\cos \theta_j) \begin{Bmatrix} -\sin m \varphi_j \\ \cos m \varphi_j \end{Bmatrix} \right] \right]$$

where $\xi_n(\kappa a) = \left[\frac{\pi \kappa a}{2} H_{n+\frac{1}{2}}^{(1)}(\kappa a) \right]$, $a \xi_n'(x) = \frac{\partial \xi_n(x)}{\partial x}$;

θ, φ — the coordinate of the j slot on the surface of sphere;

α — angle between the direction of the j slot and in parallel on the spherical surface.

RESULTS OF NUMERICAL CALCULATIONS.

Using the obtained above solutions, is carried out the numerical calculation of the synthesis of grating with the the maximum k_{nd} , that consists of the longitudinal half-wave slots, arranged/located on the arc on the surface of the ideally conducting cylinder (Fig. 1A).

Calculations were performed on TSM BESM-6 for the wide range of an electrical radius of cylinder ka , of step/pitch between emitters d and the angular dimension of arc grating $2a$.

During calculations according to the obtained above algorithm it is necessary to bound the radiation field of antenna by the final sum of its own waves. In the worked out previously approximation methods of the synthesis of cylindrical antenna arrays usually was considered the number of waves, which does not exceed an electrical radius of cylinder ka . In the present work a maximum number of the waves considered was chosen equal of ek and was conducted the accuracy analysis of the solution depending on a number of the waves considered.

While conducting of numerical calculations was assumed that value N_m entering in (22), does not depend on m and ka and it is equal to 1.4.

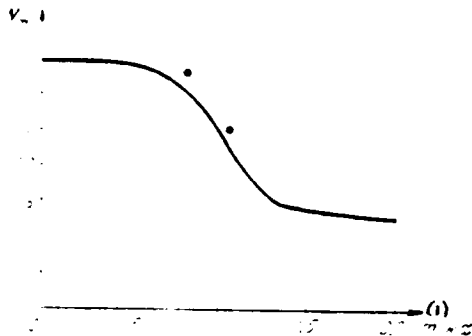


Fig. 2.

Key: (1). n/ka .

Page 61.

Fig. 2 gives the real graph/diagram of dependence η on the relative index n/ka for $ka=5$ (points noted values η_m with $ka=20$). As it follows from the graph, the done proposition is correct in region $n < ka$. However, as show the calculations, carried out taking into account precise dependence η_m on n for cylindrical antenna of radius $ka=5$, the error in the determination of the maximum η does not exceed 100%, but the error in the optimum amplitude-phase distribution proves to be still less.

Fig. 3.4 shows dependences maximum efficiency (D_{max}) of the synthesized grating on the step/pitch between emitters d/λ (dotted

curves in Fig. 3), the angular dimension of grating 2α (unbroken curves in Fig. 3) and a radius of cylinder (Fig. 4). For the clarity value D_{max} is standardized to the the maximum knd of equivalent flat/plane cophasal aperture ($D_{\text{KB}} = 2 ka$). As follows from the graphs, maximum knd of the circular grating whose electrical radius $ka \leq 20$, with the step/pitch between emitters $d = 0.5\lambda$ proves to be by approximately 40% more than the maximum knd of equivalent cophasal aperture. This phenomenon is connected with the convexity of circular grating.

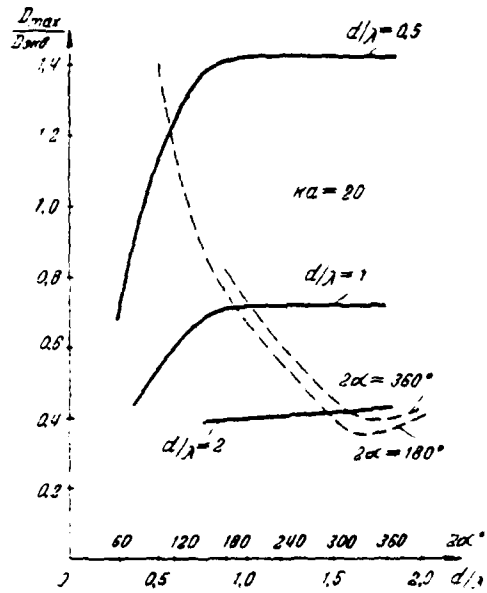


Fig. 3.

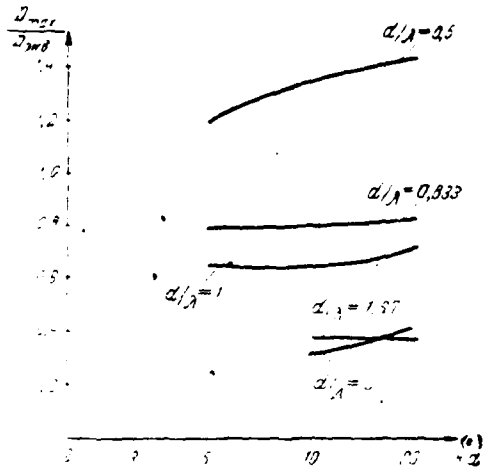


Fig. 4.

Key: (1). ka .

Page 62.

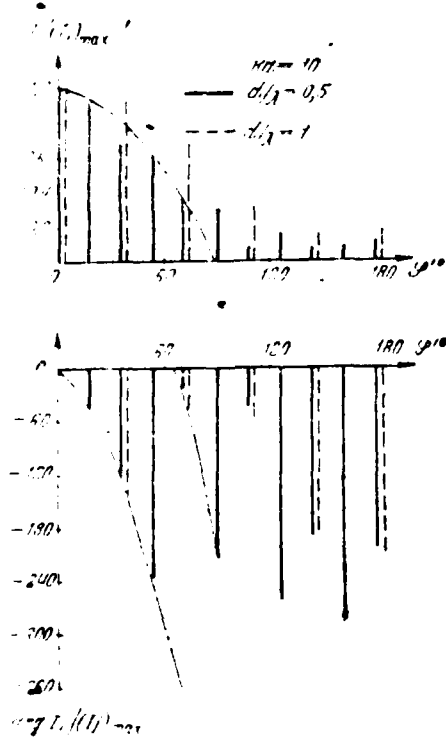


Fig. 5.

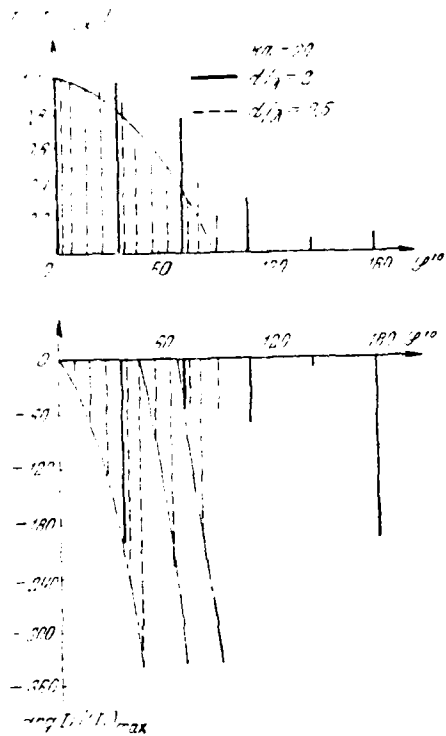


Fig. 6.

Page 63.

The extent of circular grating along the axis, which coincides with the direction of the formed/shaped ray/beam, leads to the further (in comparison with the equivalent aperture) contraction of radiation pattern both in the plane of ring and in the plane, passing through the axis of ring and with beam direction.

It should be noted that with an increase in ka from 5 to 20 values of gain in knd of the circular grating in question in comparison with the the maximum knd of equivalent cophasal aperture weakly it depends on ka . On the base of the analysis of obtained calculation data one should expect that with further how conveniently great increase in the electrical radius of ring value D_{max} in the grating in question will approach value $3.26K_0$, where K_0 - number of emitters, arranged/located on the "illuminated" part of the ring, so that with $d/\lambda=0.5$ relation $\frac{D_{max}}{D_{max}}$ will approach value 1.63.

With the decrease of the angular dimension of arc grating from $2\alpha=180^\circ$ to $2\alpha=60^\circ$ its knd is reduced approximately/exemplarily proportional to its equivalent aperture. An increase in the angular dimension of grating from 180 to 360° (excitation of "shadow" region) only insignificantly increases knd (approximately/exemplarily to $6-10\%$ with $ka=5$ and by $2-3\%$ with $ka=20$).

With an increase in the step/pitch between the emitters the value of the maximum knd of arc grating is reduced approximately proportional to a number of emitters.

Fig. 5.6 depicts the most characteristic optimum amplitude-phase

current distribution in the emitters, which ensure the maximum k_{nd} , and the corresponding to them radiation patterns (Fig. 7).

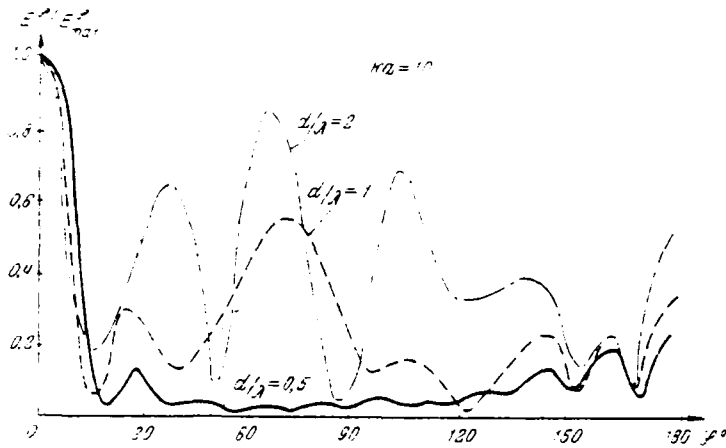


Fig. 7.

Page 64.

With the step/pitch between emitters $d=0.5\lambda$ (Fig. 5.6) amplitude current distribution has the collapsible/dropped character, and phase distribution in the "illuminated" region of grating close to the distribution, which escape/ensues from the laws of geometric optic/optics [5] (dot-dash curve). At the high values of the step/pitch between the emitters ($d=\lambda$, Fig. 5, and $d=2\lambda$, Fig. 6) amplitude current distribution approaches uniform.

From given graphs of current distribution it follows that with the step/pitch between emitters $d \gg 0.5\lambda$ of the phenomena of superdirectionality it does not appear. However, during the use/application of the algorithm examined for the synthesis of gratings with the step/pitch between emitters $d < 0.5\lambda$ amplitude-phase distribution acquires superdirectional character. Therefore with the synthesis of non-ultradirectional arrays with the low pitch between emitters ($d/\lambda < 0.5$) it is necessary to additionally introduce limitation to the superdirectionality or to pass toward the synthesis of antennas with continuous distribution [6].

In the optimum (in the sense of the maximum ^{directive gain} ~~radiation~~ radiation patterns (Fig. 7) with the step/pitch between the emitters more 0.5λ appear the diffraction peaks whose level depends on the step/pitch between the emitters and angular dimension of arrays.

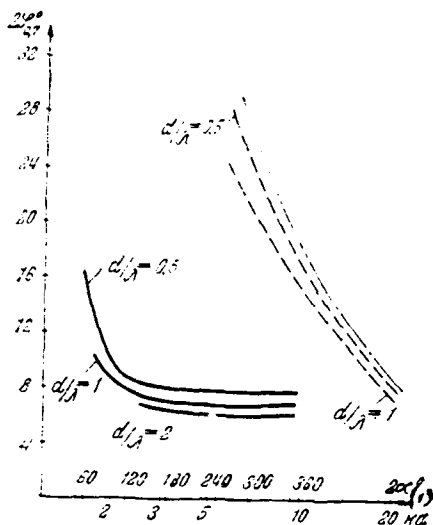


Fig. 8.

Fig. 8.

Key: (1). kA.

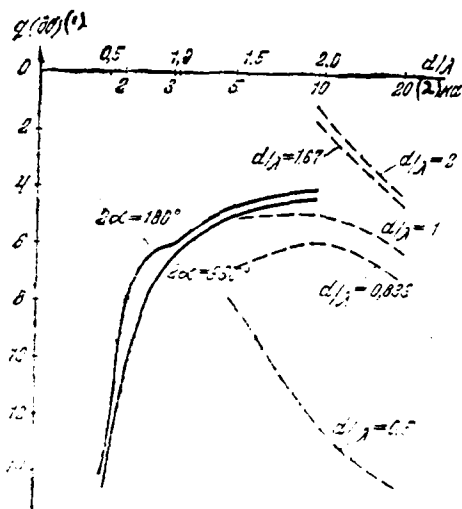


Fig. 9.

Fig. 9.

Key: (1). dv. (2). kA.

Page 65.

According to the calculated optimum radiation patterns was constructed the series of the auxiliary dependences of the beam width

$2\theta_{0.7}$ and sidelobe level η in the arc grating on a step/pitch between the emitters, an electrical radius of cylinder and angular dimension of grating. These dependences are given in Fig. 8, 9 (by dotted line - dependence on kA at $2\alpha=360^\circ$, and by unbroken curves - dependence on d/λ and $2a$ with $kA=20$).

The beam width of arc grating with maximum knd in the plane of the ring (see Fig. 8) proves to be less than the beam width of equivalent aperture (dash-line curves in Fig. 8) that it is connected with the convexity of grating.

High sidelobe level with the distance 0.833λ and is more connected with the advent of a diffraction peak.

All given above results were designed with $M=3$ kA .

Fig. 10 shows the dependences of the maximum knd of the synthesized grating on a relative quantity of those considered with calculation of its own waves M/kA for two values of an electrical radius of cylinder ($kA=5$ - unbroken curves; $kA=20$ - dotted curve).

As it follows from these dependences, upon consideration first kA of its own waves maximum knd of array is obtained by approximately 10% less than upon consideration 1.5 kA of waves. Further increase in the number of the waves considered virtually does not lead to an increase in knd .

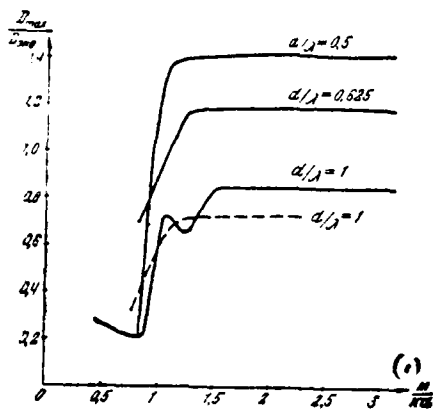


Fig. 10.

Key: (1). m/kA .

Conclusion/output.

1. Is given one of possible algorithms of solution of problem of synthesis of arc and spherical antenna arrays with use of apparatus of its own vector functions, convenient for conducting machine calculations.

2. Is carried out numerical synthesis of arc grating with maximum knd , arranged/located on surface of ideally conducting cylinder, for wide range of electrical radius of cylinder, angular dimension of grating and step/pitch between emitters.

Page 66.

As a result it is shown that:

a) for $kA \leq 20$ with the step/pitch between the emitters 0.5λ maximum knd of circular array 40% by approximately exceeds maximum knd of equivalent flat/plane cophasal aperture; with an increase in the step/pitch between the emitters maximum knd is reduced approximately/exemplarily proportional to the decrease of a number of emitters;

b) optimum amplitude current distribution depend substantially on the step/pitch between the emitters, and optimum phase current distribution close to the phase distributions, which escape/ensue from the laws of geometric optic/optics;

c) with the synthesis of arc grating with maximum knd in the numerical calculations should be considered first 1.5 kA of their own waves, upon consideration only to kA of its own waves the error comprises order 10%.

REFERENCES

1. G. T. Markov, A. F. Chaplin. Excitation of electromagnetic waves. M., "Energy", 1967.
2. D. M. Sazonov, B. A. Mishustin. Scattering matrix of antenna array. - "Proceedings of VUZ [- Institute of Higher Education]" - "Radiophysics", XII, 1969, No 4, page 597-607.
3. A. A. Pistol'kors. Radiation/emission from the longitudinal circuits in the circular cylinder. Radiation/emission from the transverse slots on the surface of circular cylinder. - "ZhTF", XVII, iss. 3, 1947, page 365-388.
4. M. I. Levin. To the theory of slot antennas in the circular waveguide. - "ZhTF", XXI, iss. 7, 1951, pages 772-786.
5. D. I. Voskresenskiy, V. S. Philipp. Directive gain of the convex highly directional antenna arrays. - "Proceedings of VUZ" - "Radio electronics", XI, 1968, NO 5, page 413-425.
6. L. I. Ponomarev. On the maximum directive gain of spherical and conical antennas. - "Proceedings of VUZ" - "Radio electronics", XI, 1968, No 5, page 426-440.

7. D. N. Sazonov, Yu. S. Ushakov. Synthesis of multiple-pronged circular antenna arrays with the full/total/complete circular symmetry. - "Radio engineering and electronics", Vol. XV, iss. 5, 1970, page 897-904.

8. B. M. Minkovich, V. P. Yakovlev. Theory of the synthesis of antennas. M., "Soviet radio", 1969.

Submitted 13/IV 1971; after treatment/processing - 1/XII 1971.

Page 67.

Formation of the antenna radiation patterns with the help of the passive slotted emitters.

I. V. Guzeyev, L. L. Zbarskaya.

Are traced laws governing the formation of the radiation/emission of slot antenna with the passive elements/cells, the loaded adjustable reactive/jet four-pole. It is shown the possibility of control over wide limits by the equatorial antenna radiation pattern, is produced the classification of diagrams according to their distinguishing features and is established/installed conformity between the parameters of antenna and the type of radiation pattern. Is in detail examined the cylindrical tri-element slotted grating whose passive emitters are loaded with the short-circuited grooves or are communicated by flat/plane waveguide.

Introduction.

Passive emitters since olden times are applied into the antenna to technology, mainly, in the composition of multiunit wire gratings

[1]. Making it possible to regulate the directivity of grating, the passive radiating elements/cells do not require the complication of its feeder system, which differ significantly then from the uniform active emitters.

In certain cases, for example, for slot antennas, arranged/located on the objects, limited by metallic surfaces, the use/application of wire elements/cells although is possible [2], on the series/row of considerations it is inconvenient. Therefore for the class of antennas indicated it is of interest to trace the possibilities of passive emitters also of the slotted type.

As far as is known, single passive elements/cells of the type of the short-circuited grooves are applied into the antenna to technology in essence only in cutoff condition of surface current (with the electrical depth of groove, close to 90°) [3, 4] ¹.

FOOTNOTE ¹. We do not stop here on the flanged structures, which are the effective means of the formation of radiation of antennas [5], giving preference to the single passive elements/cells, which have more than chances for the practical use/application. ENDFOOTNOTE.

The purpose of this work is the study of the effect of loaded passive slot antennas, arranged/located arranged/located on the metallic

cylinder, with a change of the value of load within sufficiently wide limits.

Page 68.

LEAKY-PIPE ANTENNA WITH THE PASSIVE EMITTERS. Conclusion/output of fundamental principles.

Fig. 1 schematically depicts two possible versions of antenna system with the passive slotted emitters:

a) variable-phase leaky-pipe antenna 1, formed by the grating of half-wave slots 2, with passive slots 3, loaded with the pair of short-circuited grooves 4, adjacent from without to lateral walls of waveguide;

b) the antenna of ensuing/escaping/flowing out waves 1 with passive slots 2, which are communicated by flat/plane gap 3, which partially encompasses waveguide.

In the upper part of Fig. 1 is given location of the versions of antenna systems indicated on the cylinder.

Fundamental laws governing the formation of the radiation

patterns of similar systems can be traced on the system of three narrow infinitely long parallel slots (gashed in the cylinder or the plane), one of which (average/mean) is active, and two others - passive (Fig. 2).

The passive emitters of system are assumed to be those loaded with certain cavity (in particular, it can be double-bond) whose properties do not depend on coordinate z ; in connection with this the cavity can be represented four-pole, infinitely extended and cylindrically uniform along the axis z .

For the purpose of further simplifications we will be bounded to the examination of the cases when cavity, just as the grating of emitters, is mirror symmetrical relative to the coordinate plane XOZ (see Fig. 2).

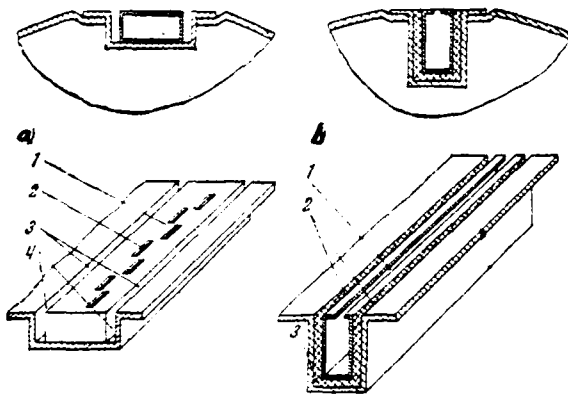


Fig. 7.

Page 69

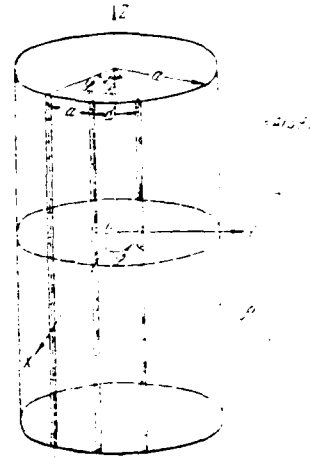


Fig. 8.

It will be shown below that in this case the four-pole formally can be replaced by the pair of the identical noninteracting two-terminal networks, which are the loads of passive slots.

The active radiators of real antennas (chain/network of discrete/digital slots, extended slot of finite length) are approximated in the selected by us model by one symmetrically arranged/located (relative to passive elements/cells) infinite continuous slot whose width the same as in real emitters, and magnetic current distribution in the aperture equal-amplitude and linear-phase with the corresponding angular coefficient in Z .

Further, it is almost obvious that in the real antenna (see Fig.

1) passive emitters affect in essence the formation of radiation pattern in the conic section, passing through the principal maximum ¹, since they change virtually only transverse current distribution.

FOOTNOTE ¹. Subsequently let us agree to call its equatorial radiation pattern. ENDFOOTNOTE.

Therefore in this work we were limited to the analysis of this most essential effect.

The described above theoretical model is most adapted for the study of the process of the formation of the azimuth radiation/emission of the highly directional line-source antennas whose primary field in the vicinity of active element/cell has a character of symmetrical conical wave. Closest to this model the antenna of the ensuing/escaping/flowing out waves (see Fig. 1b); as far as gratings are concerned discrete/digital slotted (see Fig. 1a), conformity of results, obviously, must be improved in proportion to the decrease both the longitudinal and, in particular, the transverse separation of active slots.

Fig. 3 depicts the equivalent matrix circuit of the theoretical model of radiating system. Accepting for the certainty as the terminal surfaces the apertures of emitters ² and designating through

y_{nm} ($n, m=1, 2, 3$) its own and mutual conductivities of slots (per the unit of length), and through Y_{ik} ($i, k=1, 3$) - matrix elements of the conductivity of four-pole (also per the unit of length), it is possible to record the following equations of relation between the voltages and the linear currents in the terminal sections of radiating system:

$$I_n = \sum_{m=1}^3 y_{nm} V_m \quad (n=1,2,3); \quad (1)$$

$$-I_1 = Y_{11}V_1 + Y_{13}V_3; \quad (2)$$

$$-I_3 = Y_{31}V_1 + Y_{33}V_3. \quad (2b)$$

FOOTNOTE 2. According to the theory of connected antennas [6], the terminal sections of the feeders of system should be carried out in the places of the absence of the highest transmission modes. However, in the case of electrically narrow slots in question the highest types attenuate so rapidly that the done by us selection of terminal surface virtually does not introduce errors. ENDFOOTNOTE.

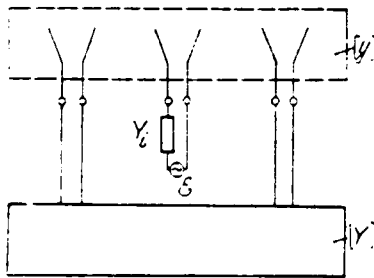


Fig. 3.

The solution of equ. (1) and (2a, b), taking into account the properties of symmetry and reciprocity of radiating system, leads to the following expression for the relative voltages:

$$\frac{V_1}{V_2} = \frac{V_3}{V_3} = \nu = - \frac{y_{13}}{y_{11} + y_{13} + Y_{11} + Y_{13}} \quad (3)$$

The equatorial radiation pattern of the narrow long slot, gashed according to the generatrix of metallic cylinder and is excited by magnetic current to equal-amplitude, linear-phase distributions [7]:

$$f(\varphi - \varphi') = \frac{1}{i\pi\nu_0 a} \left\{ \frac{1}{H_0^{(2)'}(\nu_0 a)} + 2 \sum_{m=1}^{\infty} \left[\frac{i^m \cos m(\varphi - \varphi') \frac{\sin \frac{ms}{2a}}{\frac{ms}{2a}}}{H_m^{(2)'}(\nu_0 a)} \right] \right\} \quad (4a)$$

where φ, φ' - azimuth coordinates of observation point and middle of slot respectively (see Fig. 2); a - radius of cylinder; s - width of slot; $H_m^{(2)'}(z)$ - derivative of the Hankel function of the argument; ν_0 - transverse wave number, connected with wave number k_0 in the free space with the dependence

$$\nu_0 = k_0 \sin \theta_0 \quad (4b)$$

where θ_0 - angle between Z-axis and principal maximum of meridional radiation pattern.

According to the principle of superposition, the equatorial radiation pattern of the investigated by us cylindrical system of

three slots can be described in the form

$$F(\varphi) = f(\varphi) + \alpha [f(\varphi - \varphi_0) + f(\varphi + \varphi_0)] \quad (5)$$

where $\varphi_0 = \frac{d}{2}$ - angular coordinate of the slot; α - distance between the middles of slots on the arc.

Fig. 2).

For computing the entering in (5) parameter v is necessary, in accordance with (3), the knowledge of the internal (Y_{ik}) and external (y_m) conductivities of system. The values of the latter can be obtained on the basis of work [8], where the resulting expressions of the standardized/normalized conductivities of the interesting us slots during their cophasal (y^+) and antiphase (y^-) excitations.

Page 71.

Relying on the elementarily proven equalities

$$\left. \begin{aligned} y_{11} &= \frac{1}{2} [y^{(++)} + y^{(+-)}] \\ y_{12} &= \frac{1}{2} [y^{(++)} - y^{(+-)}] \end{aligned} \right\} \quad (6a)$$

and taking into account the value of the linear conductivity of flat/plane waveguide with the inclined incident wave TEM [9]

$$\eta_0 = \frac{1}{s} \sqrt{\frac{\epsilon_0}{\mu_0}} \sin \phi_0, \quad (6b)$$

s - the height of waveguide; ϵ_0 and μ_0 - permittivity and permeability of its air filling, we obtain the following relationships/ratios:

$$y_{11} \approx \frac{v_0^2}{2\omega\mu_0} \left[1 + i \frac{2}{\pi} \ln \left(\frac{\pi e}{\gamma v_0 s} \right) \right]; \quad (7a)$$

$$y_{12} \approx \frac{v_0^2}{2\omega\mu_0} \left\{ H_0^{(2)}(v_0 d) - 0,302 \frac{\sqrt{d/a}}{\gamma v_0 a} \exp \left[-i \left(v_0 d - \frac{\pi}{4} \right) \right] \right\}, \quad (7b)$$

in which $e=2.718 28...$ and $\gamma=1.781 07...$ - respectively Napierian base

and Euler's constant, $H_0^{(2)}(\dots)$ - the Hankel function of the 2nd order
the dimensionality of conductivities - mo/meter¹.

FOOTNOTE 1. In the work is accepted the practical rationalized system
of unity MKSA. ENDFOOTNOTE.

Expression for y_{13} follows from (7b) with the substitution into its
right side $2d$ instead of d .

As far as internal conductances are concerned of slots, then
they, depending on the parameters of the cavity, included between the
passive slots, can take any composite values, which satisfy only the
necessary conditions of the physical realizability of passive
devices/equipment [10]:

$$\operatorname{Re} Y_{11} \geq 0, \quad |\operatorname{Re} Y_{13}| \leq \operatorname{Re} Y_{11}. \quad (8a)$$

In particular, if cavity is locked and free from the ohmic losses,
then matrix/die $[Y]$ - is pure imaginary and the entering in (3)
parameter

$$Y = Y_{11} + Y_{13} = iB \quad (8b)$$

varies within the limits ± 1 .

The sense of parameter Y it is easy to explain, relying on the
equations of Kirchhoff (2a, b). Assuming/setting in them due the
symmetry of system $V_1 = V_3$, we obtain (minus sign it is caused by the

external with respect to the cavity direction of standard)

$$Y = -\frac{I_1}{V_1} = -\frac{I_3}{V_3}, \quad (8a)$$

i.e. Y is operating input admittance of cavity in the mode/conditions of the equal-amplitude and cophasal excitation of its inputs.

Page 72.

Using relationships/ratios (3), (7a, b) and (8b), we obtain the following expression for the relative voltage:

$$v = \frac{H_0^{(2)}(v_0 d) - 0.302 \frac{1}{v_0} \frac{d/a}{v_0 d} \exp \left[-i \left(v_0 d - \frac{\pi}{4} \right) \right]}{1 - i \frac{2}{\pi} \ln \frac{\pi e}{\gamma v_0 s} - H_0^{(2)}(2v_0 d) - 0.302 \frac{1}{v_0} \frac{2d/a}{v_0 d} \exp \left[-i \left(2v_0 d - \frac{\pi}{4} \right) \right]} - 2\tau \quad (9a)$$

where

$$\tau = \frac{\omega \mu_0}{v_0^2} B \equiv \frac{\omega \mu_0}{v_0^2} \operatorname{Im} Y \quad (9b)$$

- parameter, which is determining (during assigned phase field distribution in the slots) exclusively by the properties of cavity.

ANALYSIS OF THE SYSTEM OF THREE INFINITE SLOTS.

Relationships/ratios (5) and (9a, b) make it possible to explain the most important laws governing the formation of the radiation/emission of slot antenna in the presence of passive slotted emitters.

The analysis of system becomes especially demonstrative, if one considers that v is the linear-fractional function τ and representation/transformation straight/direct $\text{Im}\tau=0$ on the plane complex variable v is circumference. It is not difficult to show [11] that by relationship/ratio (9a) is assigned the one-parameter family of circumferences (parameter $\delta=v_0d$), of the intersecting in the beginning coordinates; centers and radii of a circle are determined by equalities:

$$c_0 = -\frac{1}{2} \frac{H_0^{(2)}(\delta) - 0.302 \frac{1}{5} \frac{d}{v_0 a} \exp\left[-i\left(\delta - \frac{\pi}{4}\right)\right]}{1 + J_0(2\delta) - 0.302 \frac{1}{5} \frac{2d}{v_0 a} \cos\left(2\delta - \frac{\pi}{4}\right)} ; \quad (10a)$$

$$R_0 = |c_0| ; \quad (10b)$$

Fig. 4 depicts the series of circumferences $v=v(\tau, \delta)$, of corresponding to change τ within the limits $-\infty$ with the series/row fixed values $\delta=v_0d$. On one of circumferences [$\delta=\pi$] are replaced the values of variable/alternating $\xi=r-r_0$ (sense of the parameter r_0 is revealed below), which make it possible to judge rate of change in the voltage in proportion to removal/distance from the resonance.

One should emphasize that the sizes/dimensions and the location of circumferences are determined only by electrical period ($\delta=v_0d$) of system.

This means that in the system with the fixed/recorded period with a sufficiently wide change in the geometric and (or) electrical parameters the cavities, the voltage, without depending on the width of slots, pass the continuous sequence of the complex numbers, which fill the circumference, which corresponds to data v_{0d} . The radiation patterns of the system of slots, in accordance with (5), are changed in this case within the limits of one and the same sequence of forms.

However, each concrete/specific/actual value v on the circumference answers the specific combination of the parameters, which switches on also the width of slots [formula (9a, b)]. For the numerical calculations it is expedient to convert (9a) to the form

$$v = - \frac{H_0^{(2)}(\delta) - 0.302 \frac{\sqrt{d/a}}{\gamma \sqrt{v_0 a}} \exp \left[-i \left(2\delta - \frac{\pi}{4} \right) \right]}{1 - J_0(2\delta) - 0.302 \frac{\sqrt{2d/a}}{\gamma \sqrt{v_0 a}} \cos \left(2\delta - \frac{\pi}{4} \right) - 2i \xi} \quad (11a)$$

where $\xi = \tau - \tau_0$, moreover

$$\tau_0 = \frac{1}{2} \left[N_0(2\delta) - \frac{2}{\pi} \ln \left(\frac{\pi e}{\gamma \sqrt{v_0 a}} \right) - 0.302 \frac{\sqrt{2d/a}}{\gamma \sqrt{v_0 a}} \sin \left(2\delta - \frac{\pi}{4} \right) \right] \quad (11b)$$

- value of the parameter τ , which corresponds to voltage resonance in the presence of which

$$|v|_{max} = \frac{\sqrt{\left[J_0(\delta) - 0.302 \frac{\sqrt{d/a}}{\gamma \sqrt{v_0 a}} \cos \left(\delta - \frac{\pi}{4} \right) \right]^2 + \left[N_0(\delta) - 0.302 \frac{\sqrt{d/a}}{\gamma \sqrt{v_0 a}} \sin \left(\delta - \frac{\pi}{4} \right) \right]^2}}{1 + J_0(2\delta) - 0.302 \frac{\sqrt{2d/a}}{\gamma \sqrt{v_0 a}} \cos \left(2\delta - \frac{\pi}{4} \right)} \quad (11c)$$

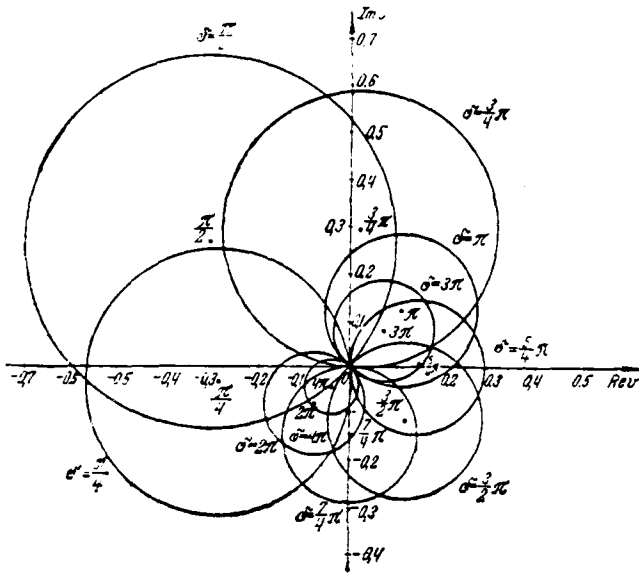


Fig. 4.

Page 74.

As we see, $|v|_{max}$ does not depend on the width of slots.

Fig. 5 depicts the dependences of amplitude and phase of the relative voltage of passive slot (calibrated to unity) in the function of "relative detuning" $\xi = \tau - \tau_0$, for the system with the electrical period $\delta = \tau$. Calculation was carried out according to formula (11a). We see that the amplitude dependence has specific resonance character and is even, and phase, with the accuracy to permanent component/term/addend [equal to

$$\pi + \text{Arg} \left| H_0^{(2)}(\delta) - 0.302 \frac{\sqrt{d/a}}{\sqrt{v_0 a}} \exp \left[-i \left(\delta - \frac{\pi}{4} \right) \right] \right|, \quad - \text{ by odd function } \xi.$$

The equatorial radiation patterns of the system of slots are symmetrical relative to main meridian cut ($\phi=0$), what is the corollary of the symmetry of system. Depending on form, radiation pattern they can be divided into three fundamental types:

- 1) narrow single-lobe;
- 2) wide single-lobe and saddle;
- 3) the intermediate form, which have several extrema, including one local maximum with $\phi=0$.

In connection with a comparatively low azimuth directivity of slot on the regular cylinder a question about affiliation of diagram to one of the types qualitatively can be solved on the basis of the analysis of the simple according to the structure equatorial radiation pattern of foil lattice, into which passes the designed cylindrical system when $v_0 a \rightarrow \infty$.

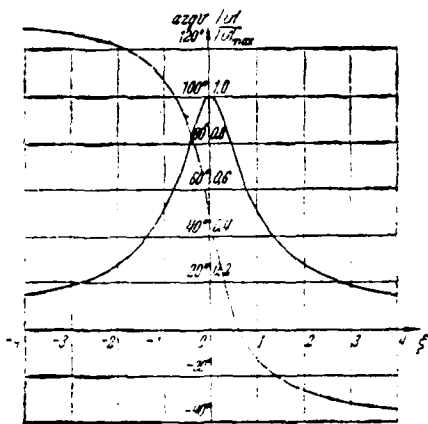


Fig. 5.

Page 75.

Relying on relationship/ratio (5) and taking into account that

$\lim_{v_0 d \rightarrow \infty} |f(\varphi)| = 1$, does not represent the work to obtain the equality:

$$\lim_{v_0 d \rightarrow \infty} F(\varphi) = 1 + 2v \cos(v_0 d \sin \varphi). \quad (12)$$

research of which shows that to the enumerated types of radiation patterns approximately corresponds the separation of plane complex variable v into three regions, demarcated by two circumferences of equation of which

$$\left[\operatorname{Re} v - \frac{1}{4} \right]^2 + [\operatorname{Im} v]^2 = \frac{1}{16}. \quad (13)$$

The numbering of regions in Fig. 6 corresponds to the indicated higher three types of radiation patterns.

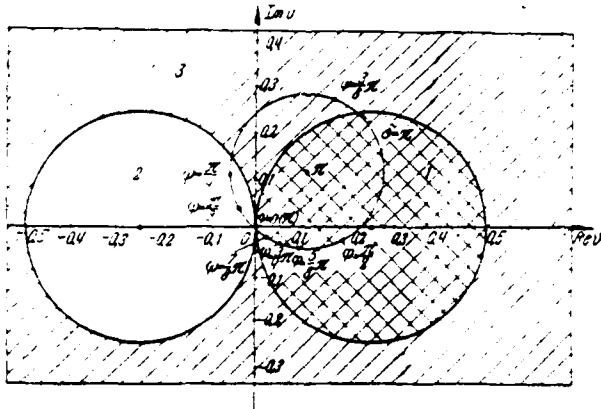


Fig. 6.

Antenna with the passive slots, loaded with grooves or communicated gaps.

Let us pause in somewhat more detail at the mentioned above two special cases, which are of practical interest:

- passive slots are loaded with the identical short-circuited grooves;

- passive slots are communicated by gap in the form of the flat/plane curved waveguide.

Assuming grooves or gap filled with uniform insulator, it

suffices to be bounded to research of the first case, since as a result of the symmetry of radiating system, in the middle of gap is established/installed the mode/conditions of idling. The second case (disregarding by heterogeneities in the inflection points of gap) formally is reduced to the first with a change in the electrical depth of grooves on $\pi/2$.

Page 76.

For determining linear input admittance of groove we will use known expression for the conductivity of the short-circuited segment of line, after replacing in it, accordingly [9], propagation constant γ and characteristic admittance Y_0 by the values:

$$\gamma_1 = k_0 \sqrt{\epsilon' \mu'} \sin \vartheta_1; \quad (14a)$$

$$Y_1 = \frac{1}{s} \sqrt{\frac{\epsilon'}{\mu'}} \sin \vartheta_1. \quad (14b)$$

where ϵ', μ' - relative permeability of insulator; s - width of groove; ϑ_1 - angle between the edge of groove and the wave standard of the propagated in it wave TEM.

The connection/communication between the angles ϑ_0 and ϑ_1 is established/installed from continuity condition of the tangential components of fields in the apertures of passive slots and takes the form (Snell law)

$$\cos \vartheta_0 = \sqrt{\epsilon' \mu'} \cos \vartheta_1. \quad (15)$$

In accordance with (9b), (14a, b) and (15) we obtain

$$\tau = \frac{\sqrt{1 - (\epsilon' \mu' - 1) \left(\frac{k_0}{v_0}\right)^2}}{\mu'} \frac{\operatorname{ctg} \Psi}{v_0^2} \quad (16a)$$

where

$$\Psi = v_0 l \sqrt{1 + (\epsilon' \mu' - 1) \left(\frac{k_0}{v_0}\right)^2} \quad (16b)$$

- electrical depth of the groove (l - its geometric depth).

Is given below the series/row of the characteristics of cylindrical three-slot grating with the load of its passive elements/cells by the short-circuited grooves with the air filling.

Fig. 7 depicts the standardized/normalized equatorial radiation patterns of grating. Calculation was carried out according to formulas (5), (9a) and (16a, b) at the values of the parameters: $\epsilon' = \mu' = 1$, $v_0 d = \pi$, $s = 0.427$, $v_0 a = 29.4$. The electrical depth of grooves $\Psi = v_0 l$ varied within the limits $0 \leq \Psi \leq \pi$ with the step/pitch $\pi/8$.

FOOTNOTE 1. The necessary for the calculations function $f(\Psi)$ was tabulated by A. V. Ivanov via the addition (on the computers) of series/row (4a) to $m=38$. ENDFOOTNOTE.

We see that the radiation patterns are changed within relatively wide limits, moreover in accordance with the introduced above classification of forms, in essence are encountered two types of

equatorial radiation patterns - single-lobe narrow 1 and wide 2. The radiation patterns of intermediate forms are encountered considerably less often. This is partly explained by the effect of the azimuth directivity of slot on the cylinder, thanks to which the equatorial radiation patterns of the intermediate forms 3 approach type 1.

Page 77.

In Fig. 6 dotted line depicted circumference $v=v(r, \varphi)$, on which are replaced values v , corresponding to electrical depths Ψ at which were designed radiation pattern. The comparison of Fig. 6 and 7 makes it possible to trace the process or the characteristic strain of radiation patterns in proportion to the transition/junction of value of v from one region to another.

It is interesting to note that the width of radiation pattern when $\psi \approx 3\pi/8$ (at the level - 3 dB) is minimum ($\sim 50^\circ$) and close to $2 \arcsin \frac{\lambda}{2(2d-s)} = 56^\circ$, which indicates that its forming currents are concentrated in essence on the opening by width $(2d+s)$. This is logical, since noted value ψ close to the resonance (Fig. 8) and the currents prove to be "forbidden" virtually in the section of the surface, limited by passive slots.

A precise value of resonance electrical depth can be obtained,

equalizing the right sides of equalities (11b) and (16a), whence

$$\psi_m = \psi_0 - m\pi, \quad m = 0, 1, 2, \dots \quad (17a)$$

$$\begin{aligned} \psi_0 = \operatorname{arccctg} \left\{ \frac{v_0 s}{2} \left[\frac{2}{\pi} \ln \left| \frac{\pi \varepsilon}{2 v_0 s} - N_0(2v_0 d) - \right. \right. \right. \\ \left. \left. \left. + 0.302 \frac{1}{v_0 d} \sin \left(2v_0 d - \frac{\pi}{4} \right) \right] \right\} \quad (17b) \end{aligned}$$

- minimum value of resonance electrical depth.

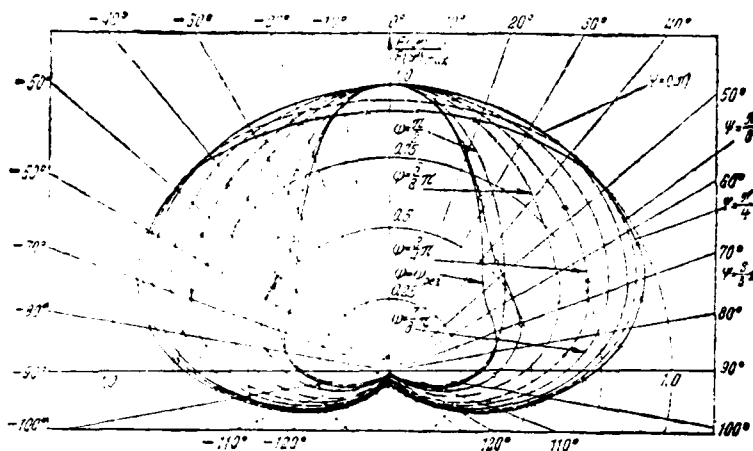


Fig. 7.

Page 78.

Fig. 8 gives dependence ψ_0 on the electrical width of groove v_0s ($v_0d = \pi$). It is interesting to note an extremely slow change in the resonance depth of groove in comparison with its width: with change v_0s from 0.1 to 0.0001, i.e., to three orders, ψ_0 was changed on $7^\circ 30'$, i.e., in all to $\sim 8.3\%$.

Should be focused attention on the criticality of voltage in the region of resonance to the depth of groove (to gap length). Relying on (16a, b), it is possible to show that the detuning in the electrical depth, which corresponds to change $|v|$ within limits $0.70|v|_{max}$, in general

$$\Delta\psi \approx \frac{\mu \sin^2 \psi_0 \Delta\tau}{\sqrt{1 + (\epsilon' \mu' - 1) \left(\frac{k_0}{v_0}\right)^2}} v_0 s. \quad (18)$$

where $\Delta\tau$ - width of "resonance curve" of $|v| = |v(\tau, \delta)|$ at the level 3 dB of lower than the maximum.

From (18) it follows that, in proportion to the contraction of slots, v runs in the circumference (see Fig. 6) near-resonance region (essential for control of the form of radiation pattern) with ever more tapered interval of depths (or gap lengths Δl) whose value order s . In this case change v in function ψ in the near-resonance region and outside it occurs according to the qualitatively different laws: relying on (9a, b) and (10a, b), it is possible to show that when $|\psi - \psi_0| \leq \Delta\psi$ and when $|\psi - \psi_0| > \Delta\psi$ the order of derivative $dv/d\psi$ proves to be equal to respectively $(v_0 s)^{-1}$ and $(v_0 s)$.

Of the aforesaid above, in particular, it follows that the use/application of excessively narrow passive slots can prove to be in practice undesirable due to the close tolerances for the geometry of grooves or gap, and also for the parameters of their filling substance.

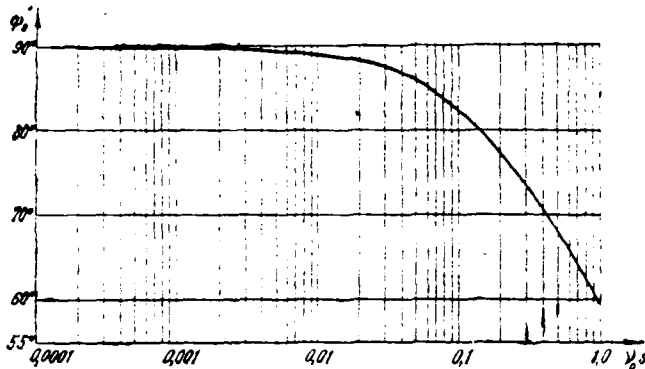


Fig. 8.

Page 79.

Conclusion/output.

1. Accepted in work simplified model of leaky-pipe antenna with passive slotted emitters in the form of system of three electrically narrow, infinitely long slots, gashed in metallic cylinder, and corresponding to it comparatively simple mathematical apparatus make it possible to explain fundamental laws governing formation of equatorial radiation patterns of antenna indicated. The behavior of the most important system characteristics yields to simple grapho-analytical interpretation, which simplifies the analysis of system.

2. Equatorial radiation pattern of system of slots is determined, mainly, by period of grating and by load of passive slots. A change in these parameters makes it possible in the relatively wide limits to control the form of radiation pattern. Depending on form, radiation pattern they can be divided into three fundamental types, each of which answers the specific range of change in the composite voltages of passive slots.

3. Independent of width of passive slots with change their loads within sufficiently wide limits of value of voltage pass constant/invariable sequence of values, and radiation patterns - constant/invariable sequence of forms, determined only by electrical period of grating. In this case the width of slots affects only the criticality of the corresponding dependences.

4. Antenna with passive emitters can be easily realized on base of leaky-pipe antennas with passive slots, adjacent to external walls of waveguide and by loaded short-circuited grooves, or by communicated flat/plane gap, which partially encompasses waveguide.

In conclusion the authors express appreciation to I. S. Pavlyushinoy for the aid while conducting of numerical calculations.

REFERENCES

1. A. A. Pistol'kors. Short-wave receiving antennas. Moscow-Leningrad, "Svyaz'tekhnizdat", 1933, page 46-65.
2. G. A. Yevstropov. Waveguide-slot antenna array. Author's certificate No 168340, kl., 21a 4601, MPK NO4, priority from 03, III, 1964.
3. La Groue A. H. Roberts G. F. «IEEE Trans on Antennas and Propagation», v. AP-14, 1966, № 1, p. 102-104.
4. R. Kyun. Microwave antennas. Translation/conversion from the German. Edited by M. P. Dolukhanov. L., "Sudostroyeniye, 1967, Section 7.2.1, pp. 330-336.
5. O. N. Tereshin. Synthesis of flat/plane and relief impedance antennas. Doctoral dissertation. MEIS, 1967.
6. Stein S. «IRE Trans on Antennas and Propagation», v. AP-10, 1962, № 5, p. 548-557.
7. D. R. White. Electromagnetic radiation from the cylindrical systems. M., "Soviet radio", 1963, page 40.
8. Nishida S. «IRE Trans. on Antennas and Propagation», v. AP-8, 1960, № 4, p. 354-360.
9. J. Slater. Transmission of ultra short waves. OGIZ, State Technical Press, 1947, page 119.
10. Theory of lines of transmission of superhigh frequencies. Vol. I. M., "Soviet radio", 1951, pages 150-151.

DOC = 30134005

PAGE

~~30~~
148

11. M. L. Lavrentyev, B. V. Shabat. Methods of the theory of complex variable functions. M., Fizmatgiz. 1958, page 125.

It acted in ed. 10/X 1970, after treatment/processing - 23/XI 1971.

Page 80.

Research of the consecutive diaphragm-forming diagrams for multiple-wires antenna.

M. A. Zhutikov, S. M. Mikheev.

Are examined the consecutive diagram-forming diagram and its modification, which makes it possible to reduce the number of elements/cells and to obtain maximum efficiency. On the base of the analysis of diagram is given the algorithm of the synthesis of amplitude-phase distributions (APR) in each channel according to the assigned values APR on the emitters, taking into account the redistribution of fields, caused by the presence of certain number of channels between the data by channel and by emitters. Are obtained the maximum energy evaluations/estimates of the work of series circuit, which depend on degree of interaction of assigned APR. Is given an example of the calculation of the modified diagram.

Introduction.

The consecutive diagram-forming schematic of multiple-pronged multichannel antenna is depicted in Fig. 19 [1]. It consists of the main-line feeder lines of transmission 1, connected with directional couplers 2 with transverse feeder lines 3, loaded to the grating of emitters 4. The latter can have any preassigned geometry. Creation on the emitters of the grating of the series/row of required APR is achieved by the selection of the coupling coefficients of the directional couplers with trunk lines and by phase wave velocity in the main-line and transverse lines.

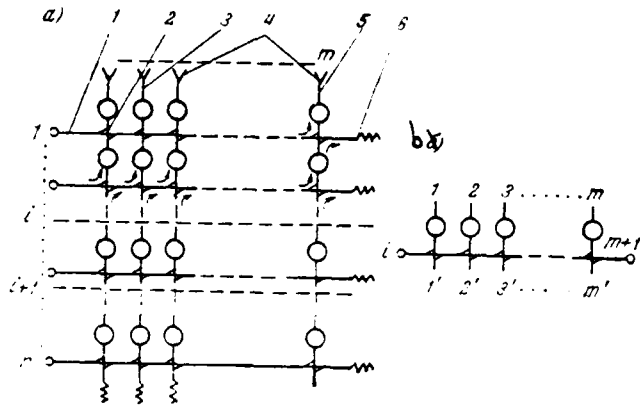


Fig. 1.

Page 31.

It is possible to assume that AFR are varied due to those concentrated phase converters 5, connected as shown in Fig. 1a. For the creation in the lines of mode of the traveling waves their ends/leads can be loaded for absorbing loads 6.

To the advantages of this diagram should be related that the fact that it is implemented from the uniform elements/cells, allows/assumes the use/application of contemporary technology of production and, which is especially important, it makes it possible without the modification to realize along each channel AFR of arbitrary form. However, for the practical realization of similar diagrams and evaluation/estimate of their maximum electrical

parameters the results, obtained in [1], are insufficient. Is conducted below detailed research of such diagrams, which contains the analysis on the basis of which are determined the maximum energy possibilities of diagram and is synthesized APR in each channel on assigned APR on the emitters. Solution of the problem of synthesis gives the possibility to reduce the calculation of the parameters of each channel to the known calculation of the feeder system of single-channel traveling-wave antenna.

Is examined the modification of series circuit, which makes it possible to reduce the number of elements/cells and the extent of feeder lines and to obtain maximum efficiency. Is given an example of the calculation of this diagram.

Examination is carried out for the grating of the matched emitters with compensated interaction on the inputs for any excitation. Couplers are assumed to be those ideally directed, but feeder lines - not having heat losses.

Analysis of diagram.

Let m - number of emitters in grating, n - number of channels of diagram. The order of numbering is shown in Fig. 1a.

Under the "i channel" of diagram we will understand both the i input of antenna and part of the diagram, included between the i-th and (i+1)-th the sections (Fig. 1a). We will speak about "its own" AFR and "its own" efficiency of the i channel, keeping in mind with respect to AFR and efficiency in by them section during the excitation of the i input.

For the analysis of diagram let us isolate the i channel (Fig. 1b). Here 1, 2, ..., m, m+1 - "output" terminals; i, 1', 2', ..., m' - "input" terminals. On terminals 1, 2, ..., m can exist both their own AFR of i channel and AFR from the channels with the higher reference number $j > i$. We will be given these AFR in the form of the columns of the composite amplitude: $a_{ij} > (j \geq i)$, calibrated to the single power of excitation.

Index i - the number of the section in question; j - number of excited channel.

Page 82.

Let us record the scattering matrix of the chosen multipole in the block form:

$$S_i = \begin{matrix} & i & 1 & \dots & m & 1' & \dots & m' & m+1 \\ \begin{matrix} i \\ 1 \\ \dots \\ m \\ 1' \\ \dots \\ m' \\ m+1 \end{matrix} & \begin{bmatrix} 0 & \langle a_{ii} \rangle & \langle 0 \rangle & f_i \\ a_{ii} \rangle & [0] & T_i & 0 \rangle \\ 0 \rangle & \tilde{r}_i & [0] & p_i \rangle \\ \tilde{j}_i & \langle 0 \rangle & \langle p_i \rangle & 0 \end{bmatrix} \end{matrix}$$

(i=1, 2, ..., n).

Here $\langle a_{ii}, a_{ii} \rangle$ - respectively row and column of dimensionless composite transmission factors from the i terminal to terminals 1, 2, ..., n, which coincide with standardized/normalized its own APR of channel;

\tilde{j}_i - transmission factor from the i terminal to terminal n+1;

$\langle p_i, p_i \rangle$ - row and column of transmission factors from terminals 1', ..., n' to terminal n+1;

T_i - square matrix/die of transmission factors from terminals 1, 2, ..., n to terminals 1', 2', ..., n';

[0], $\langle 0, 0 \rangle$ - null matrix, row and column;

- - sign of the transportation.

The zero units of matrix/die S_i consider the coordination of feeder lines and the ideal directivity of couplers.

Due to the directivity of couplers matrix/die T_i as it is not difficult to trace on the diagram, it has the triangular structure:

$$T_i = \begin{bmatrix} t_{11}' & 0 & 0 & \dots & 0 \\ t_{21}' & t_{22}' & 0 & \dots & 0 \\ t_{31}' & t_{32}' & t_{33}' & \dots & 0 \\ \dots & \dots & \dots & \dots & \dots \\ t_{m1}' & t_{m2}' & t_{m3}' & \dots & t_{mm}' \end{bmatrix} \quad (2)$$

where $t_{kk}' \neq 0 (k \leq l)$, $t_{kk}' = 0 (k > l)$ - matrix elements, $k, l = 1, 2, \dots, m$ (number of channel i in the matrix elements for the shortening is omitted).

Matrix/die T_i is not degenerated, since not some of its diagonal elements/cells it is equal to zero.

During the excitation of certain j channel on terminals $1', 2', \dots, m'$ i channel fall wave with an amplitude of $a_{i+1j} >$. In this case on terminals $1, 2, \dots, m$ will appear set/dialing $a_{ij} >$:

$$a_{ij} > = T_i a_{i+1j} >. \quad (3)$$

On the emitters during the excitation of the j channel AFR it will take the form

$$a_{1j} > = \left[\prod_{k=1}^i T_k \right] a_{ij} >. \quad (4)$$

and it can be substantially distorted and weakened on efficiency in comparison with its own AFR a_{ii} .

As can be seen from (4), for the finding AFR on radiators during the excitation of the j channel on assigned its own AFR a_{ii} it is necessary to know all matrices/dies T_k ($k=1, 2, \dots, j-1$). The elements/cells of each of these matrices/dies on the modulus/module are determined by their own AFR in the k channel, and on the phase - even and by the method of the inclusion of phase inverters in the channel. For the diagram in Fig. 1b matrix elements T_i will be

$$t_{kk'} = \sqrt{\frac{1 - \sum_{i=1}^k |a_i|^2}{1 - \sum_{i=1}^{k-1} |a_i|^2}} e^{i[\arg a_k - (k-1)\varphi]} \quad (5)$$

(diagonal elements/cells);

$$t_{ik'} = - \frac{|a_k a_i|}{\sqrt{\left(1 - \sum_{i=1}^{k-1} |a_i|^2\right) \left(1 - \sum_{i=1}^{l-1} |a_i|^2\right)}} \prod_{s=l-1}^{k-1} \cdot \times \sqrt{\frac{1 - \sum_{i=1}^s |a_i|^2}{1 - \sum_{i=1}^{s-1} |a_i|^2}} e^{i[\arg a_k - (l-1)\varphi]} \quad (6)$$

(off-diagonal elements/cells), $i, k=1, 2, \dots, n$.

Here a_k - k -th column element a_{ii} ; φ - phase change in the section of trunk line between the adjacent directional couplers. The number of channel i for the shortening is everywhere omitted.

Minus sign before the latter/last expression considers the rotation of phase on $-\pi/2$ in in l-th and k-th directional couplers.

Formulas (4)-(6) are convenient for the machine calculation AFR on the emitters according to known their own AFR.

Let us note that during the finding AFR on the emitters on assigned its own AFR the selection of the latter remains, in fact, arbitrary. Therefore more rational approach during the design of such diagrams consists of the synthesis of their own AFR on assigned AFR on the emitters. This leads to the single-valued selection of all $2n$ circuit parameters.

SYNTHESIS OF ITS OWN AMPLITUDE-PHASE DISTRIBUTIONS.

We will synthesize its own AFR $a_{ij} >$ in the arbitrary j channel on assigned AFR $a_{i1} >, a_{i2} >, \dots, a_{in} >$ ^{on} the emitters. From (3) and (4) it follows:

$$a_{i-1j} > = T_i^{-1} a_{ij} >; \quad (7)$$

$$a_{ij} > = \left[\prod_{k=1}^{j-1} T_k^{-1} \right] a_{i1} >. \quad (8)$$

Equality (8) is the unknown solution of the problem of synthesis. In practice the process of synthesis consists of the consecutive use/application of equalities from (7) to all channels from the upper to the lower ones (i.e. on index i from 1 to $n-1$). Thus, on given one a_{11} directly are designed the parameters of the 1st channel and on (5), (6) - matrix/die T_1 , then AFR a_{12} , a_{13} and so forth are counted over according to formula (7) in AFR a_{22} , a_{23} and so forth into the plane of terminals $1', \dots, m'$ the 1st channel and on a_{22} is designed the 2nd channel and matrix/die T_2 and so forth.

As can be seen from (7) and (8), calculation is connected each time with necessity of matrix inversion T_i . However, under some conditions calculation substantially is simplified. Let us consider the important case of the orthogonality of its own and any AFR in the arbitrary i section of the diagram:

$$\langle a_{ii} a_{ij}^* \rangle = 0 \quad (9)$$

$$j > i$$

(* - sign of composite coupling).

Let us introduce the relationships/ratios, which escape/ensue from the unitary matrices S_i :

$$\begin{aligned} \langle a_{ii} a_{ii}^* \rangle + |f_i|^2 &= 1, & (10) \\ \langle a_{ii} T_i^* + f_i \langle p_i^* \rangle &= \langle 0 \rangle, & (11) \\ a_{ii} \langle a_{ii}^* + T_i \tilde{T}_i^* &= E_m, & (12) \\ a_{ii} \langle f_i^* + T_i p_i^* \rangle &= \langle 0 \rangle, & (13) \\ \tilde{T}_i T_i^* + p_i \langle p_i^* &= E_m, & (14) \\ \langle p_i p_i^* \rangle + |f_i|^2 &= 1, & (15) \end{aligned}$$

where E_m - the unit matrices of order $m \times m$.

Multiplying (12) to the right on $a_{ij} \rangle$, to the left on T_i and using (7) and (9), it is not difficult to obtain

$$a_{i+1j} \rangle = \tilde{T}_i^* a_{ij} \rangle. \quad (16)$$

Thus, corresponding AFR in $(i+1)$ -th section it is calculated without the matrix inversion T_i .

let us show that if all AFR in the i section is mutually orthogonal, then AFR in $(i+1)$ -th the section they will be also orthogonal.

Actually/really, according to the condition

$$\begin{aligned} \langle a_{il} a_{ij}^* \rangle &= 0, & (17) \\ l \neq j, \quad l \geq i, \quad j \geq i. \end{aligned}$$

Taking into account (16), scalar product of vectors in $(i+1)$ -th the section will be recorded in the form

$$\langle a_{i+1l} a_{i+1j}^* \rangle = \langle a_{il} T_i^* \tilde{T}_i a_{ij}^* \rangle.$$

Page 85.

Let us multiply (12) to the left on $\langle a_{ij}$ to the right on $a_{ij}^* \rangle$. We will obtain

$$\langle a_{ij} a_{ij}^* \rangle \langle a_{ij} a_{ij} \rangle - \langle a_{ij} T_i^* \tilde{T}_i a_{ij}^* \rangle = \langle a_{ij} a_{ij}^* \rangle.$$

hence, using (17),

$$\langle a_{i+1j} a_{i+1j}^* \rangle = 0.$$

Thus, if on the emitters all assigned AFR they are mutually-orthogonal, then relationship/ratio (16) is retained at all steps/stages of calculation, which makes it possible to use it with the synthesis instead of (7). This can be recorded in the following form:

$$a_{ij} \rangle = \prod_{k=1}^{i-1} \tilde{T}_k^* a_{ij} \rangle. \quad (18)$$

Thus, the problem of the synthesis of its own AFR of each channel is reduced, in general, to turning of triangular matrices/dies with the known coefficients, and in the particular case of orthogonality AFR - to the simple operation of the multiplication of triangular matrix/die by the vector.

EFFICIENCY OF CHANNELS.

Let us rate/estimate the maximum energy circuit parameters. Let us introduce the designation: η_i - efficiency in the arbitrary i

section during the excitation of the j channel by the single power

$$\eta_{ij} = \langle a_{ij} a_{ij}^* \rangle. \quad (19)$$

In particular, η_{ii} - its own efficiency the i channel; η_{ii} - efficiency of the i channel according to the emitted power.

We trace the dependence efficiency in $(i+1)$ -th section on efficiency in the i section during the excitation of j channel ($j > i$). For this purpose let us multiply (14) to the left on $\langle a_{i+1j}$ to the right on $a_{i+1j}^* \rangle$. we will obtain

$$\langle a_{ij} a_{ij}^* \rangle = \langle a_{i+1j} a_{i+1j}^* \rangle - \langle a_{i+1j} p_i \rangle \langle p_i^* a_{i+1j}^* \rangle. \quad (20)$$

From (11) it follows that

$$\begin{aligned} \langle p_i^* a_{i+1j} \rangle &= -\frac{1}{f_i} \langle a_{ij} a_{ij}^* \rangle, \\ \langle a_{i+1j} p_i \rangle &= -\frac{1}{f_i^*} \langle a_{ij} a_{ij}^* \rangle. \end{aligned}$$

The substitution of these expressions in (20) taking into account (10) gives

$$\langle a_{ij} a_{ij}^* \rangle = \langle a_{i+1j} a_{i+1j}^* \rangle - \frac{1}{1 - \eta_{ii}} \langle a_{ij} a_{ij}^* \rangle \langle a_{ij} a_{ij}^* \rangle. \quad (21)$$

Page 86.

Let us introduce the designation

$$r_{ik} = \frac{|\langle a_{ij} a_{ik}^* \rangle|}{\sqrt{\eta_{ij} \eta_{ik}}} \quad (22)$$

- the standardized/normalized coefficient, which characterizes interaction AFR a_{ij} and a_{ik} . Index i indicates the number of section,

indices l and k - number of the channels:

$$l, k \geq i, l \neq k.$$

Coefficient r_{lk} can vary within the range of 0 to 1.

From (21) it follows

$$\eta_{i+1} = \eta_{ij} \left(\frac{1 + \eta_{ii} r_{ii}^2}{1 - \eta_{ii}} \right). \quad (23)$$

With the consecutive synthesis of diagram, described in the previous section, values η_{ii} , η_{ij} and r_{ii} are initial, and (23) gives the value of efficiency in $(i+1)$ -th section.

Transmission factor according to the power from section $i+1$ to section i of arbitrary AFR a_{i+1} :

$$q_{ij} = \frac{\langle a_{ij} a_{ij}^* \rangle}{\langle a_{i+1j} a_{i+1j}^* \rangle} = \frac{\eta_{ij}}{\eta_{i+1j}} = \frac{1 - \eta_{ii}}{1 - \eta_{ii} + \eta_{ii} r_{ii}^2}. \quad (24)$$

In particular, if AFR are orthogonal:

$$r_{ii} = 0,$$

then from (24), (25) it follows: $\eta_{i+1j} = \eta_{ij}$, $q_{ij} = 1$, power is transmitted by the vertical feeders from $(i+1)$ -th section to the i -th (Fig. 1A) without the losses.

Above it was shown that if assigned AFR on the emitters are mutually orthogonal, then all AFR were orthogonal in any section diagrams.

Thus, in this case efficiency of any channel according to the emitted power it proves to be to its equal own efficiency, caused by the losses in the load of this channel, which can be done how convenient small.

In the case of nonorthogonality of AFR

$$r_{ij} \neq 0,$$

$$q_{ij} < 1$$

and according to (23) efficiency η must grow with the increase of index i .

In particular, with $r_{ij}=1$ AFR $a_{ii} >$ and a_{i+i} they coincide:

$$q_{ij} = 1 - \eta_{ii}$$

also, when $\eta_{ii} \rightarrow 1$ $q_{ij} \rightarrow 0$, transmission of AFR $a_{i+i} >$ from section $i+1$ to section i is absent, entire/all energy is absorbed in the load of the i channel.

On the strength of the fact that value efficiency must be less than unity, increase η_{ii} with increase i is limited, that imposes the limitation to a number of channels during their assigned interaction or for interaction with the assigned number of channels.

Page 87.

We will obtain these limitations for a special case of diagram

with the uniformly effective channels during identical interaction between themselves of all AFR:

$$\eta_{1j} = \eta_1, \quad j = 1, 2, \dots, n; \quad (25)$$

$$r_{1k} = r_1, \quad l \neq k; \quad l, k = 1, 2, \dots, n. \quad (26)$$

On (23) all efficiency in the second section will be also identical:

$$\eta_{2j} = \eta_2 = \eta_1 \left(1 - \frac{\eta_1 r_1^2}{1 - \eta_1} \right). \quad (27)$$

Interaction AFR in second section:

$$r_{2lk} = \frac{1}{\eta_2} | \langle a_{2l} a_{2k}^* \rangle | = \frac{1}{\eta_2} | \langle a_{1l} \tilde{T}_1^{-1} T_1^{-1} a_{1k}^* \rangle |. \quad (28)$$

From (12) it follows

$$\tilde{T}_1^{-1} T_1^{-1} = [E - a_{1i}^* \langle a_{ii} \rangle]^{-1} = E + \frac{a_{1i}^* \langle a_{ii} \rangle}{1 - \langle a_{ii} a_{ii}^* \rangle}.$$

Is here used the known inversion formula of matrix/die [2].

Thus, from (28) it follows that

$$r_{2lk} = \frac{1}{\eta_2} \left| \langle a_{1l} a_{1k}^* \rangle + \frac{\langle a_{1l} a_{1l}^* \rangle \langle a_{1k} a_{1k}^* \rangle}{1 - \eta_1} \right|.$$

Great possible interaction (for any l and k)

$$r_{2lk \max} = r_2 = \frac{\eta_1 r_1}{\eta_2} \left(1 - \frac{\eta_1 r_1}{1 - \eta_1} \right) = \frac{r_1 (1 - \eta_1 + \eta_1 r_1)}{1 - \eta_1 + \eta_1 r_1^2}. \quad (29)$$

The conversions of form (27) and (29) will occur with each increase in the number of section; therefore for arbitrary i

$$\eta_i = \eta_{i-1} \left(1 + \frac{\eta_{i-1} r_{i-1}^2}{1 - \eta_{i-1}} \right), \quad (30)$$

$$r_{i-1} = \frac{r_{i-2}(1 - \eta_{i-2} + \eta_{i-2} r_{i-2})}{1 - \eta_{i-2} + \eta_{i-2} r_{i-2}^2}, \quad (31)$$

$$i = 1, 2, \dots, n.$$

With $i=n$ from condition $\eta_n \leq 1$ and (30)

$$\eta_{n-1} \leq \frac{1}{1 + r_{n-1}}. \quad (32)$$

Page 88.

By induction taking into account (32), (30) and (31) it is not difficult to show that

$$\eta_1 \leq \frac{1}{1 + (n+1)r_1}$$

or

$$\eta_{max} = \frac{1}{1 - (n-1)r}. \quad (33)$$

Formula (33) establishes the unknown connection/communication between maximally achievable efficiency of channels η_{max} , their number n and assigned interaction of AFR r under the conditions (25), (26). Fig. 2 this connection/communication shows graphically.

MODIFIED SERIES CIRCUIT.

Let us consider the limiting case when $\eta_{ii}=1$ ($f_i=0$). In this case the connection/communication in the latter/last coupler of the i

186

channel must be single; therefore the presence of terminals m' and $m+1$ (Fig. 1b) is deprived of sense and it is possible to reject/throw them. Discussing similarly for 1, the 2nd and so forth of channels, we come to the modified diagram, shown in Fig. 3a (two-channel diagram of this form is given in [1]).

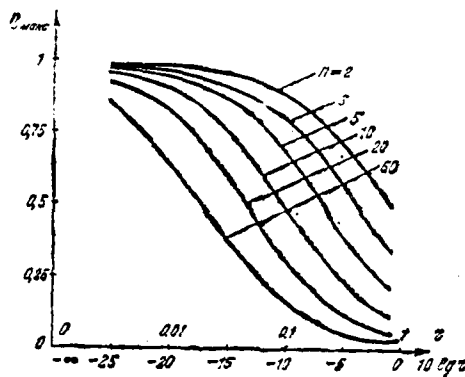


Fig. 2.

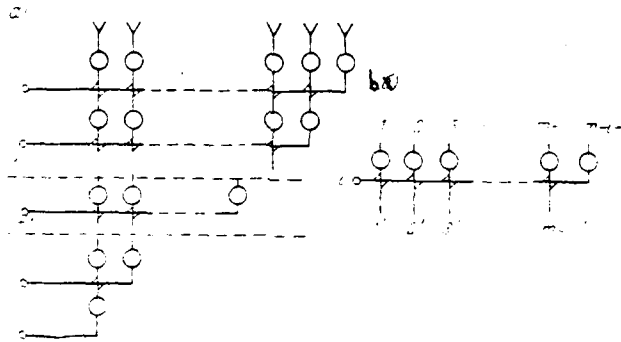


Fig. 3.

Page 39.

The arbitrary i channel of the modified diagram will have a number of output terminals $m-i+1 \leq m$, where m - number of radiators (Fig. 3b). Scattering matrix of this channel

$$S_i = \begin{matrix} & \begin{matrix} 1 \dots m-i+1 & 1' \dots m-i' \end{matrix} \\ \begin{matrix} i \\ 1 \\ \vdots \\ m-i+1 \\ 1' \\ \vdots \\ m-i' \end{matrix} & \begin{bmatrix} 0 & \langle a_{ii} & \langle 0 \\ a_{ii} & [0] & T_i \\ 0 \rangle & \tilde{T}_i & [0] \end{bmatrix} \end{matrix} \quad (34)$$

Here T_i - no longer square, but rectangular matrix/die.

From unitarity S_i we will obtain:

$$\langle a_{ii} a_{ii}^* \rangle = 1. \quad (35)$$

$$\langle a_{ii} T_i^* \rangle = \langle 0. \quad (36)$$

$$a_{ii} \rangle \langle a_{ii}^* + T_i \tilde{T}_i^* = E_{m-i+1}. \quad (37)$$

$$T_i T_i^* = E_{m-i'}. \quad (38)$$

During the excitation of terminals $1', \dots, m-i'$ the column of amplitudes $a_{i-1} \rangle$ on terminals $1, \dots, m-i+1$ will be the column

$$a_{ii} \rangle = T_i a_{i-1} \rangle \quad (39)$$

(columns $a_i \rangle$ and $a_{i-1} \rangle$ have various order).

From (38) it follows

$$\langle a_{ii} a_{ii}^* \rangle = \langle a_{i+1i} a_{i+1i}^* \rangle. \quad (40)$$

i.e. there are no power losses during the transmission from section $i+1$ to section i , as this is obvious and physically.

From the absence of power losses must follow that AFR a_{ii} and a_{i+1i} are orthogonal with any a_{i+1i} .

Is actual/real, from (36) and (39)

$$\begin{aligned} \langle a_{ii} T_i^* a_{i+1i} \rangle &= 0 \quad \text{or} \\ \langle a_{ii} a_{i+1i}^* \rangle &= 0 \end{aligned}$$

with any a_{i+1i} .

The relationship/ratio, necessary for the synthesis of its own AFR, we will obtain from (38) and (39):

$$a_{i+1i} = T_i^* a_{ii}. \quad (41)$$

to let us note that equality (41) is obtained for arbitrary a_{ii} but not for arbitrary a_{i+1i} and is applicable only for similar a_{ii} for which by selection a_{i+1i} it is possible to satisfy equality (39), i.e., for a_{i+1i} the orthogonal ones with respect to a_{ii} . In other words, with the help of this diagram it is possible to realize

completely accurately only knowingly orthogonal AFR.

Page 90.

Let us show, however, that if assigned AFR are not orthogonal, then (42) gives best approximate solution in the sense of root-mean-square deviation.

Best approximate solution of equ. (39), in the sense of root-mean-square deviation, takes form [3]

$$a_{i+1j} > = T_i^+ a_{ij} >, \quad (43)$$

where T_i^+ - pseudo-inverse matrix/die with respect to T_i determined by equality [3]:

$$T_i T_i^+ T_i = T_i. \quad (44)$$

Let us present matrix/die T_i in the form of the block:

$$T_i = \begin{pmatrix} A_i \\ < B_i \end{pmatrix},$$

where A_i - triangular matrix/die of order $m-i \times m-i$;

$< B_i$ - row.

From [3, page 64] we will obtain

$$T_i^+ = [\tilde{A}_i^* A_i + B_i^* > < B_i]^{-1} (\tilde{A}_i^* B_i^* >), \quad (45)$$

where $(\tilde{A}_i^* B_i^* >)$ - block recording of matrix/die.

But from (38) we have

$$(\bar{A}_i B_i >) \begin{pmatrix} A_i \\ < B_i^* \end{pmatrix} = [\bar{A}_i A_i^* + B_i > < B_i^*] = E,$$

therefore (45) can be presented as

$$T_i^* = (\bar{A}_i B_i >) = \bar{T}_i$$

and (43) it will be rewritten as

$$a_{i+1} > = \bar{T}_i^* a_{ij} >.$$

that it coincides with (42).

Thus, for the synthesis of the modified diagram it is necessary to use (42). If the given ones on emitter AFR are nonorthogonal, then true AFR will be nevertheless orthogonalized, but (42) will ensure best approximation to required AFR in the sense of average quadratic.

EXAMPLE OF CALCULATION BY MODIFIED DIAGRAM.

As the illustrative let us lead calculation of modified series circuit with a number of emitters $m=4$, forming four orthogonal AFR.

Page 91.

Analogous AFR can be obtained on Butler's four-channel matrix" [1]:

191

$$\begin{aligned}
 a_{11} > = \begin{bmatrix} \frac{1}{2} \\ \frac{1}{2} e^{-145^\circ} \\ \frac{1}{2} e^{-190^\circ} \\ \frac{1}{2} e^{-1135^\circ} \end{bmatrix}; \quad a_{12} > = \begin{bmatrix} \frac{1}{2} e^{-145^\circ} \\ \frac{1}{2} e^{+190^\circ} \\ \frac{1}{2} e^{-1135^\circ} \\ \frac{1}{2} \end{bmatrix}; \quad a_{13} > = \begin{bmatrix} \frac{1}{2} \\ \frac{1}{2} e^{-1135^\circ} \\ \frac{1}{2} e^{+190^\circ} \\ \frac{1}{2} e^{-145^\circ} \end{bmatrix} \\
 a_{14} > = \begin{bmatrix} \frac{1}{2} e^{-1135^\circ} \\ \frac{1}{2} e^{-190^\circ} \\ \frac{1}{2} e^{-145^\circ} \\ \frac{1}{2} \end{bmatrix}
 \end{aligned}$$

The first channel is designed directly on given one a_{11} . It is shown in Fig. 4a. In the diagram are shown crosstalk attenuations and phase shifts/shears in the degrees (phase shifts are selected taking into account supplementary phase displacement on $-\pi/2$ in the directional couplers).

Matrix/die T_1 takes the form

$$T_1 = \begin{bmatrix} \frac{\sqrt{3}}{2} e^{190^\circ} & -\frac{1}{2\sqrt{3}} e^{1135^\circ} & \frac{1}{2\sqrt{3}} & \frac{1}{2\sqrt{3}} e^{145^\circ} \\ 0 & \frac{2}{3} e^{1135^\circ} & \frac{1}{16} & \frac{1}{16} e^{145^\circ} \\ 0 & 0 & -\frac{1}{12} & \frac{1}{12} e^{145^\circ} \end{bmatrix}$$

For AFR in the second section we will obtain on (42)

$$a_{21} > = \begin{bmatrix} 0,577 e^{145^\circ} \\ 0,408 e^{-1135^\circ} \\ 0,707 e^{145^\circ} \end{bmatrix}; \quad a_{23} > = \begin{bmatrix} 0,577 e^{190^\circ} \\ 0,643 e^{118,5^\circ} \\ 0,5 e^{-145^\circ} \end{bmatrix}; \quad a_{24} > = \begin{bmatrix} 0,577 e^{-145^\circ} \\ 0,643 e^{126,5^\circ} \\ 0,5 e^{145^\circ} \end{bmatrix}$$

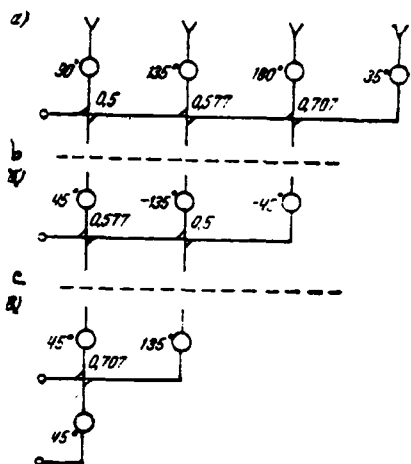


Fig. 4.

Page 92.

Second channel of diagram is shown in Fig. 4b. Matrix/die \tilde{T}_2 takes the form

$$\tilde{T}_2 = \begin{bmatrix} 0,816e^{i45^\circ} & -0,288e^{-i135^\circ} & 0,5e^{-i135^\circ} \\ 0 & 0,866e^{-i135^\circ} & 0,5e^{-i135^\circ} \end{bmatrix}$$

We will obtain on (42) for AFR in the third section

$$a_{33} > = \begin{bmatrix} 0,707e^{i135^\circ} \\ 0,707e^{-i135^\circ} \end{bmatrix}; \quad a_{34} > = \begin{bmatrix} 0,707 \\ 0,707e^{-i90^\circ} \end{bmatrix}$$

Consequently, in the latter/last node it is necessary to use the directed coupler with 3-decibel connections/communications and the phase shifts, shown in Fig. YaCh.

CONCLUSION.

In conclusion let us note that a selection of one or the other type of the diagram-forming diagram depends on the degree of interaction of assigned AFR and permissible distortions of radiation patterns. In the implementation of orthogonal AFR the modified diagram has an advantage before the usual both according to the number of elements/cells and on efficiency. With nonorthogonal assigned AFR it orthogonalizes them, respectively distorting radiation patterns. Normal series circuit in this case accurately reproduces diagrams due to the decrease efficiency.

REFERENCES

1. Microwave scanning antennas, ed by Hansen, v. 3, 1965.
2. D. K. Faddeyev, V. P. Faddeyeva. Computational methods of linear algebra. M., Fizmatgiz, 1963.
3. P. R. Gantmakher. Theory of matrices/dies. M., "Science", 1967.

It acted in ed. 22/VI 1971.

Page 93.

Algorithm of the selection of the optimum location of the emitters of linear antenna array by the method of coordinate-by-coordinate sorting.

Yu. Kh. Vernishev, V. V. Gaurman, M. B. Zakson.

Is proposed the algorithm of the global search of the optimum location of the emitters of antenna array. Algorithm is approved on the synthesis of the nonequidistant gratings, optimum in Dol6fa-Chebyshev's sense. The obtained results exceeded the achievements earlier in other works. Is formulated proposition about the possible way of the construction of nonequidistant gratings.

FORMULATION OF THE PROBLEM.

Is assigned linear equal-amplitude, symmetrical, cophasal grating with the radiation pattern

$$F(\theta) = 1 + 2 \sum_{i=1}^n \cos(2\pi x_i \sin \theta), \quad (1)$$

where x_i - distance of the i emitter from the center of grating in the wavelengths λ ; θ - direction of radiation/emission, calculated off the normal to the grating.

The position of central and outer emitters is fixed/recorded.

$$n = \frac{N-1}{2},$$

where N - number of emitters.

For the location of emitters are superimposed the limitations:

$$d_i \geq 0; \quad (2)$$

$$2 \sum_{i=1}^n d_i = L. \quad (3)$$

Here $d_i = x_i - x_{i-1}$; L - length of grating. Problem consists in

n-dimensional euclidean space $R_x (x_i \in R_x)$ selecting of the initial point, gradient search from which would lead to the global minimum of the function:

$$\Phi = \frac{|F(\theta)_{\max}|}{F(0)}, \quad (4)$$

where $F(\theta)_{\max}$ - maximum value of the side lobe of radiation pattern in the interval of angles $[\theta_0 \div \frac{\pi}{2}]$;

$F(0)$ - the value of the major lobe/lug of radiation pattern with $\theta=0$;

$2\theta_0$ - width of the fundamental maximum of radiation pattern on level of maximum side lobe.

Page 94.

Thus, discussion deals with finding of the location of emitters in the nonequidistant grating, which has the radiation pattern, close to optimum in the sense Dol'f-Chebyshev.

METHOD OF THE SOLUTION. Examples of use/application.

The proposed method is based on the use by computers. It encompasses the following sequence of operations:

1. Selection of the initial location of the emitters of grating.
2. Displacement/movement of first (near to central) emitter along aperture of grating with step/pitch ΔL and selection of its best position on criterion (4).
3. Selection by analogy of best position for second emitter in fixed/recorded positions of others, etc.

Process cyclically is continued until at least one of the emitters can be placed to the following criterion (4) position with this step/pitch of displacement/movement along the aperture ΔL .

4. Obtained solution is used as initial approximation/approach with gradient descent [1].

The described method was approved on the synthesis of lattice row. First of all let us pause at the grating by the length 40λ , which consists of 21 isotropic emitter with the half width of fundamental ray/beam $\mu_0=0.04$ and the step/pitch $\Delta L=0.1\lambda$ ($\mu_0=\sin\theta_0$). As the initial ones were undertaken three different cases of the location of emitters.

Fig. 1a, b, c shows the positions of emitters in the aperture of grating before and after conducting of operations on paragraphs 1, 2 and 3. (in view of the symmetry of grating is shown only the half aperture. Central emitter - the first to the left).

Initial location in Fig. 1a corresponds to equidistant grid with distance of d between the emitters, equal to $d=2\lambda$.

198

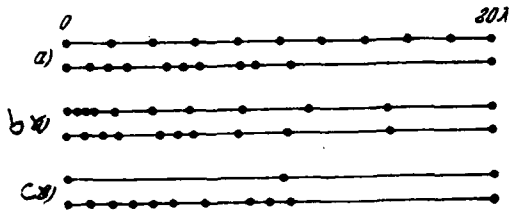


Fig. 1.

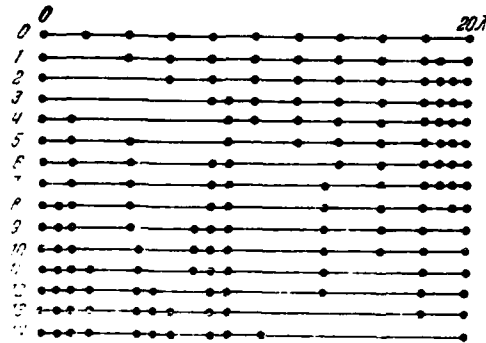


Fig. 2.

Page 95.

For this case, called further the case "a", Fig. 2 shows the sequence of changing the positions of emitters in the course of fulfilling the operations on paragraphs 1, 2, 3.

In Fig. 1b as the initial is undertaken the polynomial location during which interelemental distances d_i were calculated from the formula

$$d_i = c_0 + c_1 i + c_2 i^2, \text{ где } c_0 = 1; c_1 = -0.1; c_2 = +0.15.$$

Figure 1c corresponds to the case when all emitters of original lattice (except central and extreme ones) are assembled in each half aperture into one point.

The optimum locations of emitters, shown in Fig. 1a, b, c, led

after gradient descent of them (operation on p. 4) respectively to the following values of maximum side lobe:

-12.3 dB; -11.7 dB; -11.9 dB.

In this case the positions of emitters were changed they unessentially and virtually correspond to the positions, shown in Fig. 1. For an example Table 1 shows for the case "a" the optimum location of emitters after full/total/complete coordinate-by-coordinate sorting and subsequent gradient descent ($L=40\lambda$).

The comparison of the radiation patterns, obtained in all three cases, shows that with the full/total/complete coordinate-by-coordinate sorting the side-lobe level reached weakly depends on the selection of original lattice. (Radiation pattern for the case "a" it is given in Fig. 3).

One should take into account, however, that this factor substantially affects retrieval time. Thus, for instance, during the initial polynomial distribution was required approximately/exemplarily three times less than cycles (cycle-girder/drive of element/cell along the aperture), than in two remaining cases.

Let us note also that the gradient descent did not lead to an essential improvement in the results. Sidelobe level was improved only by 0.2-0.4 dB.

Table 1.

(1) Номер излучателя	1	2	3	4	5	6
(2) Координаты x_i	0,798 487	1,702 691	2,508 611	4,468 041	5,334 091	6,166 216
(1) Номер излучателя	7	8	9	10		
(2) Координаты x_i	7,897 522	8,721 284	10,050 423	20,000 000		

Key: (1). Number of radiator. (2). Coordinates.

Page 96.

As the second example was carried out employing the same procedure the optimization of nonequidistant grating with $L=20\lambda$, $N=21$ and $u_0=0.05$. Sidelobe level proved to be equal - 14 dB during the optimum location of emitters, shown in Fig. 4.

Was also traced grating by length $L=40\lambda$ at different values of u_0 . Fig. 5 shows the optimum locations of emitters with different width of the fundamental ray/beam u_0 . As one would expect, the expansion of fundamental ray/beam leads to a decrease in the sidelobe level. The effect of the width of fundamental ray/beam on the attained at the optimization sidelobe level Φ is shown in Table 2.

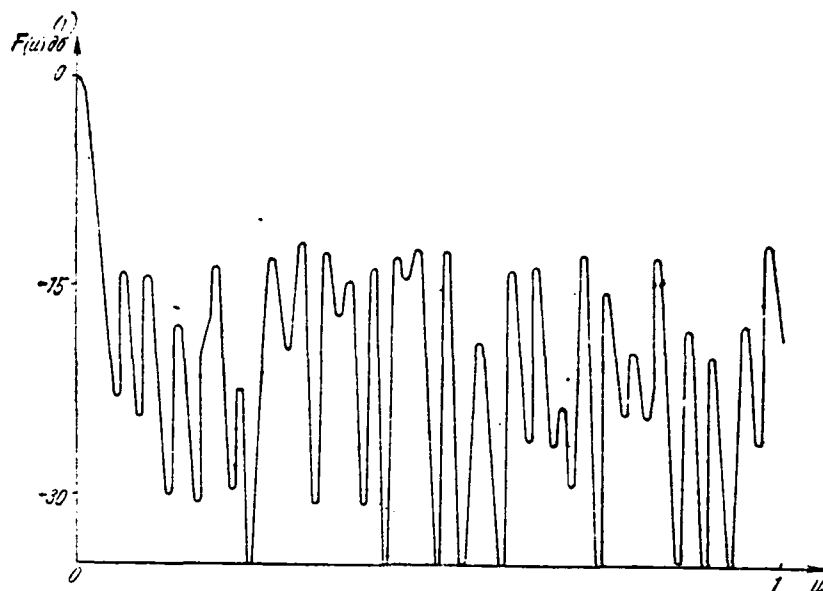


Fig. 3.

Key: (1). dB.



Fig. 4.



Fig. 5.

Page 97.

As can be seen from figures 1(a, b, c) 4 and 5, in the obtained optimum gratings are absent the interelemental distances less than the value 0.5λ . Furthermore, almost for all synthesized gratings is characteristic the appearance of equidistant sublattices with a

number of elements/cells from 2 to 6 with distances of d between them within the limits $0.6\lambda \leq d \leq 0.9\lambda$.

Thus, for the purpose of the reduction of the laboriousness for computations as the initial it would be expedient to choose precisely this group location of emitters. Furthermore, on the basis of the results, one should, apparently consider that the search of optimum in a Dol'f-Chebyshev sense gratings with interelemental distances less 0.5λ , is unsuitable.

Table 2.

(1) Ширина основ- ного луча U_0	0.02	0.03	0.04
(2) Значение Φ , дБ	-10,5	-11,5	-12,0

Key: (1). Width of the fundamental ray/beam U_0 . (2). Value Φ , dB.

INTEGRAL EVALUATION CRITERIA OF LATERAL RADIATION AND ITS COMPARISON WITH THE MINIMAX CRITERION.

For the evaluation/estimate of radiation/emission out of the fundamental ray/beam can be also used integral evaluation criteria of the lateral radiation

$$S = \int_{u_0}^1 F^2(u) du, \quad \text{where } u = \sin \theta. \quad (5)$$

An improvement in the diagram on the integral criterion leads in the considerable angular interval to its improvement and in the minimax sense. Integral criterion is convenient when integral in the right side of formula (5) can be undertaken analytically, since this allows (approximately/exemplarily to two orders in the case in question) to reduce the time of calculation, since there is no need for in the survey of radiation pattern in angular interval $[\theta_0 - \pi/2]$.

Let us give several examples of calculations according to the integral criterion.

Fig. 6 shows distribution x_0 obtained by full/total/complete coordinate-by-coordinate countershaft on criterion (5) with $L=40\lambda$ and $u_0=0.04$. As the initial was undertaken equidistant grating.

As can be seen from figure, emitters with the varied position formed equidistant sublattice with distance of d , different 0.9λ .

Page 98.

It is interesting that when as the initial was undertaken distribution x_0 which is the grouped in center equidistant sublattice with $d=0.9\lambda$ (Fig. 7) full/total/complete coordinate-by-coordinate sorting according to criterion (5) it led to the solution, which coincides with the initial distribution.

The corresponding optimum radiation pattern has a sidelobe level - 12 dB with the width of the fundamental ray/beam $u_0=0.09$.

For the more detailed research of the interconnection between the integral and minimax criteria was set the special experiment whose results illustrates Fig. 8. Along the axis of the ordinates of

figure is deposited/postponed the value of function Φ along the axis of abscissas - number of the cycle of coordinate-by-coordinate sorting on criterion Φ . Solid line shows a change in value Φ in the cycles with the initial equidistant grating. On each cycle was checked also the value of the integral criterion S . A change in value S in the cycles is shown by the dotted line (initial values S and Φ are accepted as unity). As can be seen from figure, the decrease of value Φ imply and decrease of S . This it suggests about the fact that for decreasing the retrieval time as the initial distribution during the optimization according to minimax criterion Φ should be used the solution, obtained on criterion S .

This assumption was checked based on the following example. Fig. 5c shows the optimum location of emitters after full/total/complete coordinate-by-coordinate sorting the minimax criterion from the original lattice, which corresponds to Fig. 7.

As can be seen from these figures, the displacement/movement one emitter alone proved to be sufficient in order to obtain sidelobe level Φ equal - 12 dB with the width of the fundamental ray/beam $U_0=0.04$.



Fig. 6.



Fig. 7.

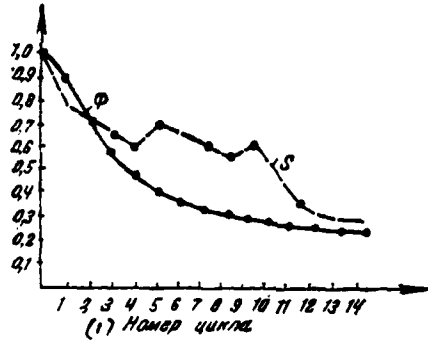


Fig. 8.

Key: (1). Number of cycle.

Page 99.

THE POSSIBLE WAY OF THE CONSTRUCTION OF NONEQUIDISTANT GRATINGS.

Generalizing the given above results, it is possible to formulate the proposition according to which the nonequidistant grating, close to the optimum in a Dol'f-Chebyshev sense, can be constructed in the form of the combination of equidistant sublattices with distances of d in the limits $0.5\lambda < d < \lambda$.

On the base of this proposition was produced the optimization of

nonequidistant grating with $L=50\lambda$, $N=21$ and $u_0=0.04$.

As the initial was undertaken the distribution, which consists of the combination of two equidistant sublattices with the distance between emitters $d=0.8\lambda$ (Fig. 9a).

For obtaining the final solution proved to be sufficient the displacement/movement only of one element/cell (Fig. 9b).

For the comparison Table 3 gives for $L=50\lambda$ the location of emitters, obtained after gradient descent with the initial approximation/approach, which corresponds to Fig. 9b, and also the location, obtained with analogous initial data by the method of dynamic programming [2].

Let us note that as a result of descent the sidelobe level was lowered with -12 dB to -12.5 dB. The obtained radiation pattern is given in Fig. 10. For the comparison dotted line here gave the radiation pattern of grating, obtained in work [2].

As can be seen from table, gradient descent did not significantly break laws governing proposed above the location of emitters in grating.

Table 4 gives the comparison of the results, obtained by the method of full/total/complete coordinate-by-coordinate sorting, with the data, undertaken from works [2, 3] ($L=50\lambda$, $N=21$, $u_0=0.04$).

As can be seen from Table 4 the method proposed is preferable both on the laboriousness for computations and on the side-lobe level reached.

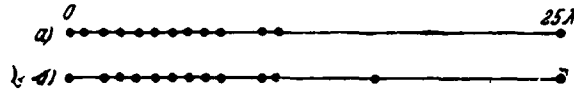


Fig. 9.

Table 3.

(1) Номер излучателя	(2) Расстояние x_i	
	(3) Покоординатный перебор и гради- ентный спуск	(4) Динамическое программиро- вание
1	1. 58 44 45	2.5
2	2. 39 67 92	3.0
3	3. 23 61 45	3.5
4	3. 97 94 69	4.0
5	4. 74 35 81	4.5
6	5. 61 21 21	5.0
7	6. 42 78 20	6.5
8	7. 20 62 58	7.5
9	8. 99 58 47	8.5
10	9. 81 40 32	10.5
11	16. 54 24 31	13.0
12	25. 00 00 00	25.0

Key: (1). Number of emitter. (2). Distance. (3).

Coordinate-by-coordinate sorting and gradient descent. (4). Dynamic programming.

Page 100.

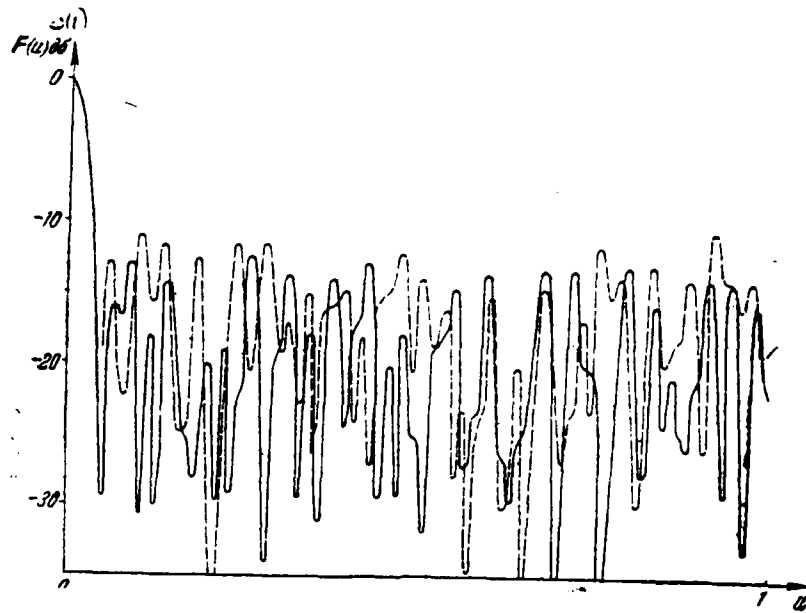


Fig. 10.

Key: (1) . dB.

TABLE 4.

(1) Метод	(2) Достигнутый уровень дб. боковых лепестков	(3) Число апробированных в процессе поиска комбинаций расположений излучателей
(4) Полного по- координатно- го перебора	-12,5	100
(5) Динамичес- кого прог- раммирования (модифици- рованный) [2]	-10,1	—
(6) Метод рабо- ты [3]	-8,5	7000

Key: (1). Method. (2). Level reached, dB, side lobes. (3). Number of approved in process of search of combinations of locations emitters. (4). Full/total/complete coordinate-by-coordinate sorting. (5). Dynamic programming (modified) [2]. (6). Method of operation [3].

Conclusion/output.

1. Is proposed algorithm of global search of location of emitters in by linear nonequidistant antenna to grating, close to optimum in Dol'f-Chebyshev's sense. As the basis of algorithm is assumed the method of the full/total/complete coordinate-by-coordinate sorting, with which is produced the cyclic permutation of emitters along the aperture of grating and the selection of the radiation patterns, best from the point of view of the criterion accepted.

2. In process of final adjustment of algorithm is traced interconnection between integral evaluation criteria of lateral radiation and minimax criterion. It is established/installed, that the process of search can be considerably accelerated, if at first the minimization of news on the integral criterion, and then on the criterion minimax.

Page 101.

3. Results, obtained during construction of series/row of nonequidistant antenna arrays, and also comparison with previously data reached testify about efficiency of algorithm proposed.

4. On base of obtained results is formulated proposition according to which nonequidistant grating, close to optimum in Dol'f-Chebyshev sense, can be constructed in the form of combination of equidistant sublattices with interelemental distances in limits $0.5\lambda < d < \lambda$.

REFERENCES

1. N. A. Martynov, E. D. Ustinov, S. A. Tsarapkin. Use/application of mathematical programming to the synthesis of antenna arrays. coll. of "Antenna", iss. 3. M, "Connection/communication", 1968.

2. Arora R. K. Krisnamaharyby N. C. V. synthesis of Unequally spaced arrays using dynamic programming. — «IEEE Trans.», v. AP-16, 1968, № 5.
3. Lo, V. T. and Lee S. W. A study of space-tapered arrays. — «IEEE Trans.» — v. AP-14, 1966.

It acted in ed. 18/VIII 1970; after treatment/processing - 13/X 1971.

Performance calculation of antenna radiation with the circular aperture.

L. Z. Pazin, Yu. S. Petreykov.

In connection with antenna with the circular aperture, field distribution in which is assigned by function $(1-\rho^2)^n$, are obtained expressions for the radiation characteristics in the region of approaching Fresnel, and also for the radiation pattern in the remote zone in the presence of quadratic phase distortions in the aperture.

These characteristics are described with the help of the proposed in the present work functions of three variable/alternating, which are the linear combinations of the Bessel functions and Lommel.

Are examined examples of the use/application of the obtained results.

Introduction.

The use/application of cylindrical functions of two variable/alternating (functions of Lommel [1, 2, 6, 7]) makes it

possible to determine the radiation characteristics of antenna with the circular aperture in the region of approaching Fresnel. Thus, for instance, in the work of Hansen [3, 4] it is shown that the combination of the functions of Lommel $U_1(m, u) + iU_2(m, u)$ describes the radiation pattern of evenly and cophasally excited circular aperture in field indicated above (in the works [3, 4] is allowed the error in the determination of the first variable/alternating function of Lommel, in the adopted there designations one should assume/set $w = ka^2/R = \pi/4\Delta$). In work [5] is introduced the function

$$W_0^n(m, u) = \left(\frac{2}{i}\right)^n \frac{\partial^n}{\partial m^n} \left\{ \frac{1}{m} [U_1(m, u) + iU_2(m, u)] \right\},$$

describing the antenna radiation pattern with the circular aperture, amplitude distribution of field in which is assigned by function $(1-t^2)^n$.

In the present work are obtained the expressions for calculating some radiation characteristics of antenna with the circular aperture with field distribution of form $(1-pt^2)^n$, which assume the use of the tabulated functions.

RADIATION PATTERN IN A REGION OF APPROACHING FRESNEL.

Field at observation point M (Fig. 1A) let us determine with the help of Kirchhoff's integral of the scalar function of field distribution in the aperture:

$$E_M = E_0 e^{ikz} = \frac{1}{\lambda} \int_S 4(\rho_1) e^{i\psi(\rho)} \frac{e^{-ikr}}{r} dS. \quad (1)$$

where $A(\rho_1)$ and $\psi(\rho_1)$ - axisymmetric functions of amplitude distribution and phase of field in the aperture with a diameter of $D=2r_1$; r - distance between the point of aperture A and observation point M ; $dS = \rho_1 d\rho_1 d\varphi$ - element of area of aperture.

Page 103.

From the examination of Fig. 1^a it follows that

$$r = R \sqrt{1 - \frac{\rho_1^2}{R^2} - \frac{2\rho_1 \sin \theta \cos(\varphi_2 - \varphi_1)}{R}}. \quad (2)$$

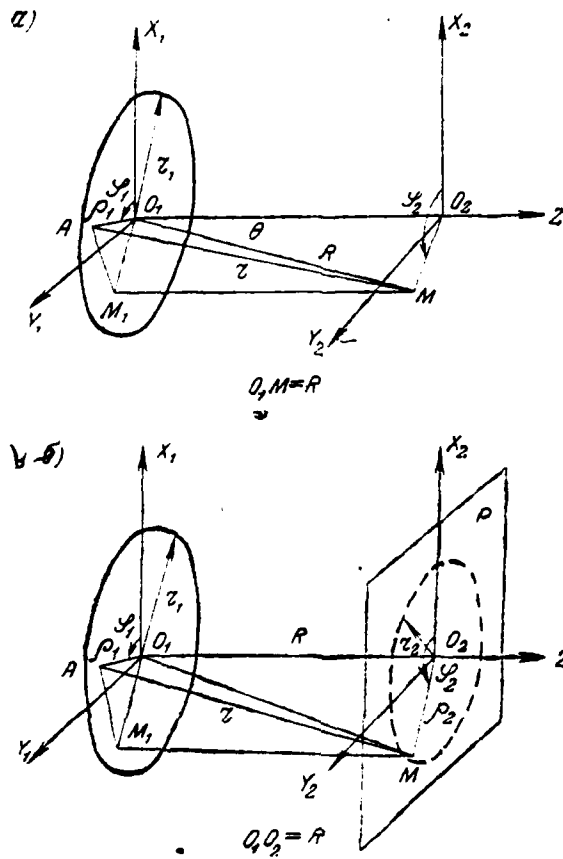


Fig. 1.

Page 104.

As is known [for 4], in the region of approaching Fresnel it is possible to assume:

- for the denominator of the integrand

$$r = R; \quad (2a)$$

- for the exponential function in the numerator (by using expansion $\sqrt{1+a} \approx 1 + \frac{a}{2}$)

$$r = R + \frac{\rho_1^2}{2R} - \rho_1 \sin \theta \cos(\varphi_1 - \varphi_2). \quad (2b)$$

Let us introduce the designations:

$$u = kr_1 \sin \theta - \text{the generalized angular coordinate}; \quad (3)$$

$$t = \frac{\rho_1}{r_1} - \text{relative coordinate of the point of aperture}; \quad (4)$$

$$m = \frac{kr_1^2}{R} - \text{dimensionless parameter (a "number of Fresnel")}. \quad (5)$$

It is easy to show that

$$m = \frac{\pi}{4\Delta}, \quad (5a)$$

where $\Delta = R\lambda/2D^2$ - the "given distance", the parameter, usually utilized in the examination of radiation characteristics in the near zone of antenna [4].

Substituting (2a) and (2b) in (1) and taking into account (3)-(5), after simple conversions it is possible to obtain, lowering permanent factors, the following expression for the radiation pattern in the region of approaching Fresnel:

$$F(u) = \int_0^1 A(t) e^{i\psi(t)} J_0(ut) e^{-i\frac{m}{2}t^2} t dt. \quad (6)$$

Subsequently we will examine the functions of the distribution only of form $A(t) = (1 - pt^2)^n$ and $\psi(t) = \varphi_m t^2$ or $\psi(t) = 0$.

Let us consider expression for the radiation pattern (in the region of approaching Fresnel) during the cophasal excitation of aperture ($\psi(t) = 0$) for the form of the function $A(t)$ accepted:

$$F(u) = \int_0^1 (1 - pt^2)^n J_0(ut) e^{-i \frac{m}{2} t^2} dt. \quad (7)$$

Representing $A(t)$ by power series, it is possible to record (7) in the form

$$F(u) = \sum_{q=0}^n (-1)^q C_n^q p^q I_0^{(2q+1)}. \quad (8)$$

where C_n^q - binomial coefficient;

$$I_0^{(2q+1)} = \int_0^1 J_0(ut) e^{-i \frac{m}{2} t^2} t^{2q+1} dt. \quad (9)$$

Page 105.

In appendix it is shown that integral (9) is led to the following expression:

$$I_0^{(2q+1)} = \frac{e^{-i \frac{m}{2}}}{m} [W_1(q, m, u) - i W_2(q, m, u)], \quad (10)$$

where $W_1(q, m, u)$ and $W_2(q, m, u)$ - function three variable/alternating, determined as follows:

$$\begin{aligned}
W_1(q, m, u) \mp i W_2(q, m, u) &= \sum_{g=0}^{q-1} \left[\sum_{s=0}^{q-1-g} (\pm i)^s C_{g-s}^g \left(\frac{2}{m}\right)^s \right] \\
&\times \frac{q!}{(q+s)!} \left[(\mp i)^{g+1} \left(\frac{u}{m}\right)^g J_g(u) \mp (\pm i)^g \sum_{g=0}^q (-1)^g C_g^g \left(\frac{2}{m}\right)^{q-g} \right] \\
&\times \frac{q!}{g!} \left(\frac{u}{m}\right)^{2g} [U_{g+1}(m, u) \mp i U_{g-2}(m, u)] (q=1, 2, 3 \dots), \quad (11)
\end{aligned}$$

in this case

$$W_1(0, m, u) \mp i W_2(0, m, u) = U_1(m, u) \mp i U_2(m, u). \quad (11a)$$

Taking into account (8) and (10) the radiation pattern can be recorded in the form

$$F(u) = \frac{e^{-i \frac{m}{2}}}{m} F_u(u), \quad (12)$$

where

$$F_u(u) = \sum_{q=0}^n (-1)^q C_n^q p^q [W_1(q, m, u) \mp i W_2(q, m, u)]. \quad (12a)$$

During the noncophasal excitation of aperture ($\psi(t) = \varphi_m t^2$) the radiation pattern also can be determined by expression (12), but during replacement of m on $(m - 2\varphi_m)$. In the case $\varphi_m = \frac{m}{2}$ the radiation pattern is described by known expression for the remote zone ¹):

$$F(u) = \int_0^u A(t) J_0(ut) dt. \quad (13)$$

FOOTNOTE ¹. The method of the definition of radiation pattern for the remote zone at comparatively small distances ($\Delta < 1$), which foresees the proper misphasing of aperture, as is known, it is proposed by N. A. Yesevkinoy. ENDFOCTNOTE.

Page 106.

EFFECT OF QUADRATIC PHASE DISTORTIONS ON THE RADIATION PATTERN IN THE REMOTE ZONE.

Assuming/setting in (6) $m=0$ and using materials of application/appendix, it is possible to obtain the following expression for the radiation pattern in the remote zone during the quadratic phase distortions in aperture ($\varphi(l) = \varphi_m l^2$):

$$F(u) = \sum_{q=0}^n (-1)^q C_n^q p^q [W_1(q, 2\varphi_m, u) - i W_2(q, 2\varphi_m, u)]. \quad (14)$$

in this case as in (12), is omitted permanent factor $\frac{e^{i\varphi_m}}{2\varphi_m}$. Fig. 2 gives the results of calculating the radiation patterns for case of $n=1$, with $p=0; 0.685; 1.0$ and $\varphi_m = \frac{\pi}{2}, \pi$ calculations were produced according to the formula

$$F(u) = [U_1(m, u) - pW_1(1, m, u)] - i[U_2(m, u) - pW_2(1, m, u)]. \quad (15)$$

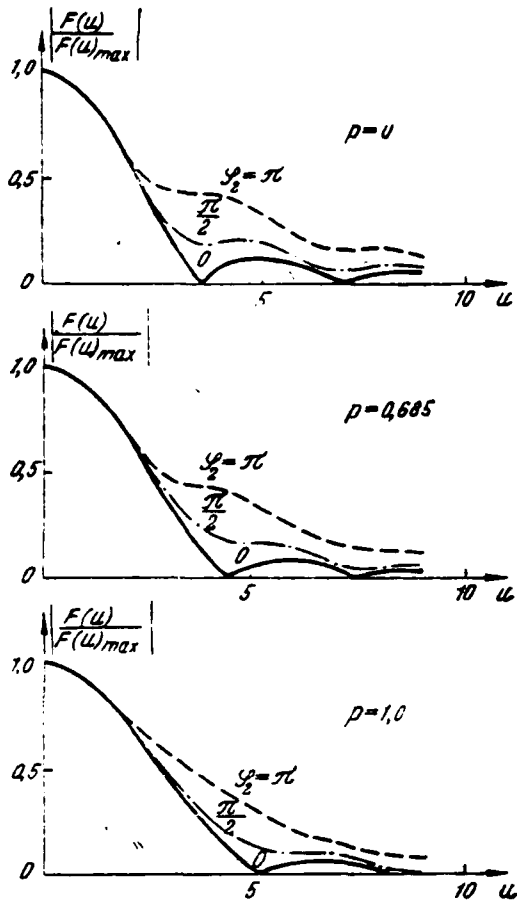


Fig. 2.

Page 107.

So, for the comparison, are shown the radiation patterns for cophasal aperture ($\varphi_m=0$), calculated by the formula

$$F(u) = \frac{1-p}{2} \Lambda_1(u) + \frac{p}{4} \Lambda_2(u). \quad (16)$$

of that obtained from (13) by simple conversions.

FIELD DISTRIBUTION IN A REGION OF APPROACHING FRESNEL.

In a number of cases of interest amplitude-phase field distribution in the region of approaching Fresnel, examined/considered usually in the planes, perpendicular to the axis of aperture. We use given above expression (1) for calculating the field at observation point M, located in plane p (see Fig. 1b). From figure it follows that

$$r = R \sqrt{1 + \frac{\rho_1^2}{R^2} + \frac{\rho_2^2}{R^2} - \frac{2\rho_1\rho_2 \cos(\varphi_2 - \varphi_1)}{R^2}} \quad (17)$$

In the region in question it is possible to assume:

- for the denominator of integrand, as earlier,

$$r = R; \quad (17a)$$

- for the exponential function in the numerator

$$r = R + \frac{\rho_1^2}{2R} + \frac{\rho_2^2}{2R} - \frac{\rho_1\rho_2}{R} \cos(\varphi_2 - \varphi_1). \quad (17b)$$

Let us introduce designation ¹⁾:

$$u = kr_1 \frac{\rho_2}{R} = m \frac{\rho_2}{r_1} \quad (18)$$

FOOTNOTE ¹⁾. It is clear that when $\rho_2 \ll R$ $u = kr_1 \frac{\rho_2}{R} = kr_1 \sin \theta$. ENDFOOTNOTE.

Substituting (17a) and (17b) into 1 and taking into account (4), (5) and (18), it is possible to obtain the following expression for

calculating the field in the region of approaching Fresnel:

$$E_M = ime^{-i\pi R} e^{-i\frac{u^2}{2m}} F(u), \quad (19)$$

where $F(u)$ is determined by expression (12).

Page 108.

Lowering in (19) and (12) permanent factors, we obtain expression for calculating amplitude distribution and phases of field in plane P of the region in question:

$$F_-(u) = e^{-i\frac{u^2}{2m}} F(u) = |F_-| e^{-i\psi_-}, \quad (20)$$

in this case $F_+(u)$ one should determine on (12a) taking into account (18), with replacement of m on $(m-2q_m)$ in the case $\psi_m = q_m t^2$

Fig. 3 gives results of the calculation of amplitude-phase field distribution for case of $\Lambda(t) = 1-pt^2$ with

$$\psi_m = 0, \quad p = 0,684, \quad m = 17 (\Delta \approx 0,046).$$

Calculation was produced according to the formula

$$F_-(u) = e^{-i\frac{u^2}{2m}} \{ [U_1(m, u) - pW_1(1, m, u)] - i[U_2(m, u) - pW_2(1, m, u)] \}. \quad (21)$$

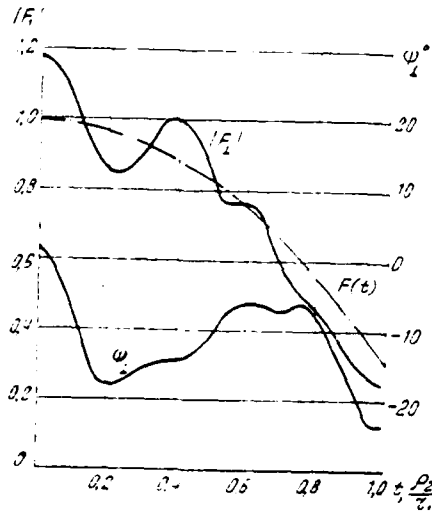


Fig. 3.

FIELD OF APPLICATION OF THE OBTAINED EXPRESSIONS.

Expressions (12), (19) and (20) can be used for performance calculation of radiation/emission in the region for which are valid placed as the basis of their conclusion/output the scalar formula of Kirchhoff and the approximation/approach of Fresnel. The boundaries of the region of applying Kirchhoff's formula it is possible to consider [4, 8] the region of angles not more than 30° from the axis of aperture and the distance to it of the order of his several diameters, for example two ([8], page 9). The boundaries of the region of applying the approximation/approach of Fresnel, i.e., representations (2a), (2b), (17a) and (17b), are determined by

amplitude and phase criteria for permissible in this case errors [4], which express through m_a and m_ϕ .

Let us consider observation point M at the maximum removal/distance r_2 from the axis of aperture in the plane, perpendicular to this axis, and let us assume, by analogy with [4], criteria indicated equal to $\lambda/8$.

Page 109.

This it indicates, in the first place, that all points of aperture are visible of the point M at angle not more $\pi/8$, in this case a change in the factor $1/r$ does not exceed 30/0; in the second place, that the difference between precise and by approximate values of r , expressed in the phase angles, does not exceed $\pi/8$. It is possible to show that the maximum limiting values of parameter m are equal in this case respectively:

$$m_a = \frac{\pi}{2.4(1+a)} \left(\frac{2r_1}{\lambda} \right), \quad m_\phi = \frac{\pi}{(1+a)^{4/3}} \left(\frac{2r_1}{\lambda} \right)^{2/3}, \quad (22)$$

where

$$a = \frac{r_2}{r_1}.$$

Fig. 4 shows the defined by expressions (22) and (23) near boundaries of the region of approaching Fresnel, and also the boundary of the use/application of Kirchhoff's scalar formula, defined as

$$m_k = \frac{\pi}{4} \left(\frac{2r_1}{\lambda} \right) \quad (24)$$

under above condition accepted.

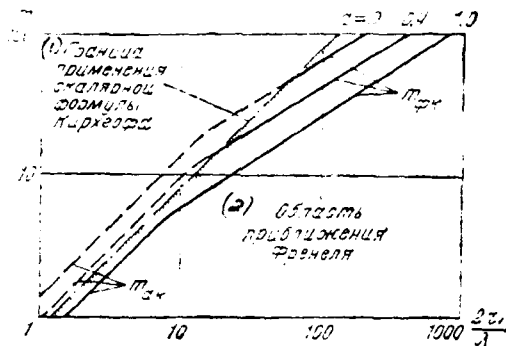


Fig. 4.

Key: (1). Boundary of the use/application of Kirchhoff's scalar formula. (2). Region of approaching Fresnel.

Conclusion.

For the antenna with the symmetrical excitation of circular aperture, the described polynomial of form $(1 - p^2)^n$, are obtained the expressions for performance calculation of radiation/emission in the near zone within the limits of the applicability of the approximation/approach of Fresnel, and also in the remote zone in the presence of quadratic phase distortions in the aperture. In the expressions indicated are used proposed in the present work functions of three of variable/alternating, that have integral representation of the type of the conversion of Hankel.

The obtained results can be propagated to any case of the described by polynomial symmetrical amplitude distribution, and also can be used for the computation of transmission factor the energies between the antennas in the near zone.

Page 110.

Application/appendix.

Calculation of the integrals of the form

$$\int_0^1 J_\nu(ut) e^{\pm i \frac{m}{2} t^2} t^{2q+1+\nu} dt.$$

On the basis of known integral representation for the functions of Lommel [2] it is possible to record

$$I_\nu = I_\nu^{(\nu+1)} = \int_0^1 J_\nu(ut) e^{\pm i \frac{m}{2} t^2} t^{\nu+1} dt = \frac{e^{\pm i \frac{m}{2}}}{m} \left(\frac{u}{m}\right)^\nu \times \\ \times [U_{\nu+1}(m, u) \pm i U_{\nu+2}(m, u)]. \quad (\text{П.1})$$

Let us show that also the integral

$$I_\nu^{(\mu)} = \int_0^1 J_\nu(ut) e^{\pm i \frac{m}{2} t^2} t^\mu dt \quad (\text{П.2})$$

can be represented when $\mu = \nu + (2q+1)$; analogously through some functions $W_{\nu+1}(q, m, n)$ and $W_{\nu+2}(q, m, n)$, expressing with the help of the Bessel functions and Lommel. We use for this method of integration in parts, making it possible "to draw together" the order of function of Bessel

and degree t in the integrand. Let us use to (p. 2) the formula of integration in parts $\int w dv = wv - \int v dw$. after assuming $w = J_\nu(u)t^{\mu-1}$; $d_v = e^{-i \frac{m}{2} t^2} dt$.

As a result it is possible to obtain the following expression:

$$I_\nu^{(\mu)} = \pm \frac{i}{m} \left[e^{\pm i \frac{m}{2}} J_\nu(u) - (\mu + \nu - 1) I_\nu^{(\mu-2)} + u I_{\nu+1}^{(\mu-1)} \right], \quad (\Pi.3)$$

where the indices of the confronting in the brackets integrals are already "approached" with the exponents $\gamma(t)$ to 2. Applying to these integrals and the further indicated method (entire q of integrations), it is possible to express integral (p. 2) through the integrals of form (p. 1) $J_\nu, J_{\nu+1}, \dots, J_{\nu+q}$ and Bessel function $J_\nu(u), J_{\nu+1}(u), \dots, J_{\nu+q-1}(u)$. Finally we have

$$\begin{aligned} I_\nu^{(\mu)} = I_\nu^{(\nu+2q+1)} &= \int_0^1 J_\nu(ut) e^{\pm i \frac{m}{2} t^2} t^{\nu+2q+1} dt = \\ &= \frac{e^{\pm i \frac{m}{2}}}{m} [W_{\nu+1}(q, m, u) \pm i W_{\nu+2}(q, m, u)], \end{aligned} \quad (\Pi.4)$$

where we have introduced functions three variable/alternating, determined as follows:

$$\begin{aligned} W_{\nu+1}(q, m, u) \mp i W_{\nu+2}(q, m, u) &= \sum_{g=0}^{q-1} \left[\sum_{s=0}^{q-1-g} (\pm i)^s \times \right. \\ &\times C_{g+s}^g \left(\frac{2}{m} \right)^s \frac{(q+\nu)!}{(q+\nu-s)!} \left. (\pm i)^{g+1} \left(\frac{u}{m} \right)^g J_{\nu+g}(u) + \right. \\ &\left. + (\pm i)^q \sum_{g=0}^q (-1)^g C_g^g \left(\frac{2}{m} \right)^{q-g} \frac{(q+\nu)!}{g!} \left(\frac{u}{m} \right)^{2g} [L_{\nu+g+1}(m, u) \mp i L_{\nu+g+2}(m, u)] \right] \\ &\quad (g = 1, 2, 3 \dots). \end{aligned} \quad (\Pi.5)$$

Page 111.

With $q=0$

$$W_\nu(0, m, u) \pm i W_{\nu+1}(0, m, u) = U_\nu(m, u) \pm U_{\nu+1}(m, u).$$

For the functions of the first and second orders, with $q=1$,

$$W_1(1, m, u) = \left(\frac{u}{m}\right)^2 U_1(m, u) + \frac{2}{m} U_2(m, u) - \frac{u}{m} J_1(u); \quad (\text{II.7})$$

$$W_2(1, m, u) = -\frac{2}{m} U_1(m, u) + \left(\frac{u}{m}\right)^2 U_2(m, u) + J_0(u). \quad (\text{II.8})$$

REFERENCES

1. LOMMEL E. Die Beugungserscheinungen einer kreisrunden Öffnung und eines kreisrunden Schirmchens theoretisch und experimentell bearbeitet. — «Abhandlungen der Math. — Phys. Klasse der König-Bayer. Akademie der Wissenschaften». XV 1886, p. 229—328.
2. G. N. Watson. Theory of Bessel functions. H. I. Publ. of ine. of lit., 1949.
3. HANSEN R. C., BAILIN L. L. A new method of near field analysis. — «IRE Transactions». AP-7, Dec. 1969. S. 458.
4. Trans. from Engl. edited by G. I. Markov and A. F. Chaplin. Scanning antenna systems SVCh. M., "Soviet radio", 1966.
5. M.-K. HU. IRE International Conv. Record, Pt. 1. 1960, 13—23.
6. Ye. N. Dekanosidze. Table of cylindrical functions from two variable/alternating. Publ. of the AS USSR, 1956.
7. HEBERMENTHL G., MINKWITZ G., SCHULZ G. Tabellen der Lommelschen Funktion $U_1(wz)$ und $U_2(wz)$ zweier Veränderlicher sowie abgeleiteter Funktionen. Berlin. Akad. Verlag, 1965.
8. A. M. Pokras. Wireless transmission lines. M., "connection/communication", 1967.

It acted in ed. 8/XII/ 1970; after treatment/processing - 25/II 1972.

Page 112.

Characteristics of two-mirror antenna, which forms radiation pattern of sum-and-difference type.

L. N. Zakhar'yev, A. A. Lemanskiy, A. Ye. Tumanskaya.

Is evaluated the effect of diffraction phenomena at the Fresnel zone of counter-reflector on the characteristics of two-mirror antenna [slope/transconductance of the differential composing diagrams, product slope/transconductance to the coefficient of the use of a surface (stalks) or the square root from the stalks]. Are given the maximum values of the characteristics indicated which it is possible to achieve due to the correction of the surface of counter-reflector. Are given the parameters of the corrected counter-reflector, which correspond to the maximum values of the characteristics of two-mirror antenna with the sum-and-difference radiation pattern.

Work [1] examines the special features/peculiarities of shaping

of field in the aperture of two-mirror antenna with the radiation pattern of total type, are given the values of its stalks and coefficient of scattering, is proposed the method of an improvement in the characteristics of two-mirror antenna indicated. In contrast to the majority previously the published works, the results, presented in article [1], are obtained taking into account the diffraction distortions of field in the Fresnel zone of counter-reflector.

In this article with the help of the method, described in work [1], is conducted the analysis of the characteristics of the two-mirror antenna, which forms sum-and-difference radiation pattern. First we will consider how is distorted differential field component in the aperture of main mirror, let us compare the values of the slope/transconductance of the direction-finding characteristic of antenna, which correspond to the calculations of field in the aperture according to the geometric optic/optics and taking into account the diffraction phenomena in the Fresnel zone of counter-reflector. Then will be given the values of slope/transconductance S and products $\sqrt{x}S \cdot xS$ (x — the stalks of antenna on the total channel), which can be achieved/reached in the classical two-mirror antenna, and also due to the correction of the surface of counter-reflector.

Page 113.

Let us suppose how in work [1], that differential field component in the aperture of irradiator takes the form:

$$\begin{aligned}\vec{H}_0(\rho, \varphi') &= A(\rho, \varphi') \vec{e}_x; \\ \vec{E}_0(\rho, \varphi') &= Z_0 A(\rho, \varphi') \vec{e}_y,\end{aligned}\quad (1)$$

where

$$\begin{aligned}A(\rho) &= B(1 - q\rho^2) \rho e^{-\gamma\rho^2} \sin\varphi', \\ \rho &= \rho' b, \quad 0 \leq \rho \leq 1;\end{aligned}$$

$2b$ - diameter of irradiator;

ρ', φ' - coordinate of point in its aperture;

Z_0 - impedance in the aperture of irradiator;

B, q, γ - parameters of amplitude-phase field distribution (1).

Considering as the given one power P_Δ in the differential channel of antenna, let us determine amplitude B :

$$B = \frac{4}{b} \sqrt{\frac{3P_\Delta}{\pi Z_0 (6 - 8q + 3q^2)}}.$$

As in work [1], it is possible to determine field in the aperture of the main mirror:

$$\vec{E}(r, \varphi) = E_x(r, \varphi) \vec{e}_x + E_y(r, \varphi) \vec{e}_y, \quad (2)$$

corresponding to distribution (1). According to the values of field (2) it is not difficult to compute slope/transconductance S of the differential diagram of the antenna:

$$S_{x, y} = \frac{k}{2\pi} \left\{ \left| \frac{\partial}{\partial \psi} \int_0^{2\pi} \int_{a_k}^a E_{x, y}(r, \varphi) e^{-ik \sin \theta \cos(\varphi - \psi)} r dr d\varphi \right| \right\}_{\psi=0} \quad (3)$$

where $d=2a_k$ - diameter of counter-reflector;

$D=2a$ - diameter of main mirror;

$k=2\pi/\lambda$.

Subsequently we will examine slope/transconductance S_y , corresponding to the fundamental component of field in the plane $\psi = \pi/2$. Values $[S_y]_{\psi=\pi/2}$ we will normalize to value

$$S_{max} \approx 7,85 \left(\frac{a}{\lambda} \right)^2 \sqrt{\frac{P_{\Delta}}{Z_0}} \quad (4)$$

- to the maximum slope/transconductance of circular aperture [2], which radiates the same power P_{Δ} , as the antenna in question. Let us designate

$$v = S_y \cdot S_{max} \quad (5)$$

Expanded/scanned field expression (2) takes the sufficiently bulky form and therefore it is not brought. Value $E(r, \theta)$ is expressed as the same special functions, as field in the aperture of two-mirror antenna with total type diagram (see [1]).

Like the characteristics of total diagram, the slope/transconductance of the differential radiation pattern of the two-mirror antenna, made on the classical diagram, as a result of the diffraction distortions of field in the Fresnel zone of counter-reflector differ significantly from slope/transconductance, which gives calculation of field in the aperture according to the geometric optic/optics. In order to be convinced of this, let us turn to the results of calculating the values $E_v(r, \varphi)$ with $\psi = \pi/2$ and v for the concrete/specific/actual two-mirror antenna with the parameters: $D=54\lambda$, $f=0.4D$ (here and subsequently we will consider that the irradiator is focused to the apex/vertex of counter-reflector and $2b \approx d$ [1]).

Page 114.

Fig. 1 gives the standardized/normalized values of the slope/transconductance of the differential radiation pattern of the antenna in question, calculated depending on power level δ^2 on the edge of counter-reflector at different values of d/D . From Fig. 1 it follows that slope/transconductance v reaches maximum value $v = v_{max} \approx 0,62$ when $\delta^2 = 0,3$ and $d = 0,2D$. If we in formula (3) supply instead of $E_v(r, \varphi)$ appropriate geometric field distribution, it will

seen that in this case when $\delta_k^2 = 0.3$ and $d = 0.2D$ $v = v = 0.88$. Thus, due to the distortions of field in the near zone of counter-reflector the real value of the slope/transconductance of the antenna in question is approximately/exemplarily to 30% lower than value $v = v_{max}$. One should note also that value $d = 0.2D_1$, which corresponds $v = v_{max}$, somewhat more than value $d = 0.16D$, with which the antenna in question has maximum of stalks along total channel [1].

In order to clarify the reason for the disagreement between $v = v_{max}$ and $v = v'$, let us turn to the results of calculating field distribution $E_v(r, \pi/2)$ into the aperture of the antenna in question. Fig. 2 gives values $|E_v(r, \pi/2)|$ (Fig. 2a) and $\arg E_v(r, \pi/2)$ (Fig. 2b, d, curves 2), appropriate $v = v_{max}$. In the same figure for the comparison are given geometrical values $|E'_v(r, \pi/2)|$ (curve 1). Comparing curves 1 and 2, it is not difficult to comprehend the reason for the disagreement between values v' and v_{max} . It is caused by the strong amplitude-phase distortions of field in the aperture. In particular, because the mirror is located in the Fresnel zone of counter-reflector, almost for all points in his aperture occurs inequality $|E_v(r, \pi/2)| < |E'_v(r, \pi/2)|$. As in the case of the diagram of total type [1], distortion of field it is not possible to substantially decrease by the corresponding tuning of irradiator or due to its displacements/movements. However, calculation they show that value v can be increased with the help of the correction of the surface

of counter-reflector similarly as is done in in the case of two-mirror antenna with the total radiation pattern [1]. If we in the antenna in question due to the identification of parameter q in field distribution (1) or diameter of irradiator $2b$ irradiate the edge of counter-reflector in the plane $\phi = \pi/2$ by power with level $S_0^2 = 0.1$ and then to increase the angle of irradiation $2\theta_0$, which ensures counter-reflector (i.e. to decrease its eccentricity), slope/transconductance v will first grow, reaching maximum, and then as a result of of the increasing "overflow" of energy of the field through the edge of antenna aperture it will begin to fall.

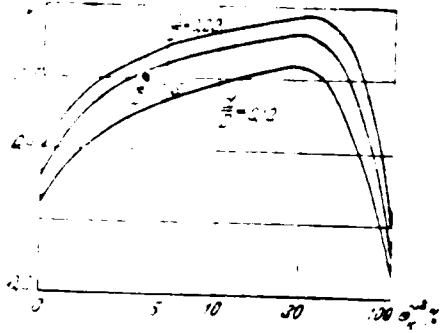


Fig. 1.

Page 115.

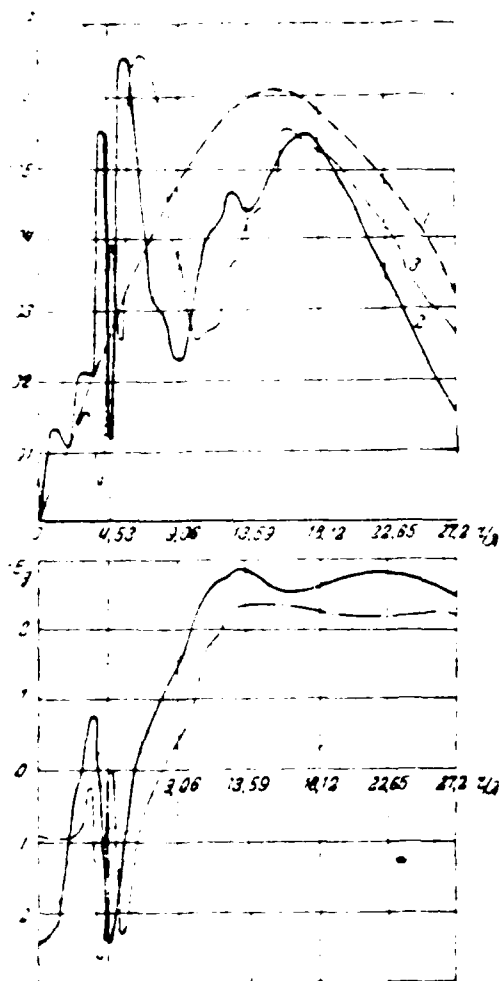


Fig. 2.

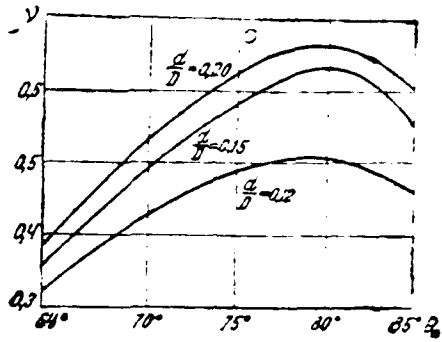


Fig. 3.

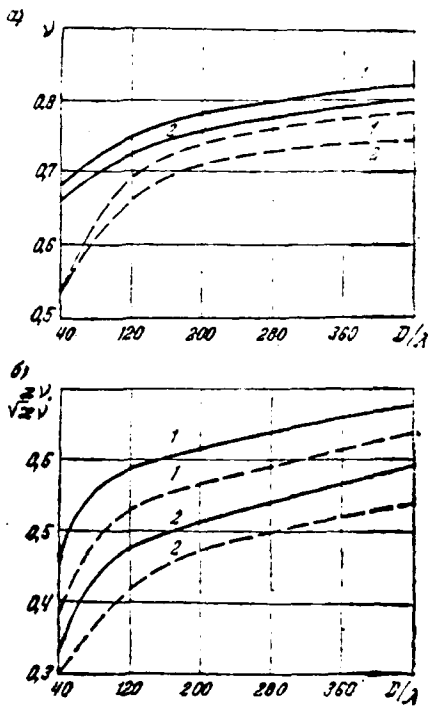


Fig. 4.

About this testify the results of calculating the value ν

depending on angle θ_0 with different d/D , represented in Fig. 3. The examination of the curves Fig. 3 shows that while conducting of the correction of the surface of hyperbolic counter-reflector indicated value v reaches maximum $v=v_0=0.69$ with $d=0.2D$ and $2\theta_0=160^\circ$, whereas the angle of the irradiation of mirror with $f/D=0.4$ is equal to 128° . Thus, the correction conducted makes it possible to raise value v from $v=v_{max}=0.62$ to $v=v_0=0.69=1.17v_{max}$. Field distribution in the aperture, which corresponds to the corrected counter-reflector, it is shown in Fig. 2a and b (curves 3).

If antenna forms/shapes sum-and-difference type diagram, its fundamental parameter is product κS or $\sqrt{\kappa} S$ — stalks along the total channel in equisignal direction, S — slope/transconductance in the zone of equisignal direction (RSN), since the measuring error of angles with the excess of the useful signal above the noise is inversely proportional to value κS or $\sqrt{\kappa} S$ (see [3]). Since the parameters of corrected counter-reflectors, which ensure maximums κ and v differ, it is expedient to find values d/D and θ_0 , with which are maximum products κv and $\sqrt{\kappa v}$. Calculation shows that for the antenna in question maximum value $\kappa v=0.375$ is reached at $d=0.18D$ and by $2\theta_0=160^\circ$. In this case $\kappa=0.55$, and $v=0.68$. The maximum of product $\sqrt{\kappa v}=0.5$ takes the pace with $d=(0.15-0.20)D$ for D and $2\theta_0=150^\circ$. In this case $\kappa=0.54-0.55$ and $v=0.67-0.68$. In connection with the given results it should be noted that in the

two-mirror antenna with $D=54\lambda$, $f/D=0.4$ carried out on the classical diagram, maximum values η_{zv} and $\sqrt{\eta_{zv}}$ compose with respect 0.3 and 0.44.

In conclusion let us present maximum values η_{zv} and $\sqrt{\eta_{zv}}$ which can be achieved/reached due to the correction of the surface of counter-reflector at different D/λ and f/D , and also the parameters of the corrected counter-reflectors.

Fig. 4a and b gives maximum values η_{zv} , $\sqrt{\eta_{zv}}$ calculated in the dependence on D/λ . Unbroken curves correspond to the focal length of $f=0.3D$, and broken $f/D=0.8$. Curves 1 in Fig. 4a correspond to the maximum values of slope/transconductance η_{zv} while curves 2 - to values η_{zv} which occur with maximum values $\sqrt{\eta_{zv}}$ and η_{zv} . The maximum values of products $\sqrt{\eta_{zv}}$ and η_{zv} are given in Fig. 4b (curves 1 they correspond to maximum $\sqrt{\eta_{zv}}$, curves 2 - maximum η_{zv}).

Page 117.

The examination of Fig. 4 shows that for obtaining the maximum values η_{zv} , $\sqrt{\eta_{zv}}$ and η_{zv} to more preferably use short-focus two-mirror antennas. For example, with $D=(50-400)\lambda$ and $f=0.8D$ maximum product $\sqrt{\eta_{zv}}$ on (10-5) o/o is more than with $f/D=0.8$, and η_{zv} - is more on (13-9) o/o. In connection with this it must be noted that from the

point of view of the realization of the maximum of stalks the short-focus antennas and long-focus in practice do not differ.

The parameters of the corrected counter-reflector, in which values $\sqrt{V_{\bar{x}v}}$ and xv are maximum, given in Fig. 5a and b (at $D \geq 80\%$), maximums $\sqrt{V_{\bar{x}v}}$ and xv reach virtually at the identical values of d/D , and maximums $\sqrt{V_{\bar{x}v}}$ and xv also, at the identical values θ_0). Solid lines in Fig. 5a correspond $f/D=0.3$, and broken - $f/D=0.8$. Curve 1 in Fig. 5b corresponds to maximum slope/transconductance, $v=v_0$ while curve 2 - to maximum products $\sqrt{V_{\bar{x}v}}$ and xv . The values of angle θ_0 , given in Fig. 5b, virtually do not depend on D/λ .

The results of calculation, represented in Fig. 4 and 5, relate to the counter-reflector of hyperbolic form. However, the calculations conducted showed that the analogous values of values $\sqrt{V_{\bar{x}v}}$, xv can be obtained, if we use counter-reflectors of parabolic and spherical form, after selecting their such that the surface of paraboloid or sphere least would deviate from the surface of the hyperbolic counter-reflector whose parameters were given in Fig. 5.

The calculations conducted showed also that even in the case of the idealized irradiator, which forms the apetalous sum-and-difference diagram of table-shaped form, it is impossible to obtain values $\sqrt{V_{\bar{x}v}}$, xv of those exceeding the values, represented

DOC = 80134008

PAGE

~~14~~
245

in Fig. 4 and which correspond to the simplest diagram of irradiator
and to the corrected counter-reflector.

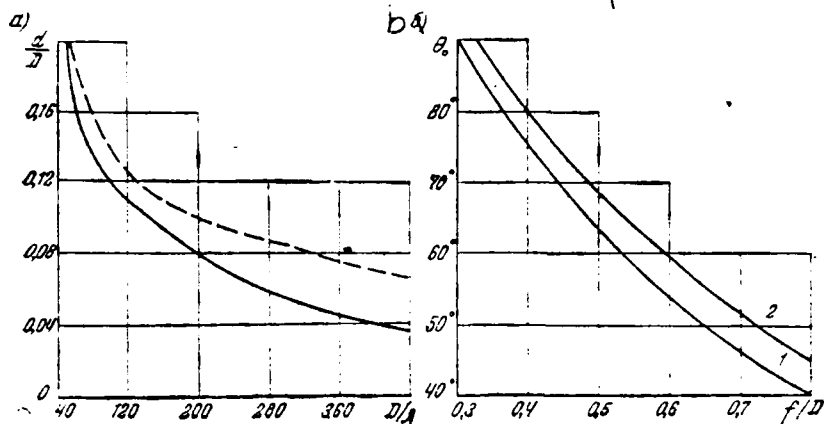


Fig. 5.

Page 118.

Therefore results of calculation, given in Fig. 4, can be considered as the maximum characteristics of the two-mirror antennas, which form radiation patterns of sum-and-difference type. It is of interest to compare these characteristics of two-mirror antenna with the analogous maximum characteristics which can be obtained with the help of the antenna, which has the circular aperture (see [2] ^{and} [4]). Comparison shows that with $D=(50-400)\lambda$ the given characteristics of two-mirror antenna are inferior to absolute maximum values on the slope/transconductance on (30-18) o/o from parameter $\sqrt{\kappa S}$ on (37-20) o/o, from parameter κS on (50-37) o/o.

REFERENCES

1. L. N. Zakhar'yev, A. A. Lemanskiy, A. Ye. Tumanskaya. On the calculation of the irradiating system of two-mirror antenna. coll. of "antenna", iss. 10. of M., "connection/communication", 1971.
2. L. N. Zakhar'yev, R. A. Konoplev. Optimum differential field distributions in antenna aperture. Coll. of "antenna", iss. 1. of M., "connection/communication", 1966.
3. P. A. Bakut et al. Questions of the statistical theory of radar. Vol. II M, "Soviet radio", 1963.
4. L. N. Zakhar'yev, R. A. Konoplev, A. A. Lemanskiy. On optimum field distribution in the aperture of the scanning antenna. coll. of "antenna", iss. 6. of M., "connection/communication", 1970.

Submitted 20 July 1970.

Page 119.

Approximate computation of the surface of a small mirror according to the strains of large mirror in Cassegrain's antenna.

Introduction.

A. L. Eizenberg, L. A. Dozorets.

Is examined the approximate geometric-optical method for calculation of the surface of a small mirror on the strains of large mirror. the new surface of a small mirror is defined as the superposition of initial surface and increments. Problem is solved for the general case of arbitrary ones, including of asymmetric ones, the strains. Taking into account evenness and smallness of strains in comparison with the linear dimensions of mirrors are obtained simple analytical expressions for Cassegrain's antenna. Calculations showed the sufficiently high accuracy of method.

As is known, in the process of manufacture and operating the large two-mirror antennas the surface of fundamental (large) mirror differs from calculated, which leads to the phase errors in the opening. One of the possible methods of fight with them - the

correction of the form of auxiliary (small) mirror [1]. Logically appears the problem of calculating the new (deformed) surface of a small mirror according to the preliminarily measured or calculated strains of large mirror. The geometry of the mirrors of initial antenna is such, that for their calculation it is possible to apply geometric-optical methods. In the case of steady and small (in comparison with the linear dimensions of mirrors) strains all parameters, which are determining the applicability of geometric optic/optics, vary unessentially; therefore for calculating the deformed system also can be used geometric-optical methods.

For using the known methods of calculation of two-mirror antennas (for example, the method of wave fronts [2]) it is necessary to determine the first new surface of large mirror. In practice the strains are assigned at discrete/digital points, in this case it comes not only the coordinate of the points of the deformed mirror, but also the vector of standard in them. In general calculation is labor-consuming operation, since it is necessary to solve the substantially three-dimensional problem (change in each of the coordinates of a small mirror is determined by a change in three coordinates of large mirror).

Furthermore, the orientation of standard must be determined with the high degree of accuracy, since in the process of computations it is necessary to use with the large lengths of optical paths and even small angular errors will involve the considerable errors in the determination of the surface of a small mirror. However, the problem of restoring the derivatives with respect to the discrete/digital values incorrectly set, and usual methods of numerical differentiation (for example, differentiation of the interpolation of Lagrange polynomial) can lead to the strongly distorted results. Most precise (method of the regularization of A. N. Tikhonov) is very complex and labor-consuming, since it is necessary to solve the integral equations of Fredholm of the first order with the disruptive kernel. Furthermore, the linear dimensions, with which they use in the process of calculation, are great; therefore independent of the accuracy of the determination of standard a relative error in the computations must be small.

In this work is posed the problem - using evenness and smallness of strains to obtain simple analytical expressions for calculating the corrective surface of a small mirror. The essence of method consists of the following. During the first stage by the values of strains and their derivatives on the large mirror are determined the shifts of the points of a small mirror and the rotation of standard in them. The deformed surface is considered then as the sum of the

initial and of the obtained increments. In this case it is not required for the high accuracy of computations, but result is weakly critical to the errors for numerical differentiation.

The method in question makes it possible to find the coordinates of points and the orientation of the standards of the deformed small mirror it is direct over the strains of large mirror and known initial surfaces of both mirrors. In the work are obtained the expressions in connection with one of the most widely used types of two-mirror systems - Cassegrain's antenna.

DETERMINATION OF THE STRAINS OF A SMALL MIRROR.

Let us introduce into the examination spherical and rectangular coordinate systems (Fig. 1). The strains of mirrors we will count off on the normals to the initial surfaces, moreover for the positive ones let us take saggings/deflections inside. Then the equation of the deformed large mirror is recorded in the form

$$\left. \begin{aligned} x_0 &= f \operatorname{tg}^2 \frac{\varphi}{2} + \Delta_n(\varphi, \psi) \cos \frac{\varphi}{2} \\ y_0 &= \left[2f \operatorname{tg} \frac{\varphi}{2} - \Delta_n(\varphi, \psi) \sin \frac{\varphi}{2} \right] \cos \psi \\ z_0 &= \left[2f \operatorname{tg} \frac{\varphi}{2} - \Delta_n(\varphi, \psi) \sin \frac{\varphi}{2} \right] \sin \psi \end{aligned} \right\} \quad (1)$$

where f - focal length of initial paraboloid $\Delta_n(\varphi, \psi)$ - the instantaneous value of the strains of the surface of large mirror.

Page 121.

We approximate the surface of the deformed large mirror in the vicinities of the arbitrary point U_0 by paraboloid of revolution with the axis, parallel to axis x (Fig. 2). The equation of the latter in general takes the form

$$\Phi(x, y, z) = 4F(x - A) - (y - B)^2 - (z - C)^2 = 0, \quad (2)$$

where F - focal length of the approximating paraboloid; A, B, C - coordinate of apex/vertex.

Let us require so that both surfaces would have general/common/total standard at point U_1 . Then from the condition of the proportionality of direction numbers we obtain

$$\frac{\frac{\partial \Phi(x, y, z)}{\partial x}}{L} = \frac{\frac{\partial \Phi(x, y, z)}{\partial y}}{M} = \frac{\frac{\partial \Phi(x, y, z)}{\partial z}}{N}, \quad (3)$$

where direction numbers normals to paraboloid (2):

$$\frac{\partial \Phi(x, y, z)}{\partial x} = 4F, \quad \frac{\partial \Phi(x, y, z)}{\partial y} = 2(B - y), \quad \frac{\partial \Phi(x, y, z)}{\partial z} = 2(C - z);$$

direction numbers normals to deformed large mirror (1):

$$L = \begin{vmatrix} \frac{\partial y_0}{\partial \varphi} & \frac{\partial y_0}{\partial \psi} \\ \frac{\partial z_0}{\partial \varphi} & \frac{\partial z_0}{\partial \psi} \end{vmatrix}, \quad M = \begin{vmatrix} \frac{\partial z_0}{\partial \varphi} & \frac{\partial z_0}{\partial \psi} \\ \frac{\partial x_0}{\partial \varphi} & \frac{\partial x_0}{\partial \psi} \end{vmatrix}, \quad N = \begin{vmatrix} \frac{\partial x_0}{\partial \varphi} & \frac{\partial x_0}{\partial \psi} \\ \frac{\partial y_0}{\partial \varphi} & \frac{\partial y_0}{\partial \psi} \end{vmatrix}.$$

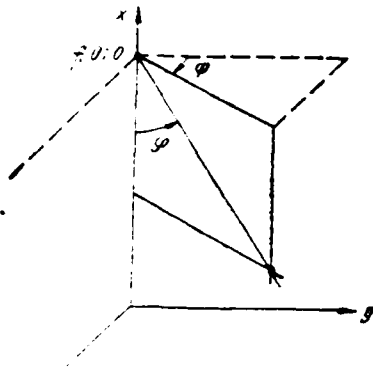


Fig. 1.

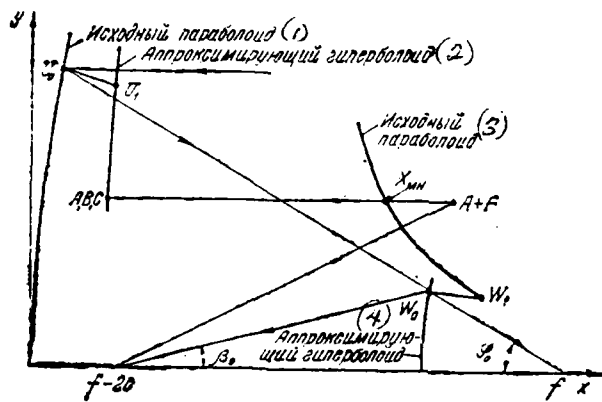


Fig. 2.

Key: (1). Initial paraboloid. (2). Approximating hyperboloid. (3). Initial paraboloid. (4). Approximating hyperboloid.

Page 122.

The front of the wave, reflected from the approximating paraboloid, will be sphere with the center at point A+F; B:C. To transform it into the spherical front with the center in the

irradiator can the hyperboloid whose foci coincide with irradiator and focus of the approximating paraboloid. The equation of this hyperboloid takes the form

$$\sqrt{(f-2c-x)^2 + y^2 + z^2} - \sqrt{(F-A-x)^2 + (y-B)^2 + (z-C)^2} = 2a_n \quad (4)$$

where $2c$ - distance between the foci of initial hyperboloid; $2a_n$ - real axis of new hyperboloid.

From the condition of equality the lengths of optical paths along any rays/beams from the opening to the emitter in the initial and deformed systems it is possible to obtain (Fig. 2):

$$2a_n = \sqrt{(f-2c-x_{MB})^2 + B^2 + C^2} - F - A - x_{MB} \quad (5)$$

where

$$x_{MB} = \frac{4a^2 + 4A^2 - 8aA - 4fa - 4fA - 4cf - 4c^2 - B^2 - C^2}{4(a+c-A)};$$

$2a$ - real axis of initial hyperboloid.

It is obvious that at certain point, which corresponds to point U_1 (conformity is determined on the optical course of ray in the deformed system), the deformed small mirror and hyperboloid (4) they coincide and have general/common/total standard. Taking into account smallness and evenness of strains, it can be assumed that point W_1 , which lies on the intersection of hyperboloid (4) it is normal to initial small mirror at point W_0 (to corresponding point U_0 of large

mirror in the reference system); it also belongs to the deformed small mirror and, therefore,

$$\sqrt{(x_{or} + \Delta_r \cos \eta - f + 2c)^2 + (y_{or} - \Delta_r \sin \eta \cos \psi)^2 + (z_{or} - \Delta_r \sin \eta \sin \psi)^2} - \sqrt{(x_{or} - F - A + \Delta_r \cos \eta - f + 2c)^2 + (y_{or} - B - \Delta_r \sin \eta \cos \psi)^2 + (z_{or} - C - \Delta_r \sin \eta \sin \psi)^2} = 2a_n, \quad (6)$$

where $x_{or} = f - \rho_r \cos \varphi$, $y_{or} = \rho_r \sin \varphi \cos \psi$, $z_{or} = \rho_r \sin \varphi \sin \psi$ — coordinates of point W_0 of initial mirror; $\rho_r = \frac{p}{1 - \varepsilon \cos \varphi}$ — radius-vector from point $f; 0; 0$, the describing initial paraboloid;

$$p = \frac{c^2 - a^2}{a} \text{ — focal parameter of hyperboloid;}$$

$$\varepsilon = \frac{c}{a} \text{ — eccentricity of hyperboloid;}$$

$\eta = \arctg \frac{\sin \varphi}{\varepsilon - \cos \varphi}$ — angle, formed normally at point W_0 of initial hyperboloid with x axis;

$$\Delta_r = W_0 W_1 \text{ — strain of a small mirror.}$$

Page 123.

As can be seen from (3) and (6), strains of a small mirror are the function of value and particular derived strains of large mirror of the angles φ and ψ spherical coordinates. Let us expand Δ_r in Maclaurin series and, taking into account smallness and evenness of

strains, we will be bounded by the members of the second order. After the appropriate conversions from (6), taking into account (3) and (5), we will obtain expression for the strains of a small mirror in the form

$$\Delta_r = \Delta_n \frac{\cos \frac{\varphi}{2}}{\cos(\varphi - \eta)} - \frac{\cos^2 \frac{\varphi}{2} \left(\frac{1}{\rho_r} - \frac{1}{f} \right)}{\cos(\varphi - \eta)} \left(\frac{\partial \Delta_n}{\partial \varphi} \right)^2 -$$

$$- \frac{(\varepsilon - 1) \sin \varphi}{\rho \cos(\varphi - \eta)} \Delta_n \frac{\partial \Delta_n}{\partial \varphi} - \frac{\frac{1}{2} - \frac{1}{\rho_r}}{2 \sin^2 \frac{\varphi}{2} \cos(\varphi - \eta)} \left(\frac{\partial \Delta_n}{\partial \varphi} \right)^2 -$$

$$\frac{\sin \varphi \operatorname{tg}(\varphi - \eta) - \sin^2 \frac{\varphi}{2} \frac{2 \operatorname{tg}^2(\varphi - \eta) \cos^2 \frac{\varphi}{2} (1 - \varepsilon \cos \varphi)}{\varepsilon^2 + 2\varepsilon \cos \varphi - 1}}{4 \rho_r \cos(\varphi - \eta)} \Delta_n^2. \quad (7)$$

DETERMINATION OF THE SURFACE OF A SMALL MIRROR.

Equations of the surface of the deformed small mirror it is possible to record in the form:

$$\left. \begin{aligned} x_m &= f - \rho_r \cos \varphi + \Delta_r \cos \eta, \\ y_m &= (\rho_r \sin \varphi - \Delta_r \sin \eta) \cos \psi, \\ z_m &= (\rho_r \sin \varphi - \Delta_r \sin \eta) \sin \psi \end{aligned} \right\}. \quad (8)$$

As noted above in practice of the strain of large mirror they were assigned discretely, therefore, expression (8) makes it possible to determine the coordinates only of the isolated points of the deformed small mirror. However, for obtaining the surface of small

mirror it is necessary to determine at these points also of standard.

Page 124.

Being guided cosines to surface (8):

$$\left. \begin{aligned} l &= \frac{Q}{\sqrt{Q^2 + S^2 + T^2}} \\ m &= \frac{S}{\sqrt{Q^2 + S^2 + T^2}} \\ n &= \frac{T}{\sqrt{Q^2 + S^2 + T^2}} \end{aligned} \right\} \quad (9)$$

where

$$Q = \begin{vmatrix} \frac{\partial y_M}{\partial \varphi} & \frac{\partial y_M}{\partial \psi} \\ \frac{\partial z_M}{\partial \varphi} & \frac{\partial z_M}{\partial \psi} \end{vmatrix}; \quad S = \begin{vmatrix} \frac{\partial z_M}{\partial \varphi} & \frac{\partial z_M}{\partial \psi} \\ \frac{\partial x_M}{\partial \varphi} & \frac{\partial x_M}{\partial \psi} \end{vmatrix}; \quad T = \begin{vmatrix} \frac{\partial x_M}{\partial \varphi} & \frac{\partial x_M}{\partial \psi} \\ \frac{\partial y_M}{\partial \varphi} & \frac{\partial y_M}{\partial \psi} \end{vmatrix}$$

it is determined from (8).

As can be seen from (6) and (8), total differential of the guides of cosines m, n, l is the function of the amount of the particular derived strains of large mirror. The rotation of standard is conveniently counted off from the radial plane, passing through point W_0 . Without the limitation of generality it is possible to consider that this plane coincides with plane $Z=0$. It differentiated (8) in terms of variable/alternating $\Delta_{\varphi}, \frac{\partial \Delta_{\varphi}}{\partial \varphi}, \frac{\partial \Delta_{\psi}}{\partial \psi}$, after some conversions we will obtain increments in the guides of the cosines of the deformed small mirror at point W_1 in comparison with the direction cosines of standard at point W_0 of the initial hyperboloid:

$$\Delta l = -\frac{\sin \eta \cos \frac{\varphi}{2}}{\rho_r} \left(\frac{\partial \Delta_n}{\partial \varphi} \right) - \frac{\sin \eta}{P (\varepsilon^2 + 2\varepsilon \cos \varphi - 1)}$$

$$\left[\varepsilon^2 \sin \frac{\varphi}{2} \left(1 + \frac{1}{2} \cos \varphi \right) - \varepsilon^2 \cos \varphi \sin \frac{\varphi}{2} - \varepsilon \left(\cos \frac{\varphi}{2} \sin^3 \varphi + \right. \right.$$

$$\left. \left. + \frac{3}{2} \cos \varphi \sin \frac{\varphi}{2} - \sin^2 \varphi \cos \frac{\varphi}{2} \right) - \frac{1}{2} \sin \frac{\varphi}{2} \right] \Delta_n;$$

$$\Delta m = \Delta l \operatorname{ctg} \eta; \quad \Delta n = -\frac{\cos \frac{\varphi}{2}}{P \sin \eta} \frac{\partial \Delta_n}{\partial \psi}.$$

Thus the methodology of the determination of the new surface of a small mirror consists of the following:

1. On assigned strains Δ_n of large mirror at discrete/digital points by the methods of numerical differentiation are determined partial derivatives $\frac{\partial \Delta_n}{\partial \varphi}$ and $\frac{\partial \Delta_n}{\partial \psi}$.

2. On known values and derivatives of strains of large mirror is determined shifts of points of small mirror, which correspond to points of large mirror in which are assigned strains.

3. With respect to known to guide cosines of normals to initial surface and their change are determined guides cosines of normals to new small mirror.

Findings it is sufficient for the construction of the surface of

new small mirror.

Page 125.

NUMERICAL CHECKING OF THE OBTAINED FORMULAS.

For checking the accuracy of the brought-out formulas was carried out the series/row of numerical calculations. Was examined the case of axisymmetric quadratic strains. In this case the radial sections of large mirror are the parabola whose focal length is excellent from the nominal, and the radial sections of a small mirror - hyperbola whose foci coincide with the focus of new parabola and the irradiator, the apex/vertex of hyperbola coincides with the nominal.

As an example were carried out the calculations for the antenna with a diameter $D_0=30$ m with the following initial geometric parameters: $\frac{f}{D_0}=0.333$; the angle of the irradiation of paraboloid $2\varphi_0=147.5$; the angle of the irradiation of hyperboloid of $2\beta_0=56^\circ$; the diameter of small mirror $d_M=0.15$.

Fig. 3 depicts the curves of the dependence of strains and maximum error $\delta\Delta_r$ (error it is reduced from the maximum on the edge of mirror to the zero on the axis antenna) in the function of strains

on the edge of large mirror. From the graphs indicated it is evident that at low values Δ_u the error is small. Thus, for instance, with $\Delta_u = -30$ mm $\delta\Delta_r = 0.05$ mm. Is at the same time evident a rapid increase in the error with an increase in the strains. Thus, with an increase in the strains from +30 to +60 mm error grows from 0.11 to 0.58 mm.

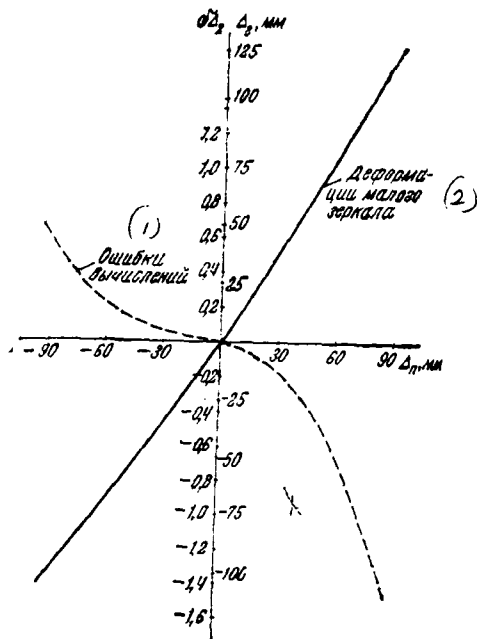


Fig. 3.

Key: (1). Errors for computations. (2). Strains of small mirror.

Page 126.

For the case of asymmetric strains were produced comparative calculations by the method proposed and the method of wave fronts. The graph of strains for one of the radial sections is given in Fig. 4. From the curves indicated it is evident that data of both methods coincide well.

CONCLUSION.

In this work is examined the approximate geometric-optical method of calculation of the corrected surface of a small mirror according to the assigned initial surfaces of mirrors and the strains of large mirror for Cassegrain's antenna. Examination is based on smallness and evenness of strains. Problem is solved for the case of arbitrary asymmetric strains.

The shift of certain point of a small mirror and the rotation of standard in it are determined on shift and rotation of the standard of the corresponding point of large mirror. The unknown values are obtained in the form of Maclaurin series for functioning three variable/alternating: the shift of point of large mirror and partial derivatives of shift of the angles ϕ and ψ spherical coordinates. The numerical calculations, carried out for the cases of asymmetric and axisymmetric strains, they showed the sufficiently high accuracy of method.

The calculation method proposed can be used both for the antenna of Cassegrain and for other types of two-mirror antennas.

REFERENCES

1. A. L. Eizenberg. Possibilities of phase correction on a small mirror in the two-mirror antenna. coll. of the "antenna" iss. 2. of M., "connection/communication", 1967.
2. Kelleher K. S. Relation concerning wave front and reflector. — <J. Appl. Phys.>. 1950, 216, 573. |

It acted in ed. 28/VIII 1970; after treatment/processing - 28/VI 1971.

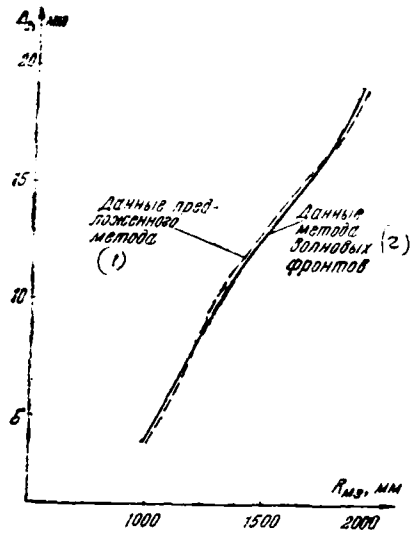


Fig. 4.

Key: (1). data of suggested method. (2). data of method of wave fronts.

Page 127.

THE PHASE CENTER OF HORN RADIATORS.

V. G. Yampol'skiy.

In the article is examined the procedure of calculation of the phase responses of the directivity of horn antennae. By the expansion of radiation patterns in the exponential series/row obtained simple formulas for determining the phase center.

Horn antennae and their modifications are used extensively in the technology SVCh both as the independent emitters and as the irradiators of optical-type antennas. Wide distribution received conical and pyramidal horn radiators. Conical horn antennae possess low side-lobe level, and their use provides usually satisfactory results [1], [2]. Recently propagation received conical horn antennae with the axisymmetric radiation patterns. The axial symmetry of diagrams is provided usually by the execution of the internal cavity of horns in the form of impedance surface with the high resistor/resistance. Such irradiators provide an increase in the

coefficient of the use of optical-type antennas and a decrease in the noise temperature. Pyramidal horn antennae are characterized by the satisfactory directed properties and ease of fabrication.

As is known, for obtaining the maximum efficiency of antenna the phase center of irradiator must be combined with the focus of antenna system. Optimum the position of irradiator is realized experimentally - either by determining its phase diagrams or by the immediate determination of the dependence of the antenna gain on the position of irradiator on the focal axis. This method of determining the position of irradiator is very labor-consuming and does not make it possible to determine the magnitude of losses of antenna gain due to the residual/remnant noncophasity of field distribution in antenna aperture, caused by the nonpointlike nature of phase center.

For many modifications of horn antennae the task of determining the phase center can be solved analytically¹.

FOOTNOTE ¹. Works [7], [8] examine the solution of this problem for some special cases. ENDFOOTNOTE.

This solution will make it possible to manage without labor-consuming and not very precise experiments, or to determine the "diffuseness" of phase center and connected with this decrease of amplification

factor.

Page 128.

The antenna radiation pattern with the circular opening at a distance of R from its aperture, as is known, it is determined by expression [1], [3]:

$$F(\theta) = \int_0^1 \int_0^{2\pi} E(r, \varphi) e^{-ikr^2 - i\alpha ar \sin \theta \cos(\varphi - \varphi')} r dr d\varphi, \quad (1)$$

where θ - current angle; $E(r, \varphi)$ - the field distribution in antenna aperture; φ' - angle between plane of reference ($\varphi=0$) and plane, in which is determined the radiation pattern; k - phase coefficient, determined by its own misphasing of horn and by misphasing, caused by the fact that the directed properties of antenna are determined in the Fresnel zone:

$$k = \frac{\alpha a^2}{2} \left(\frac{1}{T} + \frac{1}{R} \right), \quad (2)$$

a - radius of the opening of horn, T - height of horn (Fig. 1).

After decomposing exponential factor $e^{-i\alpha ar \sin \theta \cos(\varphi - \varphi')}$ in the exponential series/row, we will obtain

$$F(\theta) = \sum_{n=0}^{\infty} \frac{(-i\alpha a \sin \theta)^n}{n!} \int_0^1 \int_0^{2\pi} E(r, \varphi) \cos^n(\varphi - \varphi') e^{-ikr^2} r^{n+1} dr d\varphi. \quad (3)$$

Usually field distribution $E(r, \varphi)$ is symmetrical relative to any diameter of aperture. In this case from (3) we have

$$F(\theta) = \sum_{n=0}^{\infty} (-1)^n \frac{(\alpha a \sin \theta)^{2n}}{(2n)!} \int_0^1 \int_0^{2\pi} E(r, \varphi) \cos^{2n}(\varphi - \varphi) e^{-ikr^2} r^{2n+1} dr d\varphi. \quad (4)$$

After designating the coefficients of expansion (4) in terms of $\sin \theta$ through c_{2n} , we will obtain

$$F(\theta) = \sum_{n=0}^{\infty} c_{2n} \sin^{2n} \theta. \quad (5)$$

Let us normalize diagram $F(\theta)$ to unity in the direction $\theta=0$ and, after designating $\frac{c_{2n}}{c_0} = d_{2n} (d_0=1)$, we will obtain

$$F(\theta) = \sum_{n=0}^{\infty} d_{2n} \sin^{2n} \theta. \quad (6)$$

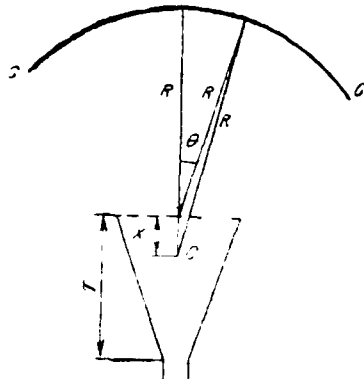


Fig. 1.

Page 129.

In the exponential form the expression for the radiation pattern takes the form

$$F(\theta) = e^{\sum_{n=1}^{\infty} A_{2n} \sin^{2n} \theta}, \quad (7)$$

where coefficients A_{2n} easily are calculated through coefficients d_{2n} . For the coefficients with small n we have:

$$A_2 = d_2; \quad A_4 = d_4 - \frac{d_2^2}{2}.$$

Coefficient A_2 in (7) determines the curvature of function $F(\theta)$ in the vicinity of direction $\theta=0$ (Fig. 1), the imaginary part of coefficient A_2 characterizing the curvature of the phase diagram of antenna, and the imaginary part of coefficient A_4 determines the "diffuseness" of the phase center of antenna.

Let us connect the position of phase center with the value of coefficient $\text{Im } A_2$. Let at a distance of R from the aperture of horn the phase radiation pattern take the form

$$\Phi(\theta) = \text{Im } A_2 \theta^2. \quad (8)$$

The position of phase center let us designate through O (Fig. 1). Then distance R' from point O to sphere CC takes the form

$$R' = \sqrt{R^2 + x^2 + 2xR \cos \theta}. \quad (9)$$

If distance R , at which is determined the radiation pattern, is considerably more than x , we have

$$R' = R + x \cos \theta = R - x - x \frac{\theta^2}{2}. \quad (10)$$

From condition $\alpha R' + \Phi(\theta) = \text{const}$ we obtain the expression, which is determining the amount of the shift of phase center relative to the aperture of horn, in the form

$$\alpha x = 2 \text{Im } A_2. \quad (11)$$

If distance R with the amount of the shift of the phase center x , formula for determining the latter commensurably takes the form

$$\alpha x = \frac{2\alpha R \text{Im } A_2}{\alpha R - 2 \text{Im } A_2}. \quad (12)$$

Obtained formulas (11) and (12) are valid only for the case when $\text{Im } A_0 = \text{Im } A_1 = \dots = 0$. The presence in the phase diagram of the terms of the expansion of higher order leads to the fact that phase field distribution is noncophasal during any selection of phase center, moreover a difference in the real phase front from the cophasal

increases with the growth θ . In other words, the position of phase center depends on angle θ .

Page 130.

Disregarding terms of expansion into $\Phi(\theta)$ above fourth, we will obtain after the simple conversions

$$\alpha x = 2\text{Im} A_2 \left[1 + \theta^2 \frac{\text{Im} A_4}{\text{Im} A_2} \right]. \quad (13)$$

Formula (13) makes it possible to determine a difference in the phase diagram from the cophasal and connected with this decrease of amplification factor.

Let us switch over to the computation of coefficients A_{2n} . Let us consider first the case of the uniform excitation of opening, i.e., $E(z, \varphi) \equiv 1$.

In this case

$$c_{2n} = 2\pi (-1)^n \frac{(\alpha a)^{2n}}{(2n)!} \int_0^1 e^{-kr^2} r^{2n+1} dr. \quad (14)$$

The integrals, entering in (14), are calculated in an explicit form. Actually/really,

$$F_0 = \int_0^1 e^{-ikr^2} r dr = \frac{1}{2} e^{-i \frac{k}{2}} \frac{\sin \frac{k}{2}}{\frac{k}{2}};$$

$$F_n = \int_0^1 e^{-ikr^2} r^{2n+1} dr = i^n \frac{d^n F_0}{dk^n} = \frac{1}{2} i^n \frac{d^n}{dk^n} \left[e^{-i \frac{k}{2}} \frac{\sin \frac{k}{2}}{\frac{k}{2}} \right]. \quad (15)$$

Hence we obtain for coefficients of $\text{Im}A_2$ and $\text{Im}A_4$ expression

$$\text{Im}A_2 = \frac{(\alpha a)^2}{8} \left(\frac{2}{k} - \text{ctg} \frac{k}{2} \right); \quad (16)$$

$$\text{Im}A_4 = \left[\frac{(\alpha a)^4}{128} - \frac{(\alpha a)^2}{24} \right] \left(\frac{2}{k} - \text{ctg} \frac{k}{2} \right). \quad (17)$$

Thus, for the case of uniform field distribution on the opening we have for the amount of the shift of phase center an expression

$$\alpha x_1 = \frac{(\alpha a)^2}{4} \left(\frac{2}{k} - \text{ctg} \frac{k}{2} \right). \quad (18)$$

If the determination of radiation pattern is conducted in the remote zone, then phase coefficient is determined only by its own misphasing of horn and is equal to $k = \alpha a / 2T^2$.

For this case we have

$$\frac{x_1}{T} = 1 - \frac{k}{2} \text{ctg} \frac{k}{2}. \quad (19)$$

Page 131.

With small k formula (19) takes the form

$$\frac{x_1}{T} = \frac{k^2}{12}. \quad (20)$$

Analysis shows that formula (19) it is possible to use during misphasings of wave in the horn, not large α . During the large

misphasings the structure of the phase front of irradiator in the limits of major lobe proves to be more complicated, and with its approximation it is necessary to consider the terms of the expansion of higher order. In this case of phase center there does not exist and the optimum position of irradiator must be determined integrally.

Large interest is horn radiators with the axisymmetric radiation pattern. In such irradiators field distribution in the aperture is approximately determined by the equality

$$E(r, \varphi) = 1 - r^2. \quad (21)$$

Coefficients $c_{2n}^{(2)}$ for this case can be determined according to the formula

$$c_{2n}^{(2)} = c_{2n}^{(1)} - c_{2n+1}^{(1)}, \quad (22)$$

where $c_{2n}^{(1)}$ is determined by expression (14).

Let us give the resultant expression for the amount of the shift of phase center from the aperture of horn, excited by field according to formula (21), in the form

$$\frac{x_2}{T} = \frac{2}{1 + \frac{1}{\left(\frac{2}{k} - \text{ctg} \frac{k}{2}\right)^2}}. \quad (23)$$

During the small misphasings

$$\frac{x_2}{T} = \frac{k^2}{18}. \quad (24)$$

Formula (23) it is possible to use with $k < \pi - 1.25\pi$. Fig. 2 gives the dependence of shifts x_1/T and x_2/T on misphasing k . Dotted line

depicted the results of calculations according to approximate formulas (20) and (24). From the figure one can see that with an increase in the misphasing the phase center of horn antenna is displaced from the plane of aperture to the throat, the amount of shift in the case of uniform field distribution in the aperture 1.5 times approximately/exemplarily exceeding the amount of shift for the horn, excited unevenly [according to the formula (21)].

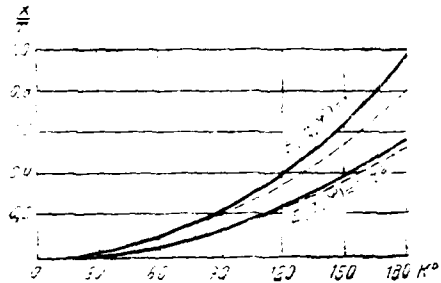


Fig. 2.

Page 132.

There is greatest practical interest in the case of exciting the horn by wave H_{11} . Field distribution in this case with a sufficient degree of accuracy can be represented by expression [1]

$$E(r, \varphi) = 1 - (p + q \cos^2 \varphi) r^2, \quad (25)$$

where $p=1/3$, $q=2/3$.

For this case coefficients c_{2n} take the form

$$c_{2n} = (-1)^n \frac{(\alpha a)^{2n}}{(2n)!} \int_0^1 \int_0^{2\pi} [1 - (p + q \cos^2 \varphi) r^2] \cos^{2n}(\varphi - \varphi') r^{2n+1} dr d\varphi. \quad (26)$$

Let us note that in plane E of horn antenna angle $\varphi' = \pi/2$, and in plane H $\varphi' = 0$.

Coefficients c_{2n} it is possible to express through known

coefficients $c_{2n}^{(1)}$, those determined by formula (14). Then we have

for plane H

$$c_{2n}^{(H)} = \frac{(2n-1)!!}{(2n)!!} \left[c_{2n}^{(1)} - \rho c_{2n+2}^{(1)} \right] - q \frac{(2n+1)!!}{(2n+2)!!} c_{2n+2}^{(1)} \quad (27)$$

for plane E

$$c_{2n}^{(E)} = \frac{(2n-1)!!}{(2n)!!} \left[c_{2n}^{(1)} - \rho c_{2n+2}^{(1)} \right] - q \frac{(2n-1)!!}{(2n+2)!!} c_{2n+2}^{(1)} \quad (28)$$

Calculating coefficients c_{2n} , we will obtain that the position of the phase center of conical horn with wave H_{11} is determined by formula (11), where

for plane H

$$\text{Im } A_2 = \text{Im} \left[\frac{i \frac{e^{-ik}}{6k} + \frac{\frac{2}{3} e^{-ik} - 1}{k^2} + \frac{5}{3} i \frac{e^{-ik} - 1}{k^2}}{\frac{2i}{k} \left(\frac{1}{3} e^{-ik} - 1 \right) + \frac{4}{3} \frac{1 - e^{-ik}}{k^2}} \right] \quad (29)$$

for plane E

$$\text{Im } A_2 = \text{Im} \left[\frac{\frac{e^{-ik}}{2k} + \frac{e^{-ik} - 1}{k^2}}{\frac{2i}{k} \left(\frac{1}{3} e^{-ik} - 1 \right) + \frac{4}{3} \frac{1 - e^{-ik}}{k^2}} \right] \quad (30)$$

Page 133.

During the small misphasings the shift of phase center can be determined:

in plane H

$$\frac{x_H}{T} = \frac{7}{144} k^2 \sim 0.049k^2; \quad (31)$$

in plane E

$$\frac{x_E}{T} = \frac{15}{144} k^2 \sim 0.104k^2. \quad (32)$$

Fig. 3 gives the dependence of the amount of the shift of the phase center of the conical horn, excited by wave H_{11} , in two principal planes. Dotted line in this figure gave the results of calculation according to approximate formulas (31) and (32). From the graphs it is evident that with an increase in the misphasing the speed of the shift of phase center in plane E more than twice exceeds the speed of shift in plane H. Therefore the equiphase frontal surface of the emitted wave has different curvatures in principal planes. This fact inevitably leads to misphasing of field into the aperture of the antenna and to the decrease of the coefficient of its amplification.

For the pyramidal horns, excited by wave H_{01} , the radiation patterns in principal planes take the form:

in plane E

$$F(\theta) = \int_{-1}^1 e^{-i\alpha_E x \sin\theta - ikx^2} dx; \quad (33)$$

in plane H

$$F(\theta) = \int_{-1}^1 \cos\left(\frac{\pi}{2}x\right) e^{-i2a_H x \sin\theta - ikx^2} dx, \quad (34)$$

where $2a_E$ and $2a_H$ - sizes/dimensions of aperture in planes E and H respectively.

In this case the integrals, entering the coefficients of expansion $F(\theta)$ in terms of $\sin^2\theta$ are not calculated in elementary functions [3]. For obtaining the calculation formulas it is expedient to use the methodology of the approximation calculus of integrals, given in [4] and valid with $k \ll \pi$.

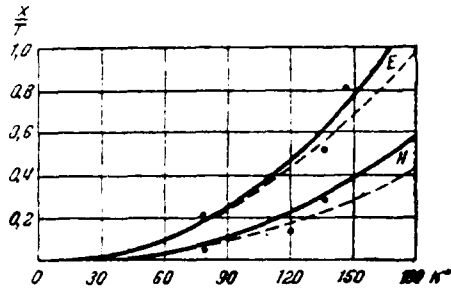


Fig. 3.

Page 134.

Final formulas for the shift of the phase center of pyramidal horn with $k \ll \omega$ take the form:

$$\frac{x_E}{T} = \frac{8}{45} k^2 \cos 0,28k \sim 0,178k^2 \cos 0,28k; \quad (35)$$

$$\frac{x_H}{T} = \frac{16}{175} k^2 \cos 0,22k \sim 0,091k^2 \cos 0,22k. \quad (36)$$

Fig. 4 gives the dependence of the amount of the shift of the phase center of pyramidal square horn in main planes. From the figure one can see that, as in the case of conical horn, the speed of the shift of phase center in plane E considerably exceeds the speed of shift in plane H. This does not allow without the acceptance of any further measures to ensure accurately cophasal field distribution in antenna aperture.

In conclusion let us note that the results of calculating the location of phase centers were compared with the available in the literature experimental data according to the phase diagrams of conical and pyramidal horns, moreover the coincidence of results was completely satisfactory. Fig. 3 and 4 depict as points the experimentally specific positions of the phase centers of horn feed, partially borrowed from [5] and [6].

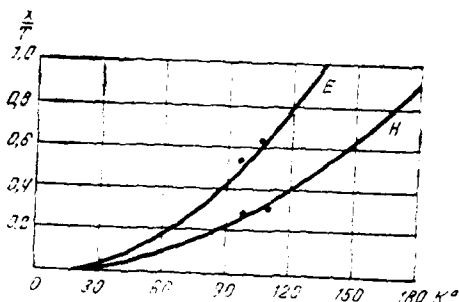


Fig. 4.

REFERENCES

1. Yu. A. Yerukhimovich, G. A. Kozrina. Radiation/emission of noncophasal circular opening. Collector/collection of works NIIR, iss. 4 (49), 1967.
2. Yu. A. Yerukhimovich, S. M. Zimin, A. A. Metrikin. Two-mirror antenna for the radio relay communication. Coll. "Antenna", iss. 7, 1970.
3. G. Z. Eizenberg. VHF antennas M., "connection/communication", 1957.
4. V. G. Yampol'skiy. Effect of phase distortions on the efficiency of surface antenna. "radio engineering", 1963, No 2.

5. Ekon Hiroshi Kokusai tsusin-no kenkyu, January, 1968, No 55.

4. Feix G. Untersuchungen von Phasenzentren an extrem langen Pyramidenhornstrahler — «MTZ» r. 19, abryer. 1966, № 18.
5. Bauer K. The phase center of aperture radiators. «Arch. Elek. Übertragung», vol. 9, 1955, p. 541—546.
6. Ujue H., Yoneyama T. and Nishida S. A consideration of the phase center of aperture antennas — «IEEE Trans. antennas Propagat (communications)», vol. AP-15, may 1967, p. 475—480.

Received 27/V 1971; after revision - 23/XI 1971.

Page 135.

DISPERSIVE CHARACTERISTICS OF MULTITURN CYLINDRICAL HELICAL ANTENNAS
WITH COUNTER WINDING.

O. A. Yurtsev.

In the article are examined normal waves in the multiturn spiral with the contrary coil/winding. Is derived and is analyzed dispersion equation, it shows that during the excitation of the first normal wave the band coverage of helical antenna increases proportional to a number of approaches.

Introduction.

In works [1-2] it is shown that the cylindrical multiturn helical antenna with the one-sided coil/winding (Fig. 1), excited in the mode/conditions of the first normal wave (amplitudes of the currents, which excite approaches, are identical, phases in the adjacent approaches differ to value $2\pi/M$, where M - number of approaches), it has axial directional characteristic and polarization in the direction of axis, close to the circular, in the range of frequencies with the coefficient of overlap $K_v = M - 1$. In work [2] it is

experimentally shown that the same range properties possesses the multiturn helical antenna with the contrary coil/winding. In contrast to the spiral with the one-sided coil/winding, this antenna depends on the method of excitation has a polarization close to circular (right or left), or linear. Theoretically this antenna in mentioned work [2] was not examined.

In this article on basis of the properties of symmetry is derived and is analyzed dispersion equation, are determined the frequency boundaries of the region of the existence of different transmission modes. On the basis of this are drawn a conclusion about the band coverage of multiturn helical antenna with the contrary coil/winding.

AD-A090 523

FOREIGN TECHNOLOGY DIV WRIGHT-PATTERSON AFB OH
ANTENNAS. (U)

F/6 9/5

UNCLASSIFIED

SEP 80
FTD-ID(RS)T-1340-80

NL

4 OF 4
AIR
AD-A090523



END
DATE
FILMED
41-80
DTIC

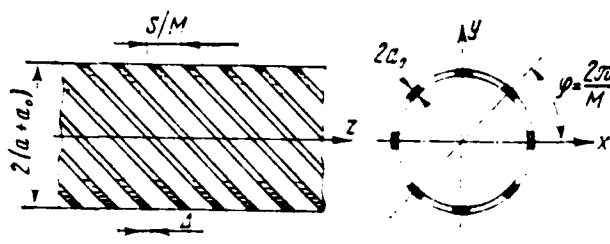


Fig. 1.

Page 136.

Symmetry of system, transmission modes.

Let us consider the system of waves in the multiturn regular spiral with the contrary coil/winding, formed by the ideally conducting tapes with the rectangular form of cross section. Let us take the following designations: M - number of approaches, wound up in one direction; $2a$, S , α - mean radius, step/pitch and winding angle of approaches; Δ - width of belt along $\frac{z}{z}$ -axis of cylindrical coordinate system: r , φ , z , moreover $\Delta \ll S/M$ and $\Delta \ll \lambda$; $2a_0$ - thickness of belt along r ; $e^{i\omega t}$ - temporary/time factor; $\sigma=0$, ϵ , μ - parameters of medium inside, also, cut of the spiral. The geometric parameters of right and left approaches are identical, which is implemented strictly, if system is the cylindrical metallic surface, perforated/punched by the openings/apertures of rhombic form (Fig.

2). In this case, naturally, between the right and left approaches in the points of their intersections there is a galvanic contact.

If $a_0 \ll a$, then equality the geometric parameters of right and left approaches can be made approximately even in the absence of the contacts between them. It must be noted that from the point of view of the retention/preservation/maintaining the properties of symmetry and, therefore, electrodynamic properties, which escape/ensue from them, the presence or the absence of the contact between the right and left approaches plays no role. The following presentation, which concerns conclusion/output and analysis of dispersion equations, assumes that $a_0/a \ll 1$. This is allowed, just as during the analysis of single-cut spiral, to seek fields only in two partial regions (with $r \leq a$ and $r \geq a$), "joining" them on the interface $r=a$.

The system of its own waves and their fundamental properties are determined by the symmetry of system.

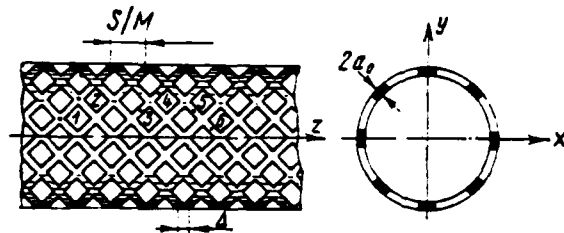


Fig. 2.

Page 137.

The spiral in question possesses the screw axis of symmetry C_{2M} . Field and currents of system with the axis of symmetry C_{2M} in the cylindrical coordinate system r, ϕ, z can be represented in the form of sum $2M$ the so-called normal waves, which satisfy boundary conditions and designed according to the formulas of work [3]:

$$E(r, \phi, z) = \sum_{n_1}^{n_2} e^{in_1\phi} (r, \phi, z) e^{-i(\beta z + \frac{2\pi n_1}{S} z)}; \quad (1)$$

$$J(r, \phi, z) = \sum_{n_1}^{n_2} J^{(n_1)}(r, \phi, z) e^{-i(\beta z + \frac{2\pi n_1}{S} z)}, \quad (2)$$

where

$$n_1 = 1 - M, n_2 = M; \quad (3)$$

β - axial phase constant of zero normal current wave.

Functions $e^{in_1\phi}$ satisfy the conditions:

$$e^{(n)}(r, \varphi, z) = e^{(n)}\left(r, \varphi, z + \frac{S}{2M}\right); \quad (4)$$

$$e^{(n)}\left(r, \varphi + \frac{2\pi}{M}, z\right) = e^{i\frac{\pi n}{M}} e^{(n)}(r, \varphi, z) \quad (5)$$

and, therefore, they can be decomposed in the Fourier series on coordinate z (period is equal to $S/2M$):

$$e^{(n)}(r, \varphi, z) = \sum_{m=-\infty}^{\infty} e_m^{(n)}(r, \varphi) e^{-i\frac{4\pi M}{S} m z}. \quad (6)$$

Representing function $e_m^{(n)}$ in the form of the sum of the azimuth three-dimensional/space harmonics:

$$e_m^{(n)}(r, \varphi) = \sum_{v=-\infty}^{\infty} e_{mv}^{(n)}(r) e^{iv\varphi}, \quad (7)$$

on the basis (5) and (6) it is possible to record

$$v\left(\varphi + \frac{\pi}{M}\right) = \frac{n\pi}{M} + v\varphi + 2\pi t, \text{ где } t=0, \pm 1, \pm 2, \dots \quad (8)$$

whence

$$v = n + 2tM.$$

Relationship/ratio (8) determines the spectrum of the azimuth three-dimensional/space harmonics, entering in n -th normal wave.

Page 138.

On the basis (1), (6), (7) and (8) it is possible to record following field expression of the n normal wave:

$$E^{(n)} = \sum_{m=-\infty}^{\infty} \sum_{l=-\infty}^{\infty} e_{ml}^{(n)}(r) e^{-i\beta_l z + i l \varphi}, \quad (9)$$

where

$$\beta_q = \beta - \frac{2\pi}{S} q; \quad q = n - 2mM. \quad (10)$$

Functions $J^{(n)}(r, \varphi, z)$ satisfy the conditions, analogous (4) and (5), and they can be represented in the form

$$J^{(n)}(r, \varphi, z) = \sum_{m=-\infty}^{\infty} \sum_{l=-\infty}^{\infty} J_{mv}^{(n)}(r) e^{-i\beta_q z + i l \varphi}. \quad (11)$$

Conditions (4) and (5) mean that the fields and currents at the symmetrical points of system in the n normal wave (point 1 and 2, 3 and 4, 5 and 6 in Fig. 2) have identical amplitude and are shifted only on the phase. This fact in the absence of losses in the system is implemented with the existence of the traveling waves of current both in the rightists and in the left approaches. The amplitudes of currents in accordance with condition (5) in the adjacent approaches, wound up in one direction, are identical, and phases in plane $z = \text{const}$ differ on

$$\Delta\psi = \frac{2\pi n}{M}. \quad (12)$$

Let us designate the composite amplitudes of currents in the right approaches through $J_+^{(n)}$, in the left - through $J_-^{(n)}$.

Condition (12) satisfy the normal waves: n -th and $(n-M)$ -th; therefore cannot be separately excited them. Instead of these two waves should be examined the total field into which enter azimuth and longitudinal three-dimensional/space harmonics with the numbers:

$$v = n + lM, \quad q = n + mM. \quad (13)$$

Moreover instead of (3) it is necessary to take $n_1=0$, $n_2=M-1$.

Currents in the right approaches satisfy the conditions of right helical symmetry; therefore in formula (11) for these currents is satisfied the condition:

$$-\beta_q \Delta z + v \Delta \varphi = -\beta \Delta z, \quad (14)$$

where Δz and $\Delta \varphi$ - arbitrary shifts of spiral along Z -axis and on the angle φ , with which right approaches are combined themselves with themselves ($\Delta z = a \Delta \varphi \operatorname{tg} a$).

Substituting in (14) expression for β_q , we obtain $-\beta \Delta z + \frac{2\pi}{S} q \Delta z + v \Delta \varphi = -\beta \Delta z$, whence $q = -v$. On the basis this expansion (11) for currents $J_{\pm}^{(n)}$ can be recorded in the form

$$J_{\pm}^{(n)} = \sum_{m=-\infty}^{\infty} J_{m\nu}^{(n)}(r) e^{-i \left(\beta + \frac{2\pi}{S} q \right) z + i m \varphi}, \quad (15)$$

where $q = n + mM$.

Page 139.

Currents in the left approaches satisfy the conditions of left helical symmetry, and it is possible to show that for them in expansion (11) $q = v$. In this case expression (11) is written/recorded in the form

$$J_{\pm}^{(n)} = \sum_{m=-\infty}^{\infty} J_{m\nu}^{(n)}(r) e^{-i \left(\beta - \frac{2\pi}{S} q \right) z + i m \varphi}, \quad (16)$$

Thus, in a H -entry symmetrical spiral with the contrary coil/winding just as into the spiral with the one-sided coil/winding, the field and currents in the approaches can be presented in the form of the sum of the normal waves each of which can be excited individually. In any normal current wave both in the rightists and in the left approaches are the traveling waves. Each longitudinal three-dimensional/space harmonic of current is connected only with one azimuth harmonic. The orthogonality of azimuth three-dimensional/space harmonics in the interval $\phi [0-2\pi]$ makes it possible to establish/install the connection/communication between the azimuth and longitudinal three-dimensional/space harmonics of field in the n normal wave and to obtain the dispersion equation of relatively phase constant β .

BOUNDARY CONDITIONS. Dispersion equation.

Using a method of the electrical and magnetic vectors of hertz, the components of vector E and H in the cylindrical coordinate system for the n normal wave in the spiral in question it is possible to record in the form (by prime is marked field with $r \leq a$, by two primes - with $r > a$):

$$\begin{aligned}
 H'_\varphi &= \sum_{l=-\infty}^{\infty} \sum_{m=-\infty}^{\infty} \left\{ -\frac{\nu\beta_q}{r} B' I_\nu(\rho_q r) - i\omega\epsilon\rho_q \right. \\
 &\quad \left. \times P_q A' I'_\nu(\rho_q r) \right\} e^{-i\beta_q z + i\nu\varphi} \\
 H'_z &= - \sum_{l=-\infty}^{\infty} \sum_{m=-\infty}^{\infty} \rho_q^2 B' I_\nu(\rho_q r) e^{-i\beta_q z + i\nu\varphi} \\
 E'_\varphi &= \sum_{l=-\infty}^{\infty} \sum_{m=-\infty}^{\infty} \left\{ -\frac{\nu\beta_q}{r} A' I_\nu(\rho_q r) - i\omega\mu\rho_q \right. \\
 &\quad \left. \times B' I'_\nu(\rho_q r) \right\} e^{-i\beta_q z + i\nu\varphi} \\
 E'_z &= - \sum_{l=-\infty}^{\infty} \sum_{m=-\infty}^{\infty} \rho_q^2 A' I_\nu(\rho_q r) e^{-i\beta_q z + i\nu\varphi}
 \end{aligned}$$

Page 140.

Field expressions with $r > a$ are obtained from (17) by the replacement:

$$I_\nu(\rho_q r) \rightarrow K_\nu(\rho_q r), \quad A' \rightarrow A'', \quad B' \rightarrow B''.$$

where I_ν and K_ν - Bessel function from the imaginary argument:

$$\rho_q = \sqrt{\beta_q^2 - k^2}, \quad k = \omega\sqrt{\epsilon\mu}.$$

Integration constant A', A'', B', B'' are found from boundary conditions with $r=a$:

$$\left. \begin{aligned}
 E'_z &= E''_z, & E'_\varphi &= E''_\varphi \\
 H'_z - H''_z &= j_\varphi, & H'_\varphi - H''_\varphi &= -j_z
 \end{aligned} \right\} \quad (18)$$

where j_φ and j_z - components of current density on surface of $r=a$.

Considering that density distribution of current along the width of the belt of approach is even, is absent transverse to the axis of belt the component j ($\Delta \ll \lambda$), amplitudes in all approaches, wound up

in one direction, are identical, and the phases of currents in the adjacent approaches differ to value $\Delta\Psi = \frac{2\pi n}{M}$. On the basis (15) and (16) it is possible to obtain the following expressions

$$\left. \begin{aligned} j_{\phi} &= \frac{M \operatorname{ctg} \alpha}{\pi a} e^{-i\beta z} \sum_{m=-\infty}^{\infty} e^{iq\phi} \left[J_0^+ e^{-i\frac{2\pi}{S} qz} - J_0^- e^{i\frac{2\pi}{S} qz} \right] \\ j_z &= \frac{M}{\pi a} e^{-i\beta z} \sum_{m=-\infty}^{\infty} e^{iq\phi} \left[J_0^+ e^{-i\frac{2\pi}{S} qz} + J_0^- e^{i\frac{2\pi}{S} qz} \right] \end{aligned} \right\} \quad (19)$$

where J_0^{\pm} - wave amplitudes of current in the right and left approaches; $q = n + mM$.

Expressions (19) correspond to the case $\Delta = 0$ and it is virtually valid with $\Delta \ll S/M$. The substitution of expressions (17) under boundary conditions (18) reduces to the system of equations relative to integration constants A' , A'' , B' , B'' . The analysis of this system, which uses a property of the orthogonality of azimuth three-dimensional/space harmonics, shows that the constants A' , A'' , B' , B'' will depend on coordinates r and ϕ in two cases:

$$- \text{ when } q = \nu \text{ and } J_0^+ = 0. \quad (20)$$

$$- \text{ when } q = -\nu \text{ and } J_0^- = 0. \quad (21)$$

In these cases solution of system of equations gives the following expressions for the integration constants:

$$\left. \begin{aligned} A' &= \frac{J_0^{\mp} M (\beta_{\pm v} \beta - k^2)}{i \omega \varepsilon \rho_{\pm v}^2 \pi} K_v(\rho_{\pm v} a) \\ A'' &= \frac{J_0^{\mp} M (\beta_{\pm v} \beta - k^2)}{i \omega \varepsilon \rho_{\pm v}^2 \pi} I_v(\rho_{\pm v} a) \\ B' &= \mp \frac{J_0^{\mp} M \operatorname{ctg} \alpha}{\rho_{\pm v} \pi} K_v'(\rho_{\pm v} a) \\ B'' &= \mp \frac{J_0^{\mp} M \operatorname{ctg} \alpha}{\rho_{\pm v} \pi} I_v'(\rho_{\pm v} a) \end{aligned} \right\} \quad (22)$$

where
$$\beta_{\pm v} = \beta \pm \frac{\operatorname{ctg} \alpha}{a} v; \rho_{\pm v} = \sqrt{\beta_{\pm v}^2 - k^2}; v = n + iM. \quad (23)$$

Phase constant β is determined from the dispersion equation, which in the case, which corresponds to condition (20), is found from the boundary condition, which requires equality zero components of vector E , tangent to the left approaches, since $J_0^{\pm} = 0$. This condition takes the form

$$E_r^{\pm} = E_z^{\pm} \sin \alpha - E_{\theta}^{\pm} \cos \alpha \quad \text{with} \quad r = a_{\pm}. \quad (24)$$

In the case, which corresponds to condition (21), dispersion equation is derived from the boundary condition, which requires the absence of the tangential component of vector E to the right approaches:

$$E_r^{\pm} = E_z^{\pm} \sin \alpha + E_{\theta}^{\pm} \cos \alpha \quad \text{with} \quad r = a + a_0. \quad (25)$$

From expressions (17), (22) and boundary conditions (24) and (25) are obtained the following two¹ dispersion equations:

$$\frac{\sum_{l=-\infty}^{\infty} \{I_{v+1}(\rho_{\pm v} a) K_{v+1}(\rho_{\pm v} a \gamma) + I_{v-1}(\rho_{\pm v} a) K_{v-1}(\rho_{\pm v} a \gamma)\}}{2 \sum_{l=-\infty}^{\infty} I_v(\rho_{\pm v} a) K_v(\rho_{\pm v} a \gamma)} = \left[\left(\frac{\beta}{k} \right)^2 - 1 \right] \operatorname{tg}^2 \alpha. \quad (26 \text{ a. b})$$

where $\gamma = 1 + \frac{\alpha_0}{a}$.

FOOTNOTE ¹. Equation (26a) for wave number ρ_{+v} . equ. (26b) - for ρ_{-v} .
ENDFOOTNOTE.

Page 142.

RESULTS OF THE ANALYSIS OF DISPERSION EQUATIONS.

The analysis of equ. (26), based on the phenomenon of three-dimensional/space resonance [4], shows that the equation with the transverse wave number ρ_{+v} (26a) determines the phase constants of those normal waves, in which resounding are three-dimensional/space harmonics with negative indices v . Equation with the transverse wave number ρ_{-v} (26b) determines normal waves, in which the resounding harmonics have $v > 0$. At the assigned value of n equ. (26) has infinite solution set. Each solution determines the wave of field, in which resounds any three-dimensional/space harmonic. The wave, in which

resounds the harmonic with index v , it is designated below through $T_{\pm(v)}$. In wave $T_{(v)}$, resounding v -harmonic has the positive phase speed, which coincides in the direction with phase wave velocity of current in the approaches of spiral. In wave $T_{-(v)}$, the resounding harmonic has negative phase speed.

During the excitation in the helical antenna of waves $T_{\pm(v)}$, where $v \neq 1$, is observed the mode of radiation/emission with conical directional characteristic. In the direction of the axis of spiral the radiation/emission is absent. The mode of straight/direct axial radiation/emission in the helical antenna is observed on waves $T_{\pm(1)}$. On wave $T_{(1)}$ the polarization in the direction of axis close to the left circular, on wave $T_{(-1)}$ - to the right circular.

On waves $T_{\pm(2)}$ in the spiral is observed the mode of reverse axial radiation/emission with the polarization in the direction of the axis, close to the circular left or the right.

As it follows from expression $v = n + tM$, of wave $T_{\pm(1)}$ they enter into first normal wave ($n=1$), waves $T_{\pm(-1)}$ - in ($M-1$) normal wave. For the excitation in the spiral of each of these waves in the pure form the approaches of spiral must be fed by the currents of identical amplitude; their phases from one approach to the next must vary according to the following laws:

- for the wave with $n = 1$ $\psi_l = \frac{2\pi}{M}(l-1)$,

- for the wave with $n = M-1$ $\psi_l = \frac{2\pi}{M}(M-1)(l-1) = -\frac{2\pi}{M}(l-1)$,

where l - number of approach.

During the excitation of approaches simultaneously by currents $J_0 e^{i \frac{2\pi}{M}(l-1)t}$ and $J_0 e^{-i \frac{2\pi}{M}(l-1)t}$ in the spiral they are excited with the identical wave amplitudes T_{+1} and $T_{(-1)}$, simultaneously resound harmonics with indices $v = \pm 1$. polarization in the direction of the axis of spiral will be linear. In this case summed current, which excites the l approach, takes form $J = J_0 \cos [2\pi/M(l-1)]$. The plane of the polarization of radiation field in the direction of the axis of helical antenna coincides with plane passing through the approach with $l=1$.

Page 143.

The mode of straight/direct axial radiation/emission on waves $T_{(\pm 1)}$ is observed in the range of values ka , in which these waves have the strong dispersion (in the region of the first three-dimensional/space resonance). Equations (26) make it possible

to determine the frequency boundaries of the region of the existence of different transmission modes in the spiral, regions of the strong and weak dispersions of the phase speed. The results of the analysis of equ. (26) are reduced to the following.

The real values βa , which correspond to ground waves, are arranged/located in the intervals:

$$|v(t)| \operatorname{ctg} \alpha + ka \leq \beta a \leq \begin{cases} |v(t-1)| \operatorname{ctg} \alpha - ka & \text{if } \frac{1}{2}\pi < \alpha < \pi \\ |v(t+1)| \operatorname{ctg} \alpha - ka & \text{if } 0 < \alpha < \frac{1}{2}\pi \end{cases} \quad (27)$$

Key: (1). for.

where $v(t) = n + tM$, $v(t \mp 1) = n + (t \mp 1)M$, $t = 0, \pm 1, \pm 2, \dots$

In each of the intervals equ. (26a) determines the phase constants of waves $T_{v(t)}$ and $T_{-v(t-1)}$, and equ. (26b) - the phase constants of waves $T_{v(t)}$ and $T_{-v(t+1)}$. Qualitative form of the dependence on βa of the left $F_1(\beta a)$ and right $F_2(\beta a)$ parts of equ. (26) is shown in Fig. 3. On the left boundary of interval (27) resonates three-dimensional/space harmonic with number $= |v(t)|$, on the right boundary - with number $= |v(t \mp 1)|$. Selecting corresponding to these harmonics terms in equ. (26) and asymptotically summarizing those remaining, that correspond to nonresonant harmonics, it is possible to obtain the following expression for for function $F_1(\beta a)$, valid in interval (27):

where

$$F_1(\beta a) \approx \frac{B_{\nu(t)-1} - B_{\nu(t)-1} + B_{\nu(t\mp 1)+1} - B_{\nu(t\mp 1)-1} + A_M}{2B_{\nu(t)} + 2B_{\nu(t\mp 1)} + A_M},$$

$$B_{\nu(t)+l} = I_{\nu(t)+l} [p_{\pm\nu(t)} a] K_{\nu(t)+l} [p_{\pm\nu(t)} a \gamma],$$

$$l = 0, \pm 1;$$

$$A_M = \frac{\operatorname{tg} \alpha}{M \gamma} \left[2 \ln \frac{1}{1 - e^{-L}} - e^{-L} \right], \quad L = M \frac{a_0}{a} \operatorname{ctg} \alpha.$$

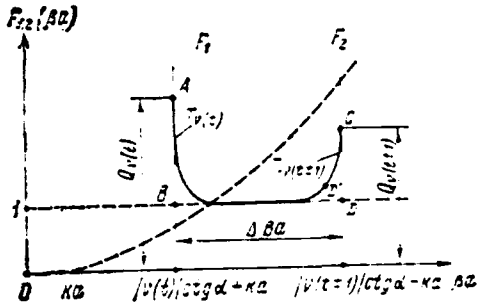


Fig. 3.

Page 144.

For the purpose of simplification in calculations $F_1(\beta a)$ during the computations of phase constants β on the left side of interval (27) it is possible to isolate only $v(t)$ member, while in the right - only $v(t=1)$, the others to sum up asymptotically. In this case

$$A_M \approx \frac{\operatorname{tg} \alpha}{M \gamma} 2 \ln \frac{1}{1 - e^{-L}}.$$

In particular, this can be done during the computation of the values of function $F_1(\beta a)$ on the boundaries of intervals - Q_v . During the more approximate computations which, as a rule, give acceptable accuracy for the practical use/application (nonresonant terms), A_M it is possible not to consider. Without account A_M is obtained the following expression for Q_v :

$$Q_v \approx \frac{v^2}{v^2 - 1}. \tag{29}$$

From equ. (26) and expression (29) are obtained the formulas, which

are determining values of ka , which limit the domains of existence of waves $T_{v(t)}$ and $T_{-v(t \pm 1)}$. Below these values are designated through $ka_{\pm v}^{min}$ and $ka_{\pm v}^{max}$. Intersection $F_1(\beta a)$ and $F_2(\beta a)$ at points A and C in Fig. 3 they correspond to values $ka_{v(t)}^{min}$ and $ka_{-v(t \pm 1)}^{min}$; the contact of these curves at point D', which is replaced by the closely spaced point D, it corresponds to values $ka_{v(t)}^{max} = ka_{-v(t \pm 1)}^{max}$. The values ka indicated are determined by the following approximation formulas:

$$ka_{v(t)}^{min} \approx \frac{|v(t)|}{\sqrt{Q_{v(t)} - \operatorname{tg}^2 \alpha - \operatorname{tg} \alpha}}; \quad (30)$$

$$ka_{-v(t \pm 1)}^{min} \approx \frac{|v(t \mp 1)|}{\sqrt{Q_{v(t \mp 1)} + \operatorname{tg}^2 \alpha - \operatorname{tg} \alpha}}; \quad (31)$$

$$ka_{v(t)}^{max} = ka_{-v(t \pm 1)}^{max} = \frac{|v(t \mp 1)| \cos \alpha}{1 + \sin \alpha}. \quad (32)$$

The region of strong wave dispersion $T_{v(t)}$ is limited by value $ka'_{v(t)}$, approximately corresponding to the passage of function $F_2(\beta a)$ through point B, and it is determined by the formula

$$ka'_{v(t)} \approx \frac{|v(t)| \cos \alpha}{1 - \sin \alpha}. \quad (33)$$

Strong wave dispersion $T_{-v(t \pm 1)}$ is observed in the entire domain of its existence. We use the obtained results for the analysis of the first and $(M-1)$ normal waves, which ensure the mode of straight/direct axial radiation/emission.

Into the normal waves indicated enter the waves of field respectively $T_{\pm(1+M)}$ and $T_{\pm(-1+(1+M))}$. For waves $T_{\pm 1}$ of appropriate $t=0$, $n=1$ and $t=-1$, $n=M-1$, from expressions (30) and (32) it follows:

$$ka_{\pm 1}^{min} = 0; \quad (34)$$

$$ka_{\pm 1}^{max} \approx \frac{(1-M) \cos \alpha}{1 + \sin \alpha}. \quad (35)$$

Page 145.

The nearest to $T_{(\pm 1)}$ transmission modes from the side of greater ka are waves $T_{-(\pm(1+M))}$ from the side of smaller ka - wave $T_{-(\pm 1)}$. For waves $T_{-(\pm(1+M))}$ from (29) and (31) we have

$$ka_{-(\pm(1+M))}^{min} \approx \frac{M-1}{\sqrt{\frac{(1-M)^2}{(1-M)^2-1} + \operatorname{tg}^2 \alpha + \operatorname{tg} \alpha}} \quad (36)$$

For waves $T_{-(\pm 1)}$ from (29), (31) and (32):

$$ka_{-(\pm 1)}^{min} = 0; \quad (37)$$

$$ka_{-(\pm 1)}^{max} \approx \frac{\cos \alpha}{1 - \sin \alpha} \quad (38)$$

The region of strong wave dispersion $T_{(\pm 1)}$ is limited from the side of high values by value $ka'_{\pm 1}$ determined on the basis (33) by the formula

$$ka'_{\pm 1} \approx \frac{\cos \alpha}{1 - \sin \alpha} \quad (39)$$

The qualitative dependences of the boundary values ka indicated from α are shown on the diagram Fig. 4. On the diagram is shown also dependence $ka_{np} = \frac{M}{2} \operatorname{ctg} \alpha$. When $ka \geq ka_{np}$ in the spiral are absent the ground waves. In the figure is shaded the part of the diagram where there are only waves $T_{\pm 1}$ and is observed the strong dispersion of their phase speed. Values ka and α from the shaded region provide the mode of straight/direct axial radiation/emission in the helical antenna.

The greatest width according to the frequency scale has the region of the mode of straight/direct axial radiation/emission when $\alpha = \alpha_{\text{opt}}$. Value α_{opt} is determined from the equation

$$ka'_{\pm 1} = ka^{\text{min}}_{-(\pm(1+M))} \quad (40)$$

and it is equal to

$$\alpha_{\text{opt}} \approx \text{arctg} \frac{(1+M)[(M+1)^2 - 2]}{2(M+2)\sqrt{M[(M+1)^2 + M]}} \quad (41)$$

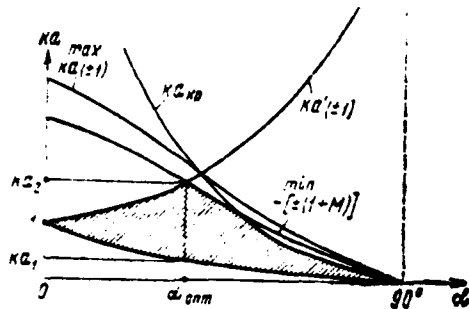


Fig. 4.

Page 146.

With $M \geq 2$ value Q_v determined by formula (29), close to unity: therefore for the approximate computations in expression (31) it is possible to assume $Q_{v(z=1)} = 1$. In this case instead of (36) we will obtain

$$ka_{-[\pm(1+M)]}^{min} \approx \frac{(1-M) \cos \alpha}{1 - \sin \alpha} \quad (42)$$

and equ. (40) gives the following value for α_{opt} :

$$\alpha_{opt} \approx \arcsin \frac{M}{M-2} \quad (43)$$

Values α_{opt} calculated according to formulas (41) and (43), are given in Table 1.

as is evident, virtually with all $M > 1$ for the calculation is possible to use formulas (42), (43). Substituting (43) into expressions (39) and (42), we obtain the following formulas for

values of $ka_{1,2}$, which limit the region of the mode of the axial radiation/emission:

$$ka_1 = ka'_{\pm 1} \approx \sqrt{\frac{1}{M-1}}; ka_2 = ka'_{\pm (1+M)} \approx \sqrt{M+1},$$

whence the overlap factor in the frequency is equal to

$$\frac{ka_2}{ka_1} \approx M+1.$$

Table 1.

M	Значения $\alpha_{\text{опт}}$, рассчитанные по формуле	
	(41)	(43)
1	16°41'	19°30'
2	29°12'	30'
3	36°35'	36°50'
4	42°35'	42°45'

Key: (1). Values $\alpha_{\text{опт}}$ calculated by formula.

Conclusion.

As a result of solving the boundary-value problem it is shown that the multiturn spiral with the contrary coil/winding possesses the same range properties as spiral with the one-sided coil/winding. Is theoretically found optimum winding angle and corresponding to it overlap factor in the frequency, which is confirmed well by the experimental data of work [2]. The system of normal waves, is examined above, it makes it possible to analyze the effect of the conditions of exciting the approaches on characteristics and parameters of helical antenna with the contrary coil/winding. The normal waves, which ensure axial radiation/emission in the helical antenna with the right and left handed circular polarization, are not depended from each other (each of them satisfies boundary conditions

in the system). This is allowed, varying the amplitudes of the waves indicated, to obtain any polarization over a wide range of frequencies.

Page 147.

REFERENCES

1. O. A. Yurtsev. Range properties of multiturn helixes. Materials of the scientific and technical conference, dedicated to seventy years from the day of the invention of radio. Minsk, 1965, page 26-29.
2. Gerst C. W., Worden R. A. Helix antennas take turn for better. — «Electronics». 1966, № 17, p. 100—116.
3. R. A. Silin, V. P. Sazonov. Circuits, M., "Soviet radio", 1966.
4. N. N. Smirnov. Propagation of waves along the infinitely long spiral. DAN USSR, 1956, 2, 108.

Received 30/III 1970; after revision - 16/IX 1971.

Pages 148-151.

No typing.

